

ELECTROPHYSIOLOGICAL AND PHARMACOLOGICAL PROPERTIES OF
THE NEURONAL VOLTAGE-GATED SODIUM CHANNEL SUBTYPE $Na_v1.7$

Patrick L. Sheets

Submitted to the faculty of the University Graduate School
in partial fulfillment of the requirements
for the degree
Doctor of Philosophy
in the Department of Pharmacology and Toxicology
Indiana University

December 2007

Accepted by the Faculty of Indiana University, in partial fulfillment of the requirements for the degree of Doctor of Philosophy

Theodore R. Cummins, Ph.D., Chair

Grant D. Nicol, Ph.D.

Doctoral Committee

Gerry S. Oxford, Ph.D.

Michael R. Vasko, Ph.D.

November 20th, 2007

John H. Schild, Ph.D.

DEDICATION

This work is dedicated to my parents, Greg and Karen Sheets, my brother, Kevin,
and to my beautiful wife, Jennifer.

ACKNOWLEDGEMENTS

This dissertation would have not been possible without the help, guidance, and support of many people whom I would like to acknowledge.

First, I want to thank God for giving me the ability to do science and putting ambition in my heart. I know none of this would have been possible without You by my side.

I would especially like to thank my mentor, Dr. Theodore Cummins. From the beginning, you have kept me progressing in the right direction with patience, humility, and ambition. You have made me a better scientist and person. In and out of the laboratory, you were an excellent role model and have taught me more than I could have imagined. I thank you for everything you have done for me and my wife. Everything I accomplish from this point on I will owe in one way or another to you. Thanks for everything.

I would like to thank Dr. Grant Nicol, Dr. Gerry Oxford, Dr. Michael Vasko, and Dr. John Schild for being an extremely fair and challenging dissertation committee. You all have contributed to my success in different ways, and I am honored to have gotten to know and work with every one of you. In and out of the laboratory you all have been truly exceptional mentors and friends, and I thank you for making my time here enjoyable and productive.

I want to thank Dr. Cynthia Hingtgen for her guidance and advice throughout my time as a Ph.D. student. I will miss the traditional Monday morning talks.

I must acknowledge everyone in the Cummins Lab, James O. Jackson II, Brian W. Jarecki, Andrew D. Piekarz, and Yucheng Xiao for all their support and assistance. James, you are a great technician and an outstanding person. You kept me leveled headed and humble throughout my time in the lab. The friendship that Jenny and I have developed with you and your family has been a truly life altering and inspiring experience. I thank you for everything. Brian, thanks for being receptive to my scientific advice and being a great friend. Yucheng, thanks for teaching me the true amount of work that should be in a normal scientific workday. Andrew, thanks for always making me laugh and forcing me to be patient. Hopefully you won't be late to your defense.

No progress would have been made in anything I have done without the help of Tina Bryant, Lisa King, Amy Lawson, Miriam Barr, Jeramy Spurgeon, Dan Smith, Amy Doherty, and Nastassia Belton in the Department of Pharmacology and Toxicology and Stark Neuroscience Research Institute. You all have helped me in one capacity or another during my graduate work, and I am very grateful for all you have done.

Thanks to all the faculty and post-docs of the Pharmacology and Toxicology Department and Stark Neuroscience Research Institute for all your scientific input and support of me and the Graduate Student Organization. Thanks as well to all of the graduate students in the Pharmacology and Toxicology Department for your help in charities, journal clubs, and seminars.

Thanks to Dr. Simon Rhodes, Jan Hodgin, Monica Henry, and Kelly Forestal in the Graduate Office for keeping me involved and on my toes. Jan,

thanks for never letting me forget anything. Thanks also to Debra Barker for making sure this dissertation fit the requirements of the Graduate School.

I would like to thank my parents, Greg and Karen Sheets, and my brother Kevin Sheets, for their undying love and support throughout my life. I love you very much.

Last and definitely not least, I would like to thank my beautiful wife, Jenny. You have been my inspiration throughout this process and without you this would have never happened. Your unconditional love has kept me strong and ambitious. I look forward to what we have ahead of us. I love you with all my heart.

ABSTRACT

Patrick L. Sheets

Electrophysiological and pharmacological properties of the neuronal voltage-gated sodium channel subtype Na_v1.7

Voltage-gated sodium channels (VGSCs) are transmembrane proteins responsible for the initiation of action potentials in excitable tissues by selectively allowing Na⁺ to flow through the cell membrane. VGSC subtype Na_v1.7 is highly expressed in nociceptive (pain-sensing) neurons. It has recently been shown that individuals lacking the Na_v1.7 subtype do not experience pain but otherwise function normally. In addition, dysfunction of Na_v1.7 caused by point mutations in the channel is involved in two inherited pain disorders, primary erythromelalgia (PE) and paroxysmal extreme pain disorder (PEPD). This indicates Na_v1.7 is a very important component in nociception. The aims of this dissertation were to 1) investigate if the antipsychotic drug, trifluoperazine (TFP), could modulate Na_v1.7 current; 2) examine changes in Na_v1.7 properties produced by the PE mutation N395K including sensitivity to the local anesthetic (LA), lidocaine; and 3) determine how different inactivated conformations of Na_v1.7 affect lidocaine inhibition on the channel using PEPD mutations (I1461T and T1464I) that alter transitions between the different inactivated configurations of Na_v1.7. Standard whole-cell electrophysiology was used to determine electrophysiological and pharmacological changes in WT and mutant sodium currents. Results from this dissertation demonstrate 1) TFP inhibits Na_v1.7 channels through the LA

interaction site; 2) the N395K mutation alters electrophysiological properties of $\text{Na}_v1.7$ and decreases channel sensitivity to the local anesthetic lidocaine; and 3) lidocaine stabilizes $\text{Na}_v1.7$ in a configuration that decreases transition to the slow inactivated state of the channel. Overall, this dissertation answers important questions regarding the pharmacology of $\text{Na}_v1.7$ and provides insight into the changes in $\text{Na}_v1.7$ channel properties caused by point mutations that may contribute to abnormal pain sensations. The results of this dissertation on the function and pharmacology of the $\text{Na}_v1.7$ channel are crucial to the understanding of pain pathophysiology and will provide insight for the advancement of pain management therapies.

Theodore R. Cummins, Ph.D.

TABLE OF CONTENTS

LIST OF TABLES	xiv
LIST OF FIGURES	xvi
LIST OF ABBREVIATIONS	xxi
I. INTRODUCTION.....	1
A. Overview	1
B. Brief history and discovery of sodium channels in the nerve.....	3
C. Voltage-gated sodium channels	4
D. Voltage-gated sodium channels in sensory neurons.....	9
E. Characteristics of the Na _v 1.7 channel subtype.....	12
F. Na _v 1.7 channels and pain	14
G. Interaction of voltage-gated sodium channels with local anesthetics.....	17
H. Na _v 1.7 and lidocaine	21
I. Hypothesis and specific aims	22
II. MATERIALS AND METHODS.....	26
A. cDNA vectors	26
B. Mutagenesis of voltage-gated sodium channels	27
C. Transfection and preparation of stably transfected cell lines.....	28
D. Transient transfection of HEK293 cells	30
E. Chemicals	31
F. Solutions	31

1. Standard bathing solution	31
2. Standard pipette solution	32
3. Pipette solution used for the CIP experiments	32
G. Whole Cell Patch-Clamp Recordings	32
1. Perfusion System.....	35
H. Data Analysis	37
III. RESULTS	39
A. Inhibition of Na _v 1.7 and Na _v 1.4 sodium channels by trifluoperazine (TFP) involves the local anesthetic interaction site	39
1. TFP decreases currents produced by Na _v 1.7 and Na _v 1.4 channels.....	39
2. TFP causes hyperpolarizing shifts in the voltage-dependence of Na _v 1.7 and Na _v 1.4 steady-state inactivation	41
3. TFP shows use-dependent inhibition of Na _v 1.7 and Na _v 1.4 during high frequency stimulation	43
4. Steady-state inactivation is altered in Na _v 1.7 but not Na _v 1.4 in the presence of 1 μM calmodulin inhibitory peptide	45
5. Calmodulin inhibitory peptide shows different effects on Na _v 1.7 and Na _v 1.4 during high frequency stimulation.....	47
6. TFP has a higher affinity for inactivated sodium channels than for resting channels.....	49
7. TFP increases the onset of inhibition and slows recovery from inhibition for Na _v 1.7 and Na _v 1.4	50

8. TFP showed attenuated effects on LA binding site mutations N434K and F1579K, but not L1280K	52
B. A channel mutation associated with primary hereditary erythromelalgia (N395K) alters electrophysiological properties of Na _v 1.7 in addition to decreasing channel sensitivity to the local anesthetic lidocaine	63
1. The N395K mutation alters electrophysiological properties of Na _v 1.7	63
2. The N395K mutation decreases Na _v 1.7 sensitivity to lidocaine.....	68
3. An erythromelalgia mutation not found in the local anesthetic binding site (F216S) did not alter Na _v 1.7 sensitivity to lidocaine	72
C. Lidocaine stabilizes Na _v 1.7 in a configuration that decreases transition to the slow inactivated state of the channel	75
1. Lidocaine alters the recovery of Na _v 1.7 channels from inactivation.....	75
2. Lidocaine attenuates the ability of Na _v 1.7 channels to transition to a state that recovers slowly from inactivation	80
3. Lidocaine exhibits different dose-response effects on Na _v 1.7 current which are dependent on voltage and pulse duration	85

4. PEPD mutations I1461T and T1464I do not alter lidocaine effects on the activation of the Na _v 1.7 channel	90
5. PEPD mutations I1461T and T1464I alter inactivation of the Na _v 1.7 channel	93
6. PEPD mutations I1461T and T1464I alter the effects of lidocaine on slow inactivation of the Na _v 1.7 channel but not fast inactivation	97
7. PEPD mutations I1461T and T1464I decrease use-dependent inhibition of the Na _v 1.7 channel by lidocaine.....	101
8. The I1461T and T1464I mutations alter the recovery of Na _v 1.7 channels from inactivation	103
9. Lidocaine alters the recovery of I1461T and T1464I channels from inactivation differently than WT channels	108
10. The I1461T and T1464I mutations alter the onset of inactivation for Na _v 1.7 channels	110
11. The I1461T and T1464I mutations alter the onset of lidocaine inhibition for Na _v 1.7 channels	112
IV. DISCUSSION	119
A. Inhibition of Na _v 1.7 and Na _v 1.4 sodium channels by trifluoperazine (TFP) involves the local anesthetic interaction site	120

B. A channel mutation associated with primary hereditary erythromelalgia (N395K) alters electrophysiological properties of Na _v 1.7 in addition to decreasing channel sensitivity to the local anesthetic lidocaine	124
C. Lidocaine stabilizes Na _v 1.7 in a configuration that decreases transition to the slow inactivated state of the channel	130
D. Summation and future directions.....	142
V. REFERENCE LIST	145

CURRICULUM VITAE

LIST OF TABLES

Table 1. Time constants for onset of TFP inhibition and recovery from TFP inhibition for WT, N434K, and F1579K channels	62
Table 2. Estimated time constants recovery from prolonged inactivation and lidocaine inhibition for Na _v 1.7 channels	78
Table 3. Estimated time constants for onset of slow inactivation for Na _v 1.7 channels	82
Table 4. Estimated time constants for onset of lidocaine inhibition of Na _v 1.7 channels	83
Table 5. Summary of IC ₅₀ values established for lidocaine inhibition of Na _v 1.7 current at different potentials and pulse durations	87
Table 6. Estimated time constants of recovery from fast inactivation for Na _v 1.7 WT, I1461T, and T1464I channels	105
Table 7. Estimated time constants of recovery from the first slow inactivation component for Na _v 1.7 WT, I1461T, and T1464I channels	107

Table 8. Estimated time constants of the onset of slow inactivation	
for Na _v 1.7 WT, I1461T, and T1464I channels	114

LIST OF FIGURES

Figure 1. Linear diagram of the α subunit for the Na _v 1.7 voltage-gated sodium channel.....	5
Figure 2. Simplified scheme of the different states of voltage-gated sodium channels.....	6
Figure 3. Schematic diagram of perfusion system used to obtain lidocaine dose response effects on Na _v 1.7 channels	36
Figure 4. Inhibition of current produced from Na _v 1.7 and Na _v 1.4 channels by TFP.....	40
Figure 5. Shift in steady-state inactivation of Na _v 1.7 and Na _v 1.4 channels in the presence of TFP.....	42
Figure 6. Use-dependent block of the Na _v 1.7 channels and Na _v 1.4 channels by TFP.....	44
Figure 7. Calmodulin inhibitory peptide effects steady-state inactivation in Na _v 1.7 channels but not Na _v 1.4 channels.....	46

Figure 8. Use-dependent block of Na _v 1.7 and Na _v 1.4 channels by calmodulin inhibitory peptide.....	48
Figure 9. Onset of TFP inhibition and recovery from TFP inhibition for Na _v 1.7 and Na _v 1.4 channels	51
Figure 10. Effects of TFP on current produced from rat Na _v 1.4 channels and rat channels having the mutations N434K, L1280K, or F1579K in the LA binding site.....	54
Figure. 11. Steady-state inactivation curves of rat wild-type channels and rat channels having the mutations N434K, L1280K, or F1579K in the LA binding site.....	57
Figure 12. State-dependent inhibitory effects of 500 nM TFP on the rat Na _v 1.4 wild-type channel and rat channels having the mutations N434K, L1280K, or F1579K in the LA binding site.....	60
Figure 13. Comparison of the activation properties between the WT and N395K Na _v 1.7 channels	64
Figure 14. Comparison of electrophysiological properties between the WT and N395K Na _v 1.7 channels	66

Figure 15. Effects of lidocaine on inactivated and resting WT and N395K channels	69
Figure. 16. Use-dependent inhibition of WT and N395K current by lidocaine.....	71
Figure 17. Inhibitory effects of lidocaine on the F216S channel compared to Na _v 1.7 WT and N395K	74
Figure 18. Recovery from prolonged inactivation and lidocaine inhibition for Na _v 1.7 channels	77
Figure 19. Onset of slow inactivation and lidocaine inhibition for Na _v 1.7 channels	81
Figure 20. Dose-response curves of lidocaine inhibition of the Na _v 1.7 at various holding potentials	86
Figure 21. Dose-response curves of lidocaine inhibition on Na _v 1.7 comparing the effects of pulse duration at various holding potentials on inhibition of channel current.....	89

Figure 22. Effects of 1 mM lidocaine on the voltage-dependence of activation and peak current for Na _v 1.7, I1461T, and T1464I channels	91
Figure 23. Effects of the I1461T and T1464I mutations on the inactivation properties of the Na _v 1.7 channel	95
Figure 24. Effects of lidocaine on the fast and slow inactivation properties of the Na _v 1.7 WT, I1461T, and T1464I channels.....	99
Figure 25. Use-dependent inhibition of Na _v 1.7 WT, I1461T, and T1464I current by lidocaine	102
Figure 26. The effects of the I1461T and T1464I mutation on recovery from prolonged inactivation for Na _v 1.7 channels	104
Figure 27. Lidocaine effects on recovery from prolonged inactivation at various potentials for Na _v 1.7 channels having the I1461T or T1464I mutation.....	109
Figure 28. Comparison of lidocaine effects on the recovery from prolonged inactivation for WT, I1461T, and T1464I channels	111

Figure 29. The effects of the I1461T and T1464I mutation on the onset of slow inactivation for Na _v 1.7 channels	113
Figure 30. Lidocaine effects on the onset of slow inactivation at various potentials for Na _v 1.7 channels having the I1461T or T1464I mutation.....	115
Figure 31. Comparison of lidocaine effects on the onset of slow inactivation for WT, I1461T, and T1464I channels	117
Figure 32. Theoretical schematic of lidocaine interaction with the Na _v 1.7 channel	141

LIST OF ABBREVIATIONS

ANOVA	Analysis of Variance
CaM	Calmodulin
CaMKII	Ca ²⁺ -Calmodulin Dependent Kinase II
CIP	Calmodulin inhibitory peptide
CNS	Central Nervous System
DI—DIV	Domains of the Voltage-gated Sodium Channel
DMEM	Dulbecco's Modified Eagle Medium
DRG	Dorsal Root Ganglion
EGFP	Enhanced Green Fluorescent Protein
G418	Neomycin
HEK293	Human Embryonic Kidney Cells
IRES	Internal Ribosome Entry Site
LA	Local Anesthetic
Lys	Lysine
Na _v	Voltage-gated Sodium Channel
NGF	Nerve Growth Factor
PE	Primary Erythromelalgia
PEPD	Paroxysmal Extreme Pain Disorder
Phe	Phenylalanine
PKA	Protein Kinase A
PKC	Protein Kinase C
PNS	Peripheral Nervous System
S1—S6	Segments within Domains of the Voltage-gated Sodium Channel
SE	Standard Error
SEM	Standard Error of the Mean
TFP	Trifluoperazine
TTX	Tetrodotoxin
TTX-S	Tetrodotoxin Sensitive
TTX-R	Tetrodotoxin Resistant
Tyr	Tyrosine
VGSC	Voltage-gated Sodium Channel
WT	Wild-type

“Problems call forth our courage and our wisdom; indeed, they create our courage and wisdom. It is only because of problems that we grow mentally and spiritually. It is through the pain of confronting and resolving problems that we learn.”

M. Scott Peck 1936—2005

American psychiatrist and writer

I. INTRODUCTION

A. Overview

Pain is a serious medical problem. The International Association for the Study of Pain (IASP) defines pain as an unpleasant sensory and emotional experience associated with actual or potential tissue damage, or described in terms of such damage. According to estimates by the American Pain Society, 75 million people are partially or totally disabled by pain and 45% of all Americans seek care for persistent pain at some point in their lives. Pain sensations typically originate in peripheral pain-sensing neurons known as nociceptors. These neurons relay information about noxious stimuli from the periphery of the human body to the central nervous system (CNS). Therefore, alterations in the homeostasis of this process can result in increased or diminished pain sensations.

Voltage-gated ion channels play a major role in determining excitability properties of peripheral and central neurons. Over the last 20 years, numerous studies have investigated the role of different ion channels in nociception, hyperexcitability, and increased pain sensitivity (Matzner and Devor, 1994; Baker and Wood, 2001). Although changes in ion channels of CNS neurons are likely to contribute to altered pain sensitivity, the vast majority of studies have focused on ion channels and ionic currents in the peripheral nervous system (PNS). Changes in the activities of many different ion channel subtypes have been identified in various pain models and there is evidence indicating several different

types of ion channels can play important roles in nociception and altered pain sensitivity.

The American Medical Association has stated that repeated evaluations of the state of pain therapy over the past 20 years suggest that many patients receive inadequate pain relief. Furthermore, pain therapeutics to date, although initially effective, have the potential to produce addiction, physical dependence, tolerance, as well as unwanted side effects. Therefore, the research and discovery of unique therapeutic targets for the treatment of pain is important. The critical role of voltage-gated sodium channels in the function of nociceptors makes them an important aspect to research for the advancement of pain mechanism and therapeutics.

The main focus in this dissertation is the modulation and pharmacology of the voltage-gated sodium channel subtype $Na_v1.7$ found primarily in peripheral sensory neurons. There is compelling support that the $Na_v1.7$ subtype is involved in pain perception due to studies of individuals that appear to have a complete insensitivity to pain (Cox et al., 2006; Goldberg et al., 2007; Ahmad et al., 2007). This provides strong evidence that complete loss of $Na_v1.7$ function results in a complete inability to sense pain. This channel is an intriguing component of pain-sensing neurons, and it is important to evaluate the pharmacology and function of $Na_v1.7$ to better understand the mechanism of pain and design more specific and effective pain therapeutics.

B. Brief history and discovery of sodium channels in the nerve

In a series of experiments using the squid giant axon, two English physiologists, Sir Alan L. Hodgkin and Sir Andrew F. Huxley, discovered that transmission of action potentials along the axon of a nerve was reliant on the permeability of sodium (Na^+) and potassium (K^+) ions across the plasma membrane (Hodgkin and Huxley, 1952, a, b, c, d). In addition to these findings, Hodgkin and Huxley discovered that membrane voltage (or potential) of the squid giant axon played a role in sodium conductance and sodium current kinetics and suggested sodium conductance was controlled by a gating mechanism (Hodgkin and Huxley, 1952, b, c, d). Thus, the term voltage-gated was born. Some years later, it was discovered the Na^+ current in squid giant axons could be selectively eliminated using a paralytic toxin called tetrodotoxin (TTX) found in the liver of the puffer fish indicating a distinct pathway for Na^+ ions to cross the plasma membrane (Narahashi et al., 1964). Pharmacologic studies using another selective blocker of Na^+ current, saxitoxin (STX), on frog and rabbit vagus nerve demonstrated the saxitoxin interacted with individual receptors to block Na^+ current (Hille, 1968; Ritchie et al., 1976). These studies together confirmed Na^+ current was 1) voltage-dependent; 2) controlled by different gating configurations; and 3) conducted by individual receptors or channels. The scientific advancement of patch-clamp recording allowing the examination of Na^+ currents in small isolated neurons (Hamill et al., 1981; Sakmann and Neher, 1984) has been pivotal in the understanding of the different subtypes of Na^+ channels found in the body. While this dissertation focuses primarily on only one voltage-gated

sodium channel subtype, it is important to introduce the structure, function, and modulation of voltage-gated sodium channels as a whole.

C. Voltage-gated sodium channels

Voltage-gated sodium channels (VGSC or Na_v) are complex transmembrane proteins that allow the influx of sodium needed to initiate action potentials in excitable tissues (Goldin, 2001). They are crucial for the excitability of neuronal, cardiac, skeletal, and smooth muscle tissue. The primary functional unit of the voltage-gated sodium channel is a 220-260 kD polypeptide known as the α subunit. The α subunit consists of four transmembrane domains (DI—DIV) with each domain consisting of six transmembrane segments (S1—S6, Figure 1). The S4 segments each contain four to eight basic amino acids (arginines or lysines) which are positively charged. These residues are thought to respond to changes in membrane voltage (or potential) and can move within the membrane creating various gating configurations (Noda et al., 1984). In a simplified scheme, VGSCs can exist in one of three gating configurations: resting (primed), open (activated), or inactivated (Figure 2). Resting or primed refers to the configuration of VGSCs, usually at hyperpolarized (or negative) membrane potentials, in which the channel is capable of opening in response to depolarization of the membrane. Open or activated is the configuration by which VGSCs allow the selective passing of Na^+ ions through the pore of the channel producing current. Current through VGSCs is terminated within 1 or 2 milliseconds by a process called fast-inactivation thought to occur when a DIII-

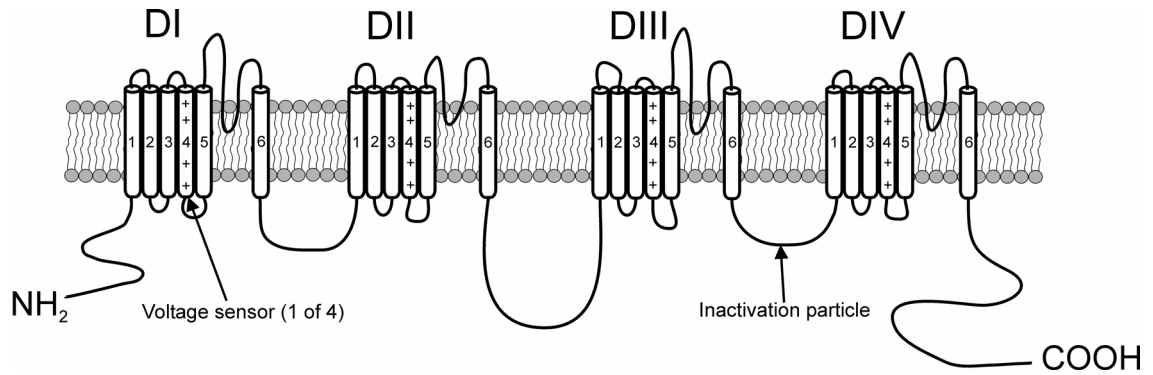


Figure 1. Linear diagram of the α subunit for the $\text{Na}_v1.7$ voltage-gated sodium channel. The α subunit consists of four transmembrane domains (DI—DIV) with each domain consisting of six transmembrane segments (S1—S6). This figure was created using CorelDraw version 9.

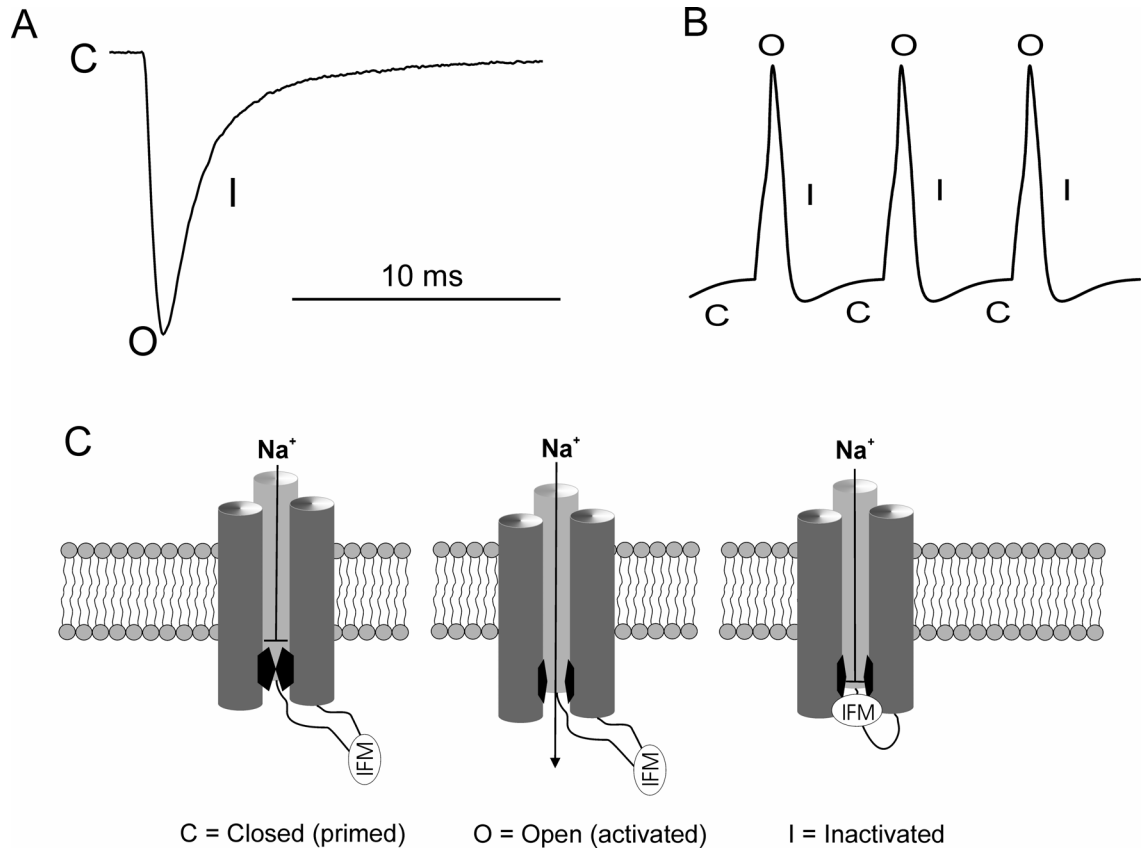


Figure 2. Simplified scheme of the different states of voltage-gated sodium channels. A, Voltage clamp recording from a single HEK293 cell transfected with Na_v1.7 cDNA showing typical voltage-gated sodium currents. The downward deflection reflects the inward movement of sodium ions in response to a depolarizing voltage pulse from a holding potential of -80 mV. The channel is closed (C) at -80 mV and when pulsed to +15 mV the channel opens (O) and rapidly inactivates (I). B, A simple action potential schematic indicating where in the action potential waveform you would expect voltage-gated sodium channels to be closed, open, or inactivated. C, Diagram indicating the proposed scheme for voltage-gated sodium channels transitions from closed to open to fast-inactivated. This figure was created using CorelDraw version 9.

DIV cytoplasmic linker (also known as the inactivation particle shown in Figure 1) binds within the pore and occludes the flow of sodium ions (West et al., 1992). In addition to fast inactivation, there have been studies showing a slower component of inactivation in neuronal (Ogata and Tatebayashi, 1992; Mickus et al., 1999), cardiac (Vilin et al., 1999) and skeletal muscle channels (Richmond et al., 1998). This slow component of inactivation is caused by prolonged depolarizations and can take seconds to minutes to recover. Fast and slow inactivation have both been proposed to play a role in the interaction of local anesthetics with VGSCs and will be discussed later.

The inner pore of the channel is thought to consist of the S6 segments of each of the four domains (Fozzard and Hanck, 1996; Marban et al., 1998; Catterall, 2000). Nine distinct voltage-gated sodium channel α subunits (Nav1.1-1.9) have been cloned from mammals (Goldin, 2002), and many of these α subunits have specific developmental, tissue, or cellular distributions. Nav1.4 is highly expressed in skeletal muscle (Trimmer et al., 1989). Although Nav1.5 is predominantly expressed in cardiac muscle (Rogart et al., 1989), Nav1.5 mRNA and current is detectable in neonatal dorsal root ganglia (DRG) neurons (Renganathan et al., 2002). Nav1.5 mRNA is also detectable in some adult DRG neurons but expression is considered to be very low under most conditions. Mature neurons typically express multiple sodium channel isoforms. Adult CNS neurons may express combinations of Nav1.1, Nav1.2 and Nav1.6 (Trimmer and Rhodes, 2004). Adult DRG sensory neurons can express combinations of Nav1.1, Nav1.6, Nav1.7, Nav1.8, and Nav1.9 (Black et al., 1996; Dib-Hajj et al.,

1998; Amaya et al., 2000). $\text{Na}_v1.3$ is predominantly expressed in immature neurons and is normally found at very low levels in adult neurons (Beckh et al., 1989). However, under certain conditions $\text{Na}_v1.3$ expression is upregulated in adult neurons and this may play a role in altered pain sensations (Waxman et al., 1994; Boucher et al., 2000). Although message for $\text{Na}_v1.2$, one of the predominant CNS isoforms, is detectable in adult DRG neurons, expression is low in these cells under most conditions (Black et al., 1996).

Since its discovery as a VGSC blocker, TTX has been identified as a highly selective blocker of CNS and skeletal muscle sodium currents ($\text{IC}_{50} \sim 5\text{-}20$ nM; (Ritchie and Rogart, 1977)) but a relatively weak blocker of cardiac muscle sodium currents ($\text{IC}_{50} \sim 1\text{-}2$ μM ; (Baer et al., 1976)), further confirming distinct VGSCs generate the sodium currents in different tissues. Based on their sensitivity to TTX, VGSCs have been divided primarily into two groups, TTX-sensitive (TTX-S) and TTX-resistant (TTX-R). While this toxin has been useful in distinguishing TTX-R and TTX-S currents in neurons, it is not effective at isolating single VGSC subtype current in neurons. Therefore, the use of heterologous (derived from tissue) cell systems such as human embryonic kidney cells (HEK293) are useful in examining current produced from a single VGSC subtype. These cells are able to internalize expression vectors containing VGSC cDNA and effectively transcribe and translate the full channel and place it in the cell membrane. We have shown that the naïve HEK293 cells exhibit negligible Na^+ current. This characteristic provides confidence that any Na^+ current observed in voltage-clamp experiments (explained in Materials and

Methods) from a single HEK293 cell after internalization of cDNA is from our channel of interest. Expression of the α -subunit alone is sufficient to produce functional sodium currents in heterologous cell systems, however β -subunits (Isom, 2001; Yu et al., 2003; Grieco et al., 2005) and other accessory proteins such as calmodulin (CaM) (Herzog et al., 2003b) or annexin II (Okuse et al., 2002) may be important modulators of VGSCs in their native environment. The role of CaM in altering VGSC function is one component of this dissertation and will be discussed later.

D. Voltage-gated sodium channels in sensory neurons

Neurons of the CNS exhibit relatively homogeneous currents characterized by rapid activation, rapid inactivation, and high sensitivity to TTX. In contrast, neurons of the DRG express more complex currents that contain both rapid-inactivating TTX-sensitive (TTX-S) components and slowly-inactivating TTX-resistant (TTX-R) components (Kostyuk et al., 1981). It was proposed the slower TTX-R currents might serve to prolong the duration of the action potential, possibly modulating neurotransmitter release at the nerve terminals. TTX-S sodium currents in most, if not all, neurons exhibit multiple kinetic components. Persistent or non-inactivating sodium current components have been identified in CNS neurons (Crill, 1996) and in DRG neurons (Baker and Bostock, 1997; Cummins and Waxman, 1997) and these currents can have significant influences on the threshold for generation of the action potential. However it was not until the advances in molecular biology and protein chemistry

of the late 1980s that the identification and cloning of individual sodium channel isoforms as well as the full complexity of VGSC and sodium currents could be adequately investigated.

Alterations in sodium currents within the PNS can contribute to changes in cellular excitability and are likely to play important roles in nociception. As mentioned earlier, adult sensory neurons can express TTX-S ($\text{Na}_v1.1$, $\text{Na}_v1.6$ and $\text{Na}_v1.7$) and TTX-R ($\text{Na}_v1.8$ and $\text{Na}_v1.9$) sodium channels. These channels are critical in producing the all-or-none depolarization that is typical of action potentials in nociceptive (pain-sensing) neurons, and understanding their pharmacologic properties is important for the development of pain therapeutics. It has been suggested the TTX-sensitive (TTX-S) channels are responsible for the initiation of action potentials in both myelinated and unmyelinated axons (Brock et al., 1998; Ritter and Mendell, 1992). These channels also have important roles in resting membrane potential and subthreshold oscillations. The difference in TTX sensitivity has been very useful in characterizing TTX-R currents in DRG neurons; however, no pharmacological tools to date are effective at discriminating the different TTX-S neuronal isoforms.

There have been several indications that changes in VGSC expression and/or modulation play a role in hyperexcitable states of neurons including inflammation, neuropathic pain, and nerve injury. Changing the gating properties of VGSCs and/or the expression of VGSCs in the membranes of nociceptive neurons could increase excitability of these neurons thus producing pain. The

inflammatory mediator prostaglandin E₂ (PGE₂) increased TTX-R current in sensory neurons and enhanced the voltage-dependence of activation for the current (Gold et al., 1996; England et al., 1996). A recent study has revealed that nerve growth factor (NGF), a neurotrophin elevated in inflammatory exudates (Weskamp and Otten, 1987), and one of its downstream signaling molecules, ceramide, enhance the excitability of DRG neurons in culture by enhancing TTX-R current (Zhang et al., 2002). In contrast, it has been shown that mice lacking a functional form of the TTX-R Na_v1.8 channel did not differ in its maximum level of hyperalgesia produced from inflammation (Akopian et al., 1999). These mice lacking Na_v1.8 did show increased levels of TTX-S currents and lower thresholds of electrical activation of small-diameter neurons. Other work has shown increased TTX-S current amplitude in DRGs of rats that have developed hyperalgesia and allodynia in response to an induced diabetic state (Hong et al., 2004). A downregulation of TTX-R current and an upregulation of rapidly repriming TTX-S current have been observed in axotomized rat spinal sensory neurons (Cummins and Waxman, 1997). Even with the findings of these studies, there still is little known about modulation of TTX-S channels that could underlie changes in nociception. However, there is now compelling evidence the TTX-S VGSC subtype Na_v1.7 (PN1) plays a critical role in nociception. To date, the modulation and pharmacology of the Na_v1.7 channel is not well characterized.

E. Characteristics of the Na_v1.7 channel subtype

The Na_v1.7 isoform was originally cloned and studied from human neuroendocrine cells and was believed to be an evolutionary link between channels from brain and skeletal muscle (Klugbauer et al., 1995). It was later observed the TTX-S Na_v1.7 channel is expressed specifically at high levels in neuronal populations throughout the peripheral nervous system and exhibits features that distinguish it from Na_v1.1, 1.2, and 1.3 channels (Toledo-Aral et al., 1997). The significant differences found from this study included some putative extracellular loops between S5 and SS1, the intracellular loop between domain I and II, and the carboxyl terminus. Na_v1.7 is expressed at high levels in rat and human dorsal root ganglia (DRG) and sympathetic ganglia (Black et al., 1996; Toledo-Aral et al., 1997; Sangameswaran et al., 1997) and responds to small, slow depolarizations thereby contributing to action potential generation. Na_v1.7 is known to be expressed abundantly in nociceptive neurons from in vivo studies using guinea-pigs showing that Na_v1.7-like immunoreactivity was greatest in cells with C-fiber axons (Djoughri et al., 2003). Na_v1.7 currents exhibit rapid activation and rapid inactivation from the open configuration (Klugbauer et al., 1995), similar to other TTX-S channels such as Na_v1.4 and Na_v1.6. However in contrast to Na_v1.4 and Na_v1.6, which exhibit rapid recovery from fast inactivation, Na_v1.7 channels exhibit substantially slower recovery from fast inactivation (Cummins et al., 1998; Herzog et al., 2003a). Biophysical properties of sodium currents generated by recombinant human Na_v1.7 channels closely resemble those of the

predominant TTX-S current expressed in small diameter neurons of the DRG (Cummins et al., 1998).

Although sodium channels are subject to extensive modulation, little is known about modulation of Na_v1.7. It has been reported recently that currents of Na_v1.7 expressed in *Xenopus* oocytes are decreased by protein kinase A (PKA) and protein kinase C (PKC) (Vijayaragavan et al., 2004). In contrast, activators of PKA had little effect on TTX-S currents of small diameter sensory neurons (Gold et al., 1996). In addition, endothelin 1, an activator of PKC, showed no effects on TTX-S currents in large diameter sensory neurons (Zhou et al., 2002). However, the direct effects of PKA and PKC on Na_v1.7 in sensory neurons have not been researched. Another intracellular signaling protein, CaM, can bind to and alter the activity of VGSCs (Deschenes et al., 2002; Tan et al., 2002). CaM, a 16.7 kDa protein is expressed in virtually all eukaryotic cells and has the ability to bind calcium ions and induce changes in target proteins. It has been shown CaM can modulate Na_v1.4 (skeletal muscle) and Na_v1.6 (neuronal) current amplitudes and properties (Herzog et al., 2003b). The C-terminus of Na_v1.7 binds CaM, although it has a lower apparent affinity than the C-termini of other TTX-sensitive isoforms. Trifluoperazine (TFP) is one of the most potent CaM inhibitors among the phenothiazine neuroleptics (Brostrom and Wolff, 1981; Levin and Weiss, 1979). Previous research has demonstrated intrathecal administration of TFP has analgesic effects at low doses (Golbidi et al., 2002). However, it is not clear how TFP is able to induce analgesia. TFP reduces peak sodium current in a concentration-dependent manner in squid giant axons

(Ichikawa et al., 1991). These studies raised the possibility TFP exerts its analgesic effects by modulating sodium currents in mammalian neurons and this might involve disruption of the CaM-channel interaction. However, it is not known if CaM, or CaM antagonists, can modulate Na_v1.7 currents.

The first goal of this dissertation was to investigate if TFP can modulate Na_v1.7 current and if this modulation was due to inhibition of the channel interaction with CaM. As previous results indicated Na_v1.7 had a lower affinity for CaM than Na_v1.4 channels (Herzog et al., 2003b), and if TFP modulates Na_v1.7 current by altering the interaction with CaM, then TFP would have dissimilar effects on Na_v1.4 and Na_v1.7. Examining the effects of TFP on Na_v1.7 could lead to a better understanding the drug's analgesic properties and possible use in regional anesthesia and thus pain management. Therefore, in order to understand the potential impact of these findings, it is important to elaborate on the importance of Na_v1.7 and its role in pain.

F. Na_v1.7 channels and pain

Recent studies (Cox et al., 2006; Goldberg et al., 2007) indicate Na_v1.7 plays a crucial role in our ability to perceive pain. Cox et al. studied several families from Northern Pakistan that contained members with an inability to experience pain. Neurological examinations indicated these individuals, age 6 to 12 years old, apparently had never experienced any pain sensations while otherwise appearing normal. The individuals were reported to have a profound, and apparently selective, inability to sense pain. It was determined the condition

was congenital and could be mapped as an autosomal-recessive trait linked to a region of chromosome 2 containing the gene *SCN9A*, which encodes for the Na_v1.7 channel. Sequence analysis of *SCN9A* found several distinct homozygous nonsense mutations in the affected individuals of each of the three families. In experiments using mutated recombinant Na_v1.7 channels it was demonstrated each of the mutations identified in the three different families eliminated functional Na_v1.7 currents in heterologous expression systems. Family members heterozygous for the *SCN9A* mutations, who therefore should have one functional *SCN9A* allele, reported normal pain phenotypes. A separate study (Goldberg et al., 2007) identified Na_v1.7 truncating mutations in patients with congenital indifference to pain from seven different countries, demonstrating loss-of-function of Na_v1.7 can result in an insensitivity to pain in multiple populations. As individuals lacking functional Na_v1.7 channels appear normal except for their complete insensitivity to pain, drugs that selectively target Na_v1.7 might be ideal analgesics.

Further support for the role of Na_v1.7 in pain includes deletion of the mouse Na_v1.7 gene in a subset of sensory neurons that are predominantly nociceptive creates decreased responses to noxious mechanostimulation and induced inflammatory pain (Nassar et al., 2004). Recently, a recombinant herpes simplex-based virus was designed to knockdown expression of the Na_v1.7 channel. When applied to the hindpaw skin of mice prior to induction of inflammation by with complete Freund's adjuvant, this virus prevented development of hyperalgesia in thermonociceptive tests (Yeomans et al., 2005).

Interestingly, mutations in the Na_v1.7 channel have been implicated in primary hereditary erythromelalgia (Yang et al., 2004; Drenth et al., 2005). Primary hereditary erythromelalgia is an inherited autosomal dominant painful neuropathy that is marked by intense burning pain and redness of the extremities and face (Van Genderen et al., 1993). Electrophysiological studies on Na_v1.7 with the I848T, L858H, or L858F mutation implicated in hereditary erythromelalgia have shown hyperpolarized voltage-dependence of activation, slower deactivation kinetics, and larger ramp currents (Cummins et al., 2004; Han et al., 2006). The L858H mutation is known to make DRG neurons hyperexcitable, while making sympathetic ganglion neurons hypoexcitable (Rush et al., 2006). DRG neurons transfected with several other Na_v1.7 mutations implicated in hereditary erythromelalgia (F1449V, A863P) have a lower threshold for firing action potentials and fire at higher-than-normal frequencies in response to suprathreshold stimulation (Dib-Hajj et al., 2005; Harty et al., 2006) which suggests these Na_v1.7 mutations increase excitability of sensory neurons. Interestingly, erythromelalgia is not the only neuropathy implicated by mutations in Na_v1.7. A recent study has shown that a family affected by paroxysmal extreme pain disorder (PEPD), characterized by rectal, ocular, and submandibular pain, also have missense mutations in the SCN9A gene encoding for Na_v1.7 (Fertleman et al., 2006). Taken together, these studies indicate that changes in Na_v1.7 properties play a crucial role in the production of pain and suggest that hereditary erythromelalgia mutations could serve as a model for examining changes in voltage-gated sodium channels that may contribute to pain

in humans. Furthermore, these studies indicate changes in $\text{Na}_v1.7$ properties play a role in the production of pain and understanding $\text{Na}_v1.7$ biophysical and pharmacological properties is crucial for the advancement of pain therapeutic design.

G. Interaction of voltage-gated sodium channels with local anesthetics

Voltage-gated sodium channels are the primary target of local anesthetics (LAs) such as lidocaine (Taylor, 1959; Hille, 1966; Hille, 1977). The main use of LAs is to prevent or relieve pain by reversibly preventing action potential propagation through the inhibition of VGSCs. One problem with LAs is that they interact with most VGSCs in the body. This non-selectivity of LAs is cause for concern in regards to unwanted side effects. Since VGSCs reside in cardiac and muscle tissue, it is predictable LAs can cause a decreased activity of the heart, bowel, and skeletal muscle. In fact, the LA lidocaine can be administered intravenously to patients as short-term management of ventricular arrhythmias. Thus, establishing a detailed pharmacologic and molecular basis for the complex interaction of LAs with the different VGSC subtypes throughout the body remains an important goal.

A common theory for the dynamic and complex interaction between LAs and VGSCs has been termed the modulated receptor hypothesis (Hille, 1977). The modulated receptor hypothesis states that 1) affinity of a channel for LAs changes with channel state while access to the channel remains constant, 2) LAs can bind to any channel state, 3) LA bound states are non-conducting until LA

unbinds from the channel, 4) binding of LAs to the channel obeys first-order reaction kinetics, and 5) unbinding of LAs from the channel obeys zero-order kinetics. Further investigation led to the discovery that LA inhibition of VGSCs is dependent on voltage and frequency of activation (Strichartz, 1973; Courtney, 1975; Khodorov et al., 1976; Hille, 1977; Schwarz et al., 1977). Another model for interaction of LAs with VGSCs has been termed the guarded receptor hypothesis (Starmer et al., 1984; Starmer and Grant, 1985). In this model, the site of LA interaction with VGSC is “guarded” when the channel is in the closed or inactivated state. Only when the channel opens does the binding site become “unguarded” by channel configuration allowing LAs to effectively interact with the channel.

To date, the interaction of local anesthetics with the individual gating configurations of VGSCs remains controversial. LAs are thought to interact with residues in the middle of the S6 transmembrane segments within domains I, III, and IV in the α -subunit of VGSCs (Ragsdale et al., 1994; Wang et al., 2000; Yarov-Yarovoy et al., 2002; Yarov-Yarovoy et al., 2001; Wright et al., 1998). The S6 segments as mentioned earlier are thought to be arranged as α -helices that line the inner (cytoplasmic) portion of the pore in VGSCs (Fozzard and Hanck, 1996; Catterall, 2000; Marban et al., 1998). Point mutations of residues located in the S6 transmembrane segments can reduce high affinity binding of LAs to the inactivated state of the channel (Ragsdale et al., 1994; Wright et al., 1998; Li et al., 1999; Nau et al., 1999; Nau et al., 2003). These results have provided further evidence as to the potential molecular site within VGSCs at which LAs interact.

However, the accessibility and configuration of these sites continue to be explored.

One study done in squid giant axon showed that elimination of the fast inactivation mechanism after intracellular pronase treatment did not completely eliminate time- and voltage-dependent inhibition of Na⁺ current by LAs (Cahalan, 1978). However, in this same study, and in an additional study (Yeh, 1978), voltage-dependent and use-dependent inhibitory effects of QX-314, a quaternary ammonium derivative of lidocaine, on Na⁺ currents were eliminated meaning the fast inactivation mechanism of VGSCs important for QX-314 interaction with the channels. In addition, other studies in the human cardiac VGSC showed that elimination of fast inactivation by mutation also reduced lidocaine induced use-dependent inhibition (Bennett et al., 1995). These studies provide evidence the fast inactivation component of Na⁺ channels play a role in use-dependent lidocaine inhibition. Experiments using cardiac and skeletal muscle VGSCs in tissue or heterologous expression systems indicated the open-state of channel was not important for lidocaine interaction (Bean et al., 1983; Bennett et al., 1995; Balser et al., 1996a) but in fact lidocaine served to enhance VGSC inactivation. This idea was supported by a study showing that in rat Na_v1.4 channels, lidocaine increased the closure of the fast inactivation gate but did not cause the accumulation of fast-inactivated channels during use-dependent block (Vedantham and Cannon, 1999). In other words, lidocaine does not trap the rat Na_v1.4 channel into a fast-inactivated conformation.

Other theories in regard to LA interaction with VGSCs involve interaction of LAs with the slow-inactivated state of the channel. One study done in *Xenopus* oocytes suggested lidocaine block on rat Na_v1.4 channels was similar for fast-inactivated and slow-inactivated states of the channel (Balsler et al., 1996b). Other studies done in rat Na_v1.4 channels proposed that lidocaine interaction with the channel induced a transition to a slow-inactivated state (Chen et al., 2000; Fukuda et al., 2005). Additional findings suggest use-dependent block of lidocaine creates a configuration of rat Na_v1.4 channels similar to the slow-inactivated state (Ong et al., 2006). These hypotheses propose slow inactivation in VGSCs is important in lidocaine block of the channel. However, data from this dissertation conflict with these hypotheses.

Opposing viewpoints support the idea that channel activation is critical in high affinity lidocaine interaction with VGSCs. A study using squid giant axon showed that lidocaine competes for a similar site to which the fast inactivation gate may interact (Yeh and Oxford, 1985). Not long after this discovery, it was discovered that eliminating Na⁺ channel inactivation in squid giant axon using chloramine-T had no effect on the potency of QX-314 and that channel activation was critical for interaction of LA with the channel (Wang et al., 1987). A supporting study demonstrated LAs interact with inactivation-deficient rat Na_v1.4 channels expressed in HEK293 cells (Wang et al., 2004b). Hanck et al. (2000) indicated lidocaine modified the S4 segments important in voltage-sensing of human Na_v1.5 channels and have recently stated that the S4 segments of DIII and DIV are more important in this modification (Sheets and Hanck, 2007). In

addition to these findings, it was concluded the fast inactivation gate was not necessary for lidocaine binding but is crucial for lidocaine to interact to the Na_v1.5 channel with high affinity (Sheets and Hanck, 2007). These studies indicate the possibility that lidocaine interacts directly with the pore of VGSCs and becomes stabilized by the fast inactivation gate.

Therefore, different mechanisms have been proposed regarding the state-dependent block VGSCs by lidocaine. However, to date the interaction of LAs with VGSCs is still not entirely understood and remains a matter of debate. Since lidocaine is used to prevent or relieve pain by reversibly blocking action potential propagation through the inhibition of VGSCs in sensory neurons and the Na_v1.7 channel is highly implicated in pain production, then understanding the interaction of lidocaine with Na_v1.7 becomes more important when considering lidocaine as a pain therapeutic.

H. Na_v1.7 and lidocaine

To date there is very little information regarding the interaction of lidocaine with the Na_v1.7 channel. One study compared the effects of lidocaine on Na_v1.7 channels versus Na_v1.8 channels in *Xenopus* oocytes (Chevrier et al., 2004). This study revealed Na_v1.8 was more sensitive to lidocaine than Na_v1.7 which was consistent with findings indicating TTX-R currents displayed more use-dependent inhibition by lidocaine compared to TTX-S currents in DRG neurons (Roy and Narahashi, 1992). However, this study also showed that TTX-S current was more sensitive to resting lidocaine block than TTX-R currents. The

Cummins lab has also shown that TTX-R channels in DRG neurons are more sensitive to lidocaine than $\text{Na}_v1.7$ channels expressed in a heterologous expression system (Sheets et al., 2007b). It must be noted that this discrepancy in sensitivity was only observed at voltages where channels are resting/closed or completely inactivated. Interestingly, when holding the channels at a potential close to or at threshold for firing (-50 mV), the differences in lidocaine inhibition between $\text{Na}_v1.7$ and TTX-R channels is eliminated. Chevrier et al. (2004) concluded that lidocaine enhances entry into the slow-inactivated state for $\text{Na}_v1.7$ and $\text{Na}_v1.8$ channels. This conclusion was investigated in this dissertation and the data obtained argue against it.

I. Hypothesis and specific aims

Previous research demonstrated that intrathecal administration of trifluoperazine (TFP) has analgesic effects at low doses (Golbidi et al., 2002). However, it is not clear how TFP is able to induce analgesia. TFP is one of the most potent CaM inhibitors among the phenothiazine neuroleptics (Brostrom and Wolff, 1981; Levin and Weiss, 1979). Several studies indicate CaM can bind to and alter the activity of voltage-gated sodium channels (Deschenes et al., 2002; Tan et al., 2002), and it was previously shown CaM can modulate $\text{Na}_v1.4$ (skeletal muscle) and $\text{Na}_v1.6$ (neuronal) current amplitudes and properties (Herzog et al., 2003b). TFP is also able to reduce peak sodium current in a concentration-dependent manner in squid giant axons (Ichikawa, et al., 1991). This raised the possibility TFP could exert its analgesic effects by modulating

sodium currents in mammalian neurons by disrupting the CaM-sodium channel interaction. Therefore, it was hypothesized TFP can alter the electrophysiological properties of the Na_v1.7 channel by disrupting the CaM-channel interaction.

Therefore, the first aim of this dissertation was to investigate if TFP can modulate Na_v1.7 current and if this modulation was due to inhibition of the channel interaction with CaM. Due to previous results indicating Na_v1.7 channels have a lower affinity for CaM than Na_v1.4 channels (Herzog et al., 2003b), it was predicted if TFP could modulate Na_v1.7 current by altering the interaction with CaM, then TFP would have dissimilar effects on Na_v1.4 and Na_v1.7. Understanding the effects of TFP on Na_v1.7 could lead to a better understanding of the drug's analgesic properties, possible use in regional anesthesia, and pain management.

Interestingly, a mutant Na_v1.4 channel (N434K) used in the first specific aim of this dissertation stimulated the idea for the second specific aim of this dissertation. Lysine substitution at this residue (N434K) in the rat Na_v1.4 sodium channel reduces local anesthetic block of channel current (Nau et al., 1999). One mutation in primary hereditary erythromelalgia that has been associated with a severe phenotype is the N395K Na_v1.7 mutation (Drenth et al., 2005), located in the S6 segment of domain I. This N395 residue in Na_v1.7 corresponds to N434 in the rat Na_v1.4 sodium channel. Unfortunately both of the affected individuals in the original family with the N395K mutation (Drenth et al., 2005) are now deceased and data on sensitivity of these patients to local anesthetics

cannot be attained. However, a recent study showed treatment of erythromelalgia with lidocaine relieves pain in only 55% of afflicted patients (Davis and Sandroni, 2005). Due to the multiple mutations involved in hereditary erythromelalgia, it may be possible some but not all of these mutations alter local anesthetic binding to Na_v1.7, and this may contribute to the variability in patients responding to lidocaine. Thus, it was hypothesized the N395K mutation in Na_v1.7 would alter interaction of lidocaine with the channel whereas another erythromelalgia mutation (F216S) not in the local anesthetic binding site would not change this interaction. Therefore, the second aim of this dissertation was to 1) examine electrophysiological changes in Na_v1.7 produced by the N395K mutation and 2) determine if the N395K mutation or F216S mutation in Na_v1.7 changes the effects of lidocaine on sodium channel current.

Results from the second aim showed that a two-site binding model gave a much better fit to the concentration-response curve for lidocaine inhibition of Na_v1.7 channel current. This fit indicated two possible lidocaine interaction configurations of Na_v1.7, one exhibiting high affinity lidocaine binding and another exhibiting low affinity binding. Therefore, the final hypothesis for this dissertation was that the high affinity and low affinity populations represent channels in different inactivated conformations. Based on this hypothesis, the aims for the final part of this dissertation were to 1) determine how different inactivated conformations of Na_v1.7 affect lidocaine inhibition on the channel and 2) use PEPD mutations (I1461T and T1464I) that alter transitions between the different inactivated configurations of Na_v1.7 to determine how these alterations

affect lidocaine's ability to inhibit channel current. Together, these findings will begin to answer questions about the complex interaction of lidocaine with the Na_v1.7 channel.

Overall, this dissertation answers important questions regarding the pharmacology and biophysics of the understudied neuronal VGSC subtype, Na_v1.7. The recent evidence indicating Na_v1.7 as a critical factor of pain in humans (Drenth et al., 2005; Michiels et al., 2005; Cox et al., 2006; Fertleman et al., 2006; Goldberg et al., 2007) makes researching this channel important in the advancement to more efficient pain therapy.

II. MATERIALS AND METHODS

A. cDNA vectors

The voltage-gated sodium channel subtype human Na_v1.7 was previously cloned and constructed into a modified pcDNA 3.1 (-) vector (Klugbauer et al., 1995). This vector was used for all transfections and mutagenesis of the Na_v1.7 channel. The human Na_v1.4 subtype was previously cloned (George Jr. et al., 1992) and constructed into the expression vector pRc/CMV (Wang et al., 1996). This vector was used to produce the HEK293 cell line that stably expressed the Na_v1.4 channel. The rat Na_v1.4 cDNA (Trimmer et al., 1989) had been previously cloned into a RBG4 vector (Ukomadu et al., 1992) and was characterized in HEK293 cells (Ukomadu et al., 1992; Cummins et al., 1993). This vector was used in transient transfections of the rat Na_v1.4 channel. The rat Na_v1.4 mutant channels were generous gifts from laboratory of Dr. Ging Kuo Wang. The mutagenesis was originally done on the rNa_v1.4-pcDNA/amp to create N434K (Nau et al., 1999), L1280K (Wang et al., 2000), and F1579K (Wright et al., 1998) mutant channels.

The vectors for the human β_1 and β_2 subunits were pCD8-IRES-h β_1 and pEGFP-IRES-h β_2 (CD8: cluster of differentiation 8, IRES: internal ribosome entry site, EGFP: enhanced green fluorescent protein) and have been used in previous studies (Lossin et al., 2002; Lossin et al., 2003). Vectors containing an IRES allow for the production of two proteins from the same mRNA sequence. Thus, in a mammalian expression system, the pCD8-IRES-h β_1 vector will produce CD8

and the human β_1 protein, while the pEGFP-IRES-h β_2 vector will produce EGFP and the human β_2 protein. CD8 and EGFP are used as markers to confirm expression of the human β_1 protein and human β_2 protein, respectively. In this dissertation, human β_2 protein expression was confirmed by the presence of EGFP fluorescence in HEK293 cells. Human β_1 protein expression was assumed to correlate with human β_2 protein expression and was not tested in experiments performed for this dissertation. However, other experiments from this laboratory (done by Andrew D. Piekarz) show that cotransfection of the pCD8-IRES-h β_1 vector and the pEGFP-IRES-h β_2 vector in HEK293 cells produce expression of the human β_1 protein in approximately 89% of cells expressing the human β_2 protein. These experiments were done by testing for the presence of CD8 in EGFP positive cells using Dynabeads (Dyna[®], Brown Deer, WI, U.S.A.) which interact with the CD8 protein being expressed extracellularly.

B. Mutagenesis of voltage-gated sodium channels

Site directed mutagenesis of Na_v1.7 was performed with the Na_v1.7-pcDNA 3.1 (-) vector by means of the QuikChange[®] II XL Site-Directed Mutagenesis Kit (Stratgene, La Jolla, CA, U.S.A.). Mutagenic primers containing the desired mutation were designed to anneal to the same sequence on opposite strands of the plasmid. The potential mutants were identified by restriction enzyme digestion and confirmed by DNA sequencing with appropriate primers near the mutated region of the plasmid. DNA sequencing was performed at the DNA Sequencing Core Facility in the Biochemistry Biotechnology Facility of

Indiana University (Indianapolis, IN, U.S.A.). Site directed mutagenesis of rat Na_v1.4 was previously performed (Wang and Wang, 1997; Nau et al., 1999) with the Na_v1.4-pcDNA1/amp vector using the Transformer Site-Directed Mutagenesis Kit (Clontech Inc., Palo Alto, CA, U.S.A.).

C. Transfection and preparation of stably transfected cell lines

Experiments investigating the effects of TFP on human Na_v1.7 and Na_v1.4 channels were done using stably transfected cell lines. To obtain these cell lines, human embryonic kidney cells (HEK293 cells; American Type Culture Collection; Manassas, VA, U.S.A.) were grown under standard tissue culture conditions (5% CO₂; 37 °C) in Dulbecco's Modified Eagle Medium (DMEM; Invitrogen, Grand Island, NY, U.S.A.) supplemented with 10% fetal bovine serum (FBS; Cellgro, Herndon, VA, U.S.A.) and 1% penicillin/streptomycin (Invitrogen, Grand Island, NY, U.S.A.). Transfections of Na_v1.4 and Na_v1.7 cDNA were performed using the calcium phosphate precipitation technique. No human β subunits were transfected with the channels as previous studies have shown β subunits do not alter the effect of CaM on sodium currents in HEK293 cells (Deschênes et al., 2002; Young and Caldwell, 2005). In addition, it has been demonstrated addition of human β₁ and human β₂ subunits had no effect on Na_v1.3 voltage-dependent properties in HEK293 cells (Cummins et al., 2001). For these experiments the calcium phosphate precipitation technique consisted of adding the following solutions together:

Solution 1

40 μ l 2X HEPES buffer

Solution 2

2.75—3 μ g channel cDNA (at 1 μ g/ μ l concentration)

5 μ l 2M CaCl₂

sterile water (bring volume to 40 μ l)

Solution 2 was added to Solution 1 dropwise and was gently mixed and bubbled using a 100 μ l pipettor. The calcium phosphate-DNA mixture was incubated at room temperature for 30 minutes after which time it was added to naïve HEK293 cells contained within serum-free DMEM on a 100 x 20 mm culture dish. After 15-20 hours of incubation at 37 °C, the cells were washed with fresh complete DMEM medium (10% FBS, 1% pen/strep). The Na_v1.7 and Na_v1.4 cDNA had been cloned in the pcDNA 3.1 (-) vector which contains the neomycin (G418) resistant gene for selection of stable cell lines using G418. Therefore, after 48 hours, antibiotic (G418, Geneticin[®]; Cellgro, Herndon, VA) was added to select for neomycin-resistant cells. After 2-3 weeks in G418, HEK293 cell colonies resistant to G418 grew and were picked, allowed to grow on 12 mm glass coverslips (Microscope Cover Glass; Fisherbrand[®], Pittsburgh, PA, U.S.A.) previously coated in laminin and subsequently tested for Na_v1.7 or Na_v1.4 channel expression using whole-cell patch-clamp recording techniques (discussed later). Cells producing more than 1 nA of sodium current were used for subsequent experiments.

D. Transient transfection of HEK293 cells

Transient transfections were used for all experiments excluding those investigating the effects of TFP on human Na_v1.7 and Na_v1.4 channels. For transient transfections, HEK293 cells were grown under standard tissue culture conditions (5% CO₂; 37 °C) in DMEM supplemented with 10% fetal bovine serum and 1% penicillin/streptomycin. Transfections of rat wild-type Na_v1.4, rat mutant Na_v1.4 (N434K, L1280K, F1579K), human wild-type Na_v1.7, and human mutant Na_v1.7 (N395K, F216S, I1461T, T1464I) were performed using the calcium phosphate precipitation technique explained above. However, for transient transfections, the calcium phosphate-DNA mixture was added to naïve HEK293 cells contained within DMEM supplemented with 5% fetal bovine serum and 1% penicillin/streptomycin on a 100 x 20 mm culture dish 1 minute after combining solution 1 and solution 2. The mixture was left on the cells in culture for 3-6 hr, after which time the cells were washed with fresh DMEM supplemented with 10% fetal bovine serum. For experiments involving transient transfections of wild-type, N395K, I1461T, and T1464I Na_v1.7 channels, human β1 and β2 subunits were cotransfected to enhance expression of the channel in HEK293 cells. When the human β1 and β2 subunits were included in the transfection, 0.4 µg of each subunit was included in Solution 2.

E. Chemicals

For application during voltage-clamp experiments, trifluoperazine (TFP, Sigma Aldrich Co., St. Louis, MO) was dissolved in sterile water to give stock solutions of 10 mM and 300 μ M, respectively. Calmodulin inhibitory peptide (CIP, EMD Biosciences, Inc., San Diego, CA) was dissolved in sterile water to give a stock solution of 240 μ M. Lidocaine hydrochloride (Sigma Aldrich Co.) was dissolved in standard bathing solution to give a stock solution of 100 mM. Subsequent dilutions were performed in standard bathing solution to give concentrations of (in mM): 0.1, 0.3, 1, 3, 10, and 30.

F. Solutions

1. *Standard bathing solution*

The standard bathing solution was used to bath cells during all voltage-clamp whole-cell electrophysiology experiments. The composition of the standard bathing solution was as follows (in mM): 140 NaCl, 1 MgCl₂, 3 KCl, 1 CaCl₂, and 10 HEPES, pH 7.3 (adjusted with NaOH). TFP was diluted in standard bathing solution before being externally applied to the stable HEK293 lines.

2. *Standard pipette solution*

The standard pipette solution was used in all experiments except for those involving the use of the CIP. The composition of the standard pipette solution was as follows (in mM): 140 CsF, 10 NaCl, 1.1 EGTA, and 10 HEPES, pH 7.3 with CsOH.

3. *Pipette solution used for the CIP experiments*

A different pipette solution was used when testing the effects of CIP on Na_v1.7 or Na_v1.4 channels. Since the effectiveness of CIP to inhibit calmodulin is based on intracellular Ca²⁺ levels, a more effective Ca²⁺ chelator, BAPTA, to better control the level of intracellular Ca²⁺ when looking at the effects of CIP on channel properties was used. The pipette solution used for the CIP experiments had the following composition (in mM): 90 CsF, 10 BAPTA, 10 NaCl, 10 HEPES, pH 7.3. CsOH was used to adjust pH for the pipette solutions. CIP was added to this solution when testing its effects on channel properties.

G. Whole Cell Patch-Clamp Recordings

Whole cell patch-clamp recordings were conducted at room temperature (~21 °C) using a HEKA EPC-10 double amplifier. Data were acquired on a Windows-based Pentium IV computer using the Pulse program (v 8.65, HEKA Electronic, Lambrecht/Pfalz, Germany). Fire-polished electrodes (0.9—1.3 MΩ)

were fabricated from 1.7 mm VMR Scientific (West Chester, PA, U.S.A.) capillary glass using a Sutter P-97 puller (Novato, CA, USA). For holding coverslips containing transfected HEK293 cells during whole cell patch-clamp recordings, lids from 35 mm cell culture dishes (Corning Inc.[®], Corning, NY, U.S.A.) were filled with silicone elastomer base (Sylgard[®], World Precision Instruments Inc., Sarasota, FL, U.S.A.), mixed with a curing agent, and allowed to solidify. After solidification, a scalpel was used to cut around a single 12 mm coverslip into the silicone creating a reservoir that could hold a coverslip and approximately 300 μ l of bath solution.

The recording dish containing transfected cells was mounted on an inverted Leitz Fluovert microscope equipped with a fluorescent light source and Hoffman modulated contrast objectives. The microscope was on a vibration isolation table with a 2 inch stainless steel laminate (63-500 Series, Technical Manufacturing Company, Peabody, MA, U.S.A.) to counter all negative effects of vibration on the experiments. All electrophysiological experiments were performed without the use of a Faraday cage. However, multiple wires were used to ground all metal surfaces having the potential to serve as an antenna for aberrant electrical noise. These wires converged at a single point on the air table from which a single wire was connected to the ground input of the amplifier.

Isolated cells for whole-cell electrophysiology were chosen by morphology and/or expression of EGFP. A fresh electrode back-filled with the appropriate intracellular solution was used each time a new electrophysiological experiment was started. Once filled with the appropriate intracellular solution, the recording

electrode had an approximate resistance of 1.0—1.2 M Ω . The EPC10 amplifier's offset potential was zeroed with the electrode almost touching the cell of interest. A silver chloride (AgCl) coated silver wire served as a reference electrode with one end connected to the ground input of the amplifier headstage and the AgCl coated end placed directly into the bath solution. The liquid junction potential for all solutions was not corrected for during these experiments and data analysis. After obtaining a cell membrane-glass interaction creating over 1 G Ω resistance, suction was used to establish the whole-cell recording configuration. Series resistance errors were compensated to be less than 3 mV and the capacitance artifact was canceled using computer-controlled circuitry of the patch-clamp amplifier. Linear leak subtraction, based on resistance estimates from four to five hyperpolarizing pulses applied before the depolarizing test potential, was used for all voltage-clamp recordings. Recordings were always started at least 3 min after establishing the whole-cell configuration. Membrane currents were filtered at 5 kHz and sampled at 20 kHz. Cells having a leak current of more than 10% of the peak sodium current were discarded and not used for analysis. Time-dependent shifts in current amplitude and voltage-dependence were calculated for all paired experiments. Specific voltage protocols are described within the Results section of this dissertation. When the perfusion system (described below) was not used, compounds were added to the bath compartment by first withdrawing 25 μ l of bathing solution, then adding 25 μ l of 10-fold concentrated compound and mixing 10-15 times with a 25 μ l pipettor.

1. Perfusion System

For obtaining lidocaine dose-response curves for inhibition of Na_v1.7 channel current in Figures 19 and 20, a SF-77B Perfusion Fast-Step system (Warner Instruments, LLC, Hamden, CT, U.S.A.) was used to deliver different concentrations of lidocaine focally onto the transfected HEK293 cell in whole cell configuration (Figure 3). During these experiments, coverslips containing transfected HEK293 cells were placed into a RC-26 Open Diamond Bath perfusion chamber (Warner Instruments, LLC, Hamden, CT, U.S.A.) with a small amount of Vaseline. This chamber allows a constant laminar flow of bath solution across the cells which was perfused at approximately 1 ml/min using gravity flow and removed using a Masterflex[®] C/L[®] Single Channel Variable-Speed peristaltic pump (Cole-Parmer Instrument Company, Vernon Hills, IL, U.S.A.). The perfusion system was constructed using various sizes of polyethylene tubing (Warner Instruments, LLC, Hamden, CT, U.S.A.). The drug delivery 3-barrel tube was placed near the transfected HEK293 cell, and its positioning was calibrated before each experiment. The position of the drug delivery tube was controlled manually by a stepper motor which could change the positioning in about 20 milliseconds. Concentrations of lidocaine were applied in random order and were allowed to interact with the cell 30 seconds prior to recording. All solutions were kept at room temperature (~21 °C). After experiments were completed for the day, all tubing was cleaned thoroughly with deionized water and, once a week, the tubing was cleaned with 70% ethanol.

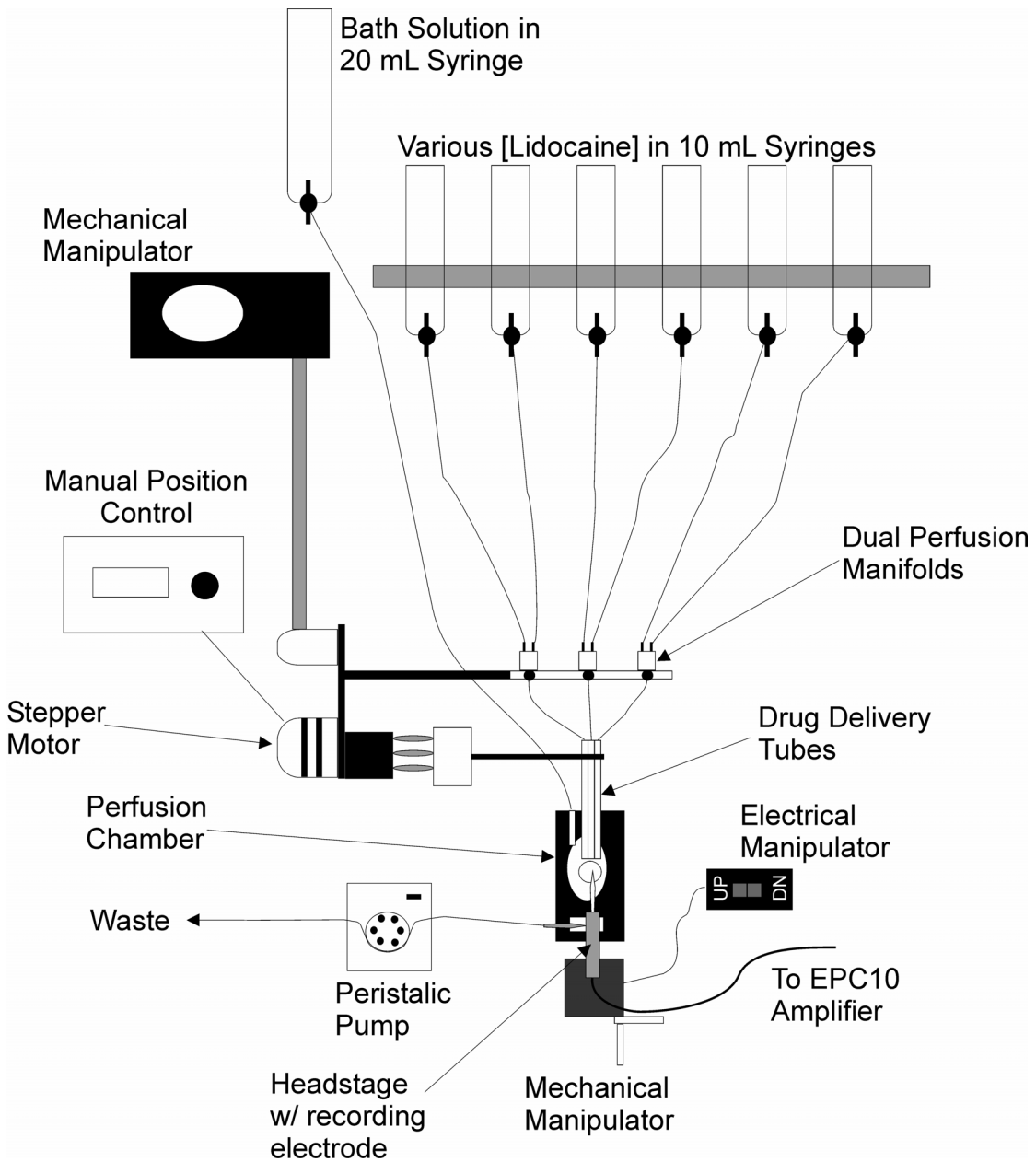


Figure 3. Schematic diagram of perfusion system used to obtain lidocaine dose response effects on $Na_v1.7$ channels.

H. Data Analysis

Voltage-clamp experimental data were analyzed using the Pulsefit (v 8.65, HEKA Electronic, Germany) and Origin (OriginLab Corp., Northampton, MA, U.S.A.) software programs. Slope factors of activation and steady-state inactivation curves were calculated using the general Boltzmann function:

$$I / I_{\max} = \left(\frac{1}{1 + e^{(V - V_{0.5})/k}} \right) \text{ where } I = \text{measured current, } I_{\max} = \text{maximum current, } V =$$

command voltage, $V_{0.5}$ = voltage at which the normalized current value is 0.5, and k = slope factor describing the steepness of the relationship. An offset value was added to the Boltzmann equation when fitting to some slow inactivation profiles to address incomplete inactivation. The equation used for the one-site binding curve and two-site binding curves for dose-inhibition relationship for lidocaine and the Na_v channels were as follows:

$$1) \text{ One-site binding curve: } v = \frac{[\text{Lidocaine}]_{\text{free}}}{[\text{Lidocaine}]_{\text{free}} + K_d}$$

$$2) \text{ Two-site binding curve: } v = \frac{[\text{Lidocaine}]_{\text{free}}}{[\text{Lidocaine}]_{\text{free}} + K_{d_1}} + \frac{[\text{Lidocaine}]_{\text{free}}}{[\text{Lidocaine}]_{\text{free}} + K_{d_2}}$$

Parameters for exponential fitting are presented in the Results section of the dissertation. The order (i.e. first-order, second-order) of exponential fit was chosen after an increase in the order of the fit produced an extra parameter that 1) was less than 5% of the total fit and 2) produced an estimated tau value outside the range of the fit. Goodness of fit was set at $R^2 > 0.90$ for all fits.

Results are presented as mean \pm S.E.M., and error bars in the figures represent SEs. Statistical significance was set at $p < 0.05$ for all experiments.

III. RESULTS

A. Inhibition of Na_v1.7 and Na_v1.4 sodium channels by trifluoperazine (TFP) involves the local anesthetic interaction site

1. *TFP decreases currents produced by Na_v1.7 and Na_v1.4 channels*

To determine if TFP could affect mammalian voltage-gated sodium currents, TFP was applied externally to HEK293 cells stably-transfected with human Na_v1.7 or human Na_v1.4 channels, and sodium currents were monitored using whole-cell voltage clamp techniques. Cells were held at -100 mV and pulsed to 0 mV every five seconds to elicit channel current. In the presence of 500 nM or 2 μM TFP, sodium currents rapidly declined and stabilized within 15 seconds and 25 seconds for Na_v1.7 and Na_v1.4, respectively (Figure 4, A and C). Although a small hyperpolarizing shift in the current-voltage relationship for Na_v1.7 and Na_v1.4 was observed following application of 2 μM TFP (Figure 4, B and D), these shifts were not significantly different from the time-dependent shifts observed in control cells. Na_v1.7 showed decreases in peak sodium currents of $19.4 \pm 6.0 \%$ (n = 6) and $76.7 \pm 4.6 \%$ (n = 6) after approximately 2.5 minutes during application of 500 nM and 2 μM TFP, respectively. Under the same conditions the same two concentrations of TFP produced decreases in peak Na_v1.4 currents of $14.7 \pm 7.3 \%$ (n = 6) and $59.4 \pm 7.8 \%$ (n = 5), respectively.

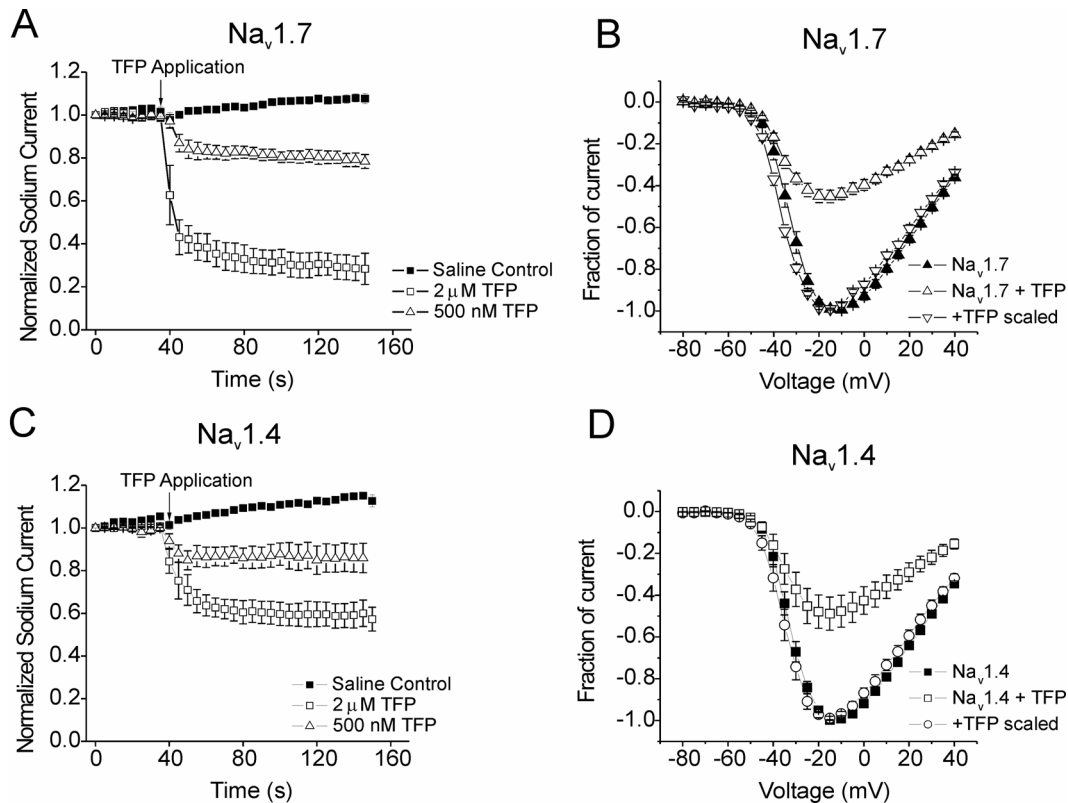


Figure 4. Inhibition of current produced from $\text{Na}_v1.7$ and $\text{Na}_v1.4$ channels by TFP. A and C, comparison of effects of two different TFP concentrations on currents produced by $\text{Na}_v1.7$ (A) and $\text{Na}_v1.4$ (C) channels. Saline controls represent the change in sodium current after application of cold external bath solution. The external bath solution was cold because TFP was kept cold in order to maintain its integrity. Drug or cold external bath solution was added to the external bath solution approximately 45 seconds into the protocol. B and D, effects of 2 μM TFP on the current-voltage relationship for $\text{Na}_v1.7$ (B) and $\text{Na}_v1.4$ (D) channels. The scaled group represents current values of the TFP treated channels normalized to the peak current of the control channels. Data is presented as mean normalized sodium current \pm S.E.M.

2. *TFP causes hyperpolarizing shifts in the voltage-dependence of Na_v1.7 and Na_v1.4 steady-state inactivation*

To understand how TFP reduces sodium current amplitude the effect of TFP on steady-state inactivation was investigated. Application of 500 nM and 2 μ M TFP to cells expressing Na_v1.7 caused hyperpolarizing shifts of -5.0 ± 0.87 mV ($n = 6$) and -18.4 ± 2.3 mV ($n = 6$) in the $V_{1/2}$ of steady-state inactivation, respectively (Figure 5, A and B), where $V_{1/2}$ was determined by fitting the data with the standard Boltzmann function as described in the Methods. The slope factor of the steady-state inactivation curve for Na_v1.7 in the absence of TFP was 6.6 ± 0.1 mV⁻¹. Following application of 500 nM and 2 μ M TFP the slope factors were 7.0 ± 0.3 mV⁻¹ and 10.2 ± 0.5 mV⁻¹, respectively. Application of the same two concentrations of TFP to cells containing Na_v1.4 caused hyperpolarizing shifts in the $V_{1/2}$ of steady-state inactivation of -5.0 ± 0.87 mV ($n = 5$) and -11.4 ± 0.80 mV ($n = 6$), respectively (Figure 5, D and E). The slope factor of the steady-state inactivation curve for Na_v1.4 in the absence of TFP was 6.0 ± 0.1 mV⁻¹. Following application of 500 nM and 2 μ M TFP the slope factors were 5.9 ± 0.1 mV⁻¹ and 6.6 ± 0.3 mV⁻¹, respectively. In control experiments (without TFP application) time-dependent shifts were observed in the $V_{1/2}$ of steady-state inactivation taken 7 minutes apart for Na_v1.7 channels (-2.6 ± 0.43 mV; $n = 6$) and Na_v1.4 channels (-4.7 ± 1.1 mV; $n = 5$). Thus, application of 500 nM TFP did not cause a significant hyperpolarizing shift in the $V_{1/2}$ of steady-state inactivation of Na_v1.7 or Na_v1.4 compared to the hyperpolarizing shift that was

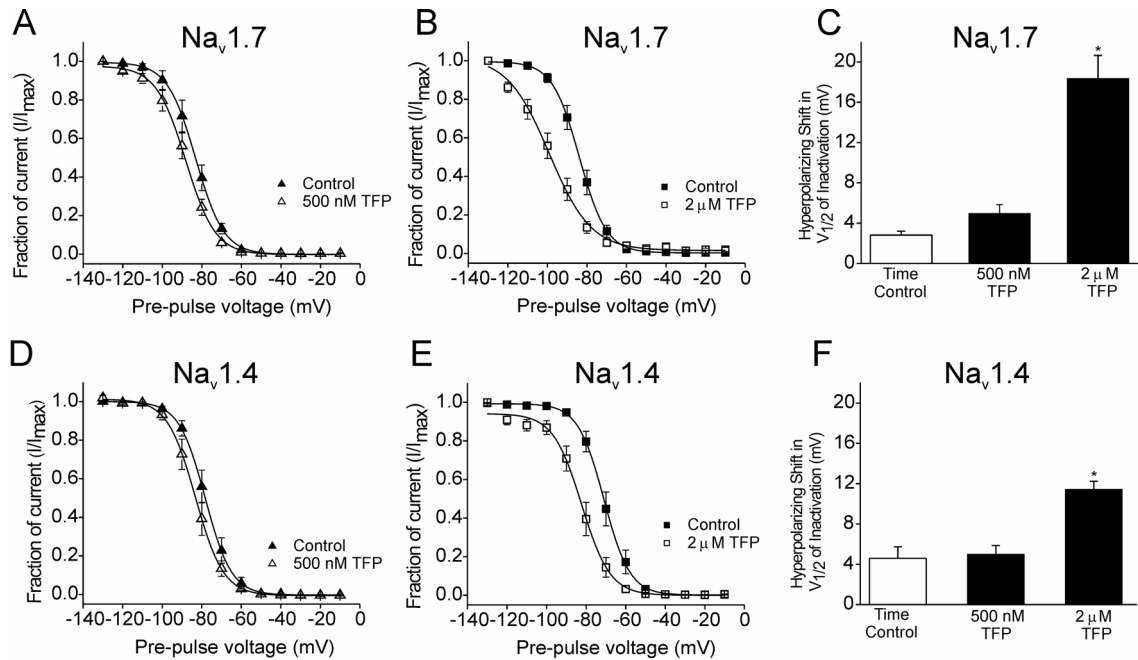


Figure 5. Shift in steady-state inactivation of $Na_v1.7$ and $Na_v1.4$ channels in the presence of TFP. Cells containing the channels were held at -100 mV and stepped to an inactivating pre-pulse (-130 to 40 mV) for 500 ms. The channels available after each inactivating pre-pulse were assessed by the peak current produced during a test pulse to -10 mV for 25 ms. A and B, 500 nM (A) and 2 μ M TFP(B) caused hyperpolarizing shifts in steady-state inactivation curves of $Na_v1.7$ channels. The average value of $V_{1/2}$ of inactivation for control conditions of $Na_v1.7$ channels was -83.9 ± 1.5 mV which was averaged from experiments in A and B. C, TFP and time caused hyperpolarizing shifts (mV) in $V_{1/2}$ of inactivation for $Na_v1.7$ channels. TFP (2 μ M) in the external bath solution was the only condition to cause a significant shift in $V_{1/2}$ of inactivation compared to the time-dependent control. D and E, 500 nM (D) and 2 μ M TFP (E) caused hyperpolarizing shifts in steady-state inactivation curves of $Na_v1.4$ channels. The average value of $V_{1/2}$ of inactivation under control conditions for $Na_v1.4$ channels was -74.8 ± 2.0 mV which was averaged from experiments in D and E. F, TFP and time also caused hyperpolarizing shifts (mV) in $V_{1/2}$ of inactivation for $Na_v1.7$ channels. Statistical significance was determined using a Student's paired t test (* = $p < 0.05$).

observed in these channels over the same period of time in control experiments. However, 2 μ M TFP did cause a significant hyperpolarizing shift in the $V_{1/2}$ of steady-state inactivation of $Na_v1.7$ channels and $Na_v1.4$ channels compared to time-dependent controls (Figure 5, C and F). Mechanistically, changes in slope factors caused by TFP cannot be readily explained.

3. TFP shows use-dependent inhibition of $Na_v1.7$ and $Na_v1.4$ during high frequency stimulation

The hyperpolarizing shifts of steady-state inactivation of both $Na_v1.7$ and $Na_v1.4$ by 2 μ M TFP indicates that TFP enhances sodium channel inactivation and led to the proposal that TFP might exhibit use-dependent inhibition of sodium channels. This was investigated by pulsing the transfected cells to -10 mV at a frequency of 5 Hz in the absence and presence of drug. Figure 6 (A and B) displays examples of results obtained under control conditions (left) and in the presence of 2 μ M TFP (right) for both $Na_v1.7$ and $Na_v1.4$. In the presence of 500 nM TFP, there were 67.6 ± 3.3 % ($n = 6$) and 54.1 ± 6.7 % ($n = 5$) decreases in the current amplitudes evoked by the first pulse to the current amplitudes evoked by the last pulse in the protocol for $Na_v1.7$ and $Na_v1.4$, respectively. In the presence of 2 μ M TFP, decreases of 73.8 ± 5.6 % ($n = 6$) and 80.4 ± 3.4 % ($n = 6$) were observed for $Na_v1.7$ and $Na_v1.4$, respectively. All decreases in peak current amplitudes were significant compared to time-dependent decreases in peak current amplitudes in the absence of drug (Figure 6, C and D).

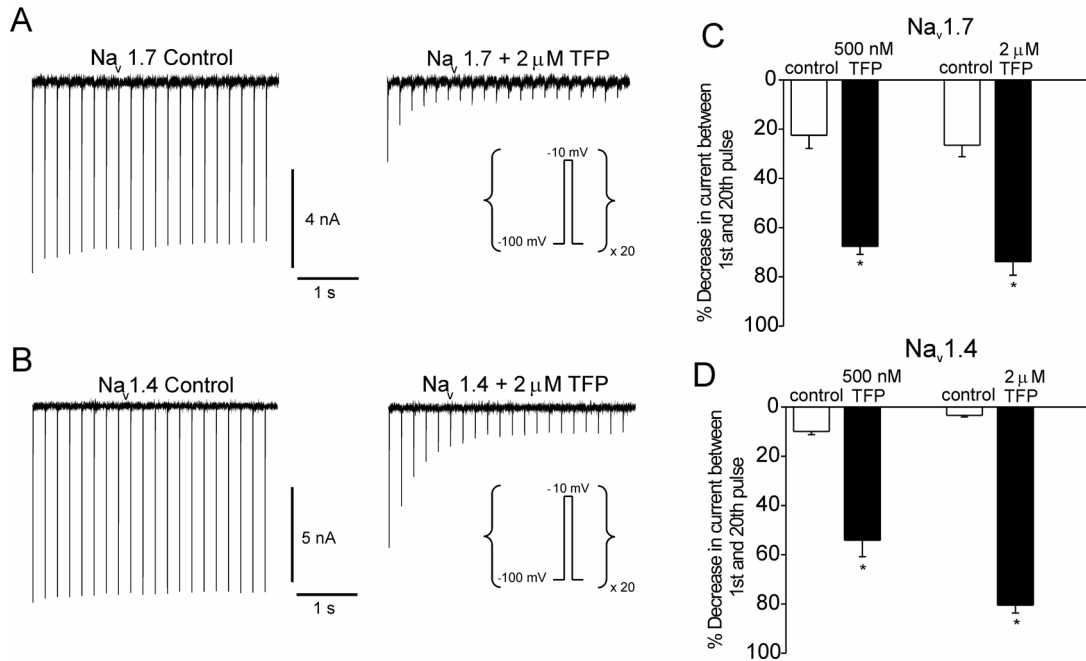


Figure 6. Use-dependent block of the Na_v1.7 channels and Na_v1.4 channels by TFP. High frequency stimulation consisted of pulses from a holding potential of -100 mV to -10 mV at a frequency of 5 Hz to evoke sodium currents. A (left), example of peak sodium currents produced by Na_v1.7 channels during high frequency stimulation under control conditions. A (right), peak currents from the same Na_v1.7 channels during high frequency stimulation in the presence of 2 μM TFP. B (left), example of peak sodium currents produced by Na_v1.4 channels during high frequency stimulation under control conditions. B (right), peak currents from the same Na_v1.4 channels during high frequency stimulation in the presence of 2 μM TFP. C and D, displays the decrease of peak sodium current produced by Na_v1.7 channels (C) and Na_v1.4 channels (D) from the first pulse to the last pulse of the high frequency stimulation protocol under control conditions compared to in the presence of drug. Data are presented as mean % decrease in current between the 1st and 20th pulse ± S.E.M. Statistical significance was determined using a Student's paired t test (* = p < 0.05).

4. *Steady-state inactivation is altered in Na_v1.7 but not Na_v1.4 in the presence of 1 μM calmodulin inhibitory peptide*

To determine if the mechanism by which TFP altered the currents conducted by Na_v1.7 and Na_v1.4 involved inhibition of the CaM-sodium channel interaction, currents were observed in the presence of a more specific CaM inhibitor. For these experiments a CaM inhibitory peptide, a 17-residue peptide based on the CaM-binding domain of myosin light chain kinase that binds to CaM with a K_d of 6 pM (Torok, et al., 1998) was used. The CaM inhibitory peptide is not cell permeable and had to be added directly to the pipette solution. Recordings were taken 12 minutes after obtaining whole-cell configuration to allow for adequate diffusion of the peptide into the cell. For control experiments, no peptide was added to the pipette solution.

Changes in steady-state inactivation of Na_v1.7 were observed in the presence of 1 μM CaM inhibitory peptide (Figure 7A). The mean V_{1/2} of steady-state inactivation of Na_v1.7 in the presence of 1 μM calmodulin inhibitory peptide was significantly hyperpolarized compared to without the peptide (Figure 7C). In contrast, steady-state inactivation of Na_v1.4 was unaffected by the presence of 1 μM calmodulin inhibitory peptide (Figure 7B). The mean V_{1/2} of inactivation of Na_v1.4 in the presence and absence of the peptide were not statistically different (Figure 7C). These results reveal specific inhibition of CaM had significant effects on Na_v1.7 steady-state inactivation while having no effect on Na_v1.4 steady-state inactivation.

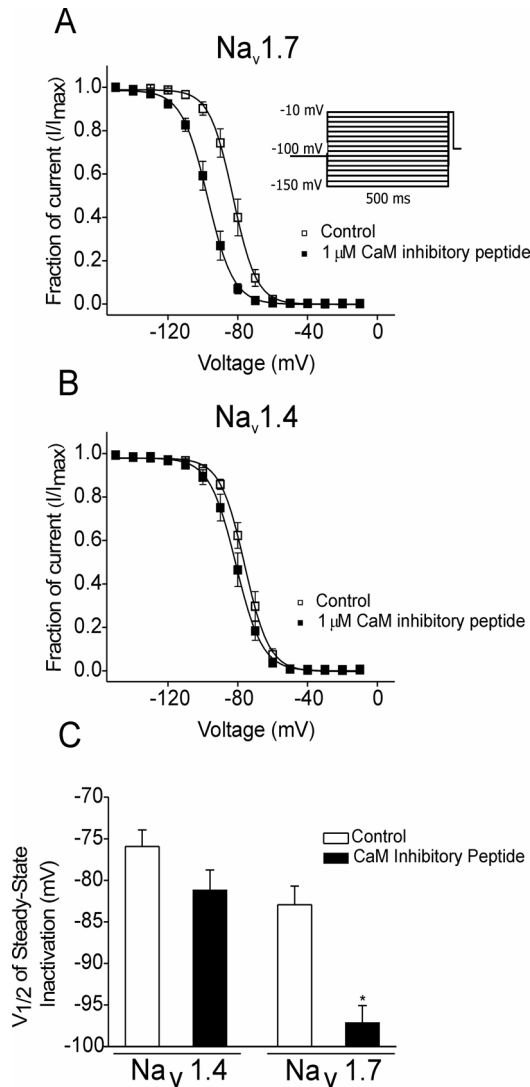


Figure 7. Calmodulin inhibitory peptide affects steady-state inactivation in Na_v1.7 channels but not Na_v1.4 channels. Cells containing the channels were held at -100 mV and stepped to an inactivating pre-pulse (-130 to 40 mV) for 200 ms. The channels that remain available after each inactivating pre-pulse were assessed by the peak current produced during a test pulse to -10 mV for 25 ms. A, Steady-state inactivation curves for Na_v1.7 current with (n = 5) and without (n = 5) 1 μ M calmodulin inhibitory peptide. B, Steady-state inactivation curves for Na_v1.4 current with (n = 3) and without (n = 3) 1 μ M calmodulin inhibitory peptide. C, 1 μ M calmodulin inhibitory peptide causes a significant hyperpolarizing shift in the $V_{1/2}$ of steady-state inactivation for the Na_v1.7 channel. 1 μ M calmodulin inhibitory peptide had no significant effects on the $V_{1/2}$ of steady-state inactivation for the Na_v1.4 channel. Statistical significance was determined using a Student's unpaired t test (* = p < 0.05).

5. *Calmodulin inhibitory peptide shows different effects on Na_v1.7 and Na_v1.4 during high frequency stimulation*

Calmodulin inhibitory peptide induction of use-dependent inhibition on voltage-gated sodium currents was also examined. Figure 8, A and B, displays examples of the protocol results in the presence of 1 μ M calmodulin inhibitory peptide for Na_v1.7 and Na_v1.4, respectively. In cells recorded with 1 μ M calmodulin inhibitory peptide added to the pipette solution the use-dependent decrease of Na_v1.4 current amplitudes was small (12.43 ± 1.69 %; n = 5), but significantly larger compared to the use-dependent decrease in cells recorded in pipette solution without the peptide (4.19 ± 0.19 %; n = 5, Figure 7C). Calmodulin inhibitory peptide (1 μ M) in the pipette solution induced a small but significant use-dependent effect on currents produced by Na_v1.7 stimulated at high frequency (Figure 8C). Na_v1.7 stimulated at high frequency with the pipette solution alone showed a 16.6 ± 5.1 % (n = 5) decrease in current. This decrease was significantly smaller than the 32.4 ± 4.3 % (n = 5) decrease in current seen with 1 μ M CaM inhibitory peptide in the pipette solution (Figure 8C). The use-dependent effects of the CaM inhibitory peptide on Na_v1.7 and Na_v1.4, although significant, were not as large as the effects seen with TFP. This result, in conjunction with the observation the calmodulin inhibitory peptide had no effect on Na_v1.4 steady-state inactivation, led to the hypothesis that the effects of TFP on these channels is the result of something other than blocking CaM-channel interactions.

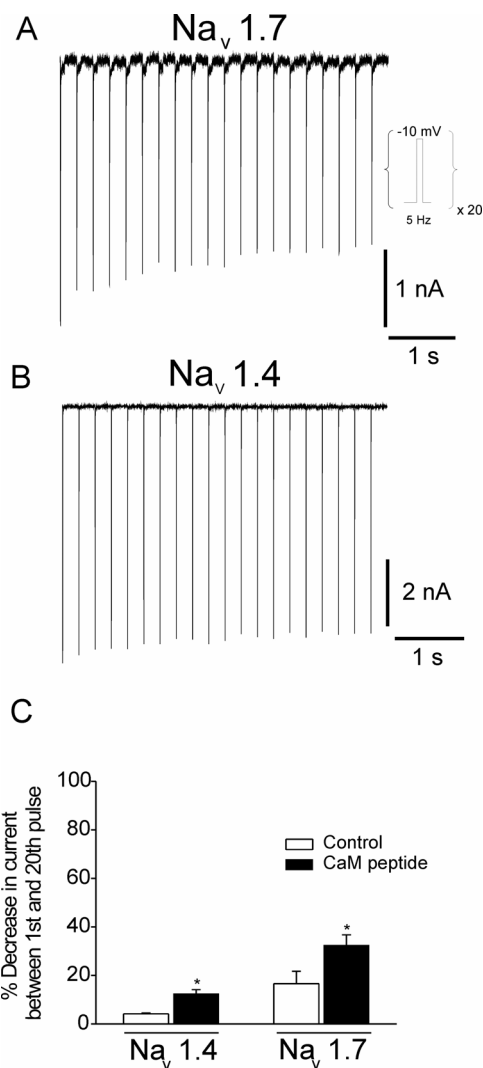


Figure. 8. Use-dependent block of Na_v1.7 and Na_v1.4 channels by calmodulin inhibitory peptide. High frequency stimulation followed the same protocol as shown in Figure 4. Since the calmodulin inhibitory peptide is not cell permeable it was added to the pipette solution. Control conditions represent pipette solution without the peptide. The high frequency stimulation protocol was performed 12 minutes after attaining whole-cell configuration. A, example of peak sodium currents produced by Na_v1.7 channels during high frequency stimulation in the presence of 1 μM calmodulin inhibitory peptide. B, example of peak sodium currents from Na_v1.4 channels during high frequency stimulation in the presence of 1 μM calmodulin inhibitory peptide. C, displays the decrease of peak sodium current produced by Na_v1.7 channels and Na_v1.4 channels from the first pulse to the last pulse of the high frequency stimulation protocol under control conditions compared to in the presence of the peptide. Data are presented as mean % decrease in current between the 1st and 20th pulse ± S.E.M. Statistical significance was determined using a Student's unpaired t-test. (* = p < 0.05).

6. *TFP has a higher affinity for inactivated sodium channels than for resting channels*

As local anesthetics (LA) exhibit use-dependent inhibition of sodium currents and induce a negative shift in the voltage-dependence of sodium channel steady-state inactivation, it was hypothesized TFP might be acting as a LA. According to the modulated receptor hypothesis of LA inhibition of sodium channels, the affinity of the LAs for sodium channels depends on the state of the channel, with inactivated channels exhibiting much higher affinities than resting channels. Therefore the ability of 2 μM TFP to block $\text{Na}_v1.7$ and $\text{Na}_v1.4$ channels in the resting state was tested using a holding potential of -140 mV. Current was elicited with a pulse to 0 mV every 5 s and TFP caused an $8.3 \pm 0.5\%$ ($n = 10$) and $8.4 \pm 1.1\%$ ($n = 10$) decrease in $\text{Na}_v1.7$ and $\text{Na}_v1.4$ current, respectively. This indicates that block of resting channels by TFP is similar for $\text{Na}_v1.7$ and $\text{Na}_v1.4$, with an estimated IC_{50} of $\sim 22 \mu\text{M}$. To examine TFP effects on inactivated channels, cells were held at -120 mV and pre-pulsed to -60 mV for 10 seconds, pulsed to -120 mV for 50 ms to allow for recovery from fast inactivation, and then pulsed to 0 mV to elicit current. With this protocol, TFP caused an $85.6 \pm 2.1\%$ ($n = 5$) and $87.4 \pm 8.2\%$ ($n = 5$) decrease in $\text{Na}_v1.7$ and $\text{Na}_v1.4$ current, respectively. This indicates block of inactivated channels by TFP is also similar for $\text{Na}_v1.7$ and $\text{Na}_v1.4$, with an estimated IC_{50} of $\sim 300 \text{ nM}$. These data suggest that, like LA inhibition, TFP inhibition is dependent on the configuration or state of VGSCs (i.e. state-dependent). Therefore, the disparity in block of $\text{Na}_v1.7$ and $\text{Na}_v1.4$ currents by 2 μM TFP observed in Figure 4 can be explained by

differences in steady-state availability rather than differences in channel affinities for TFP.

7. TFP increases the onset of inhibition and slows recovery from inhibition for Na_v1.7 and Na_v1.4

The effect of TFP on Na_v1.7 and Na_v1.4 currents was further investigated by examining the time course for onset of inhibition and recovery from inhibition for Na_v1.7 and Na_v1.4 currents. Figure 9A (top) displays the protocol used to examine the onset of TFP inhibition for Na_v1.7 and Na_v1.4 currents. In the absence of TFP, this protocol will display the onset of slow inactivation for Na_v1.7 and Na_v1.4. The onset of inhibition for Na_v1.7 and Na_v1.4 currents by 2 μM TFP was rapid compared to the development of slow inactivation observed under control conditions (Figure 9A bottom). The time constants for the inhibition of Na_v1.7 and Na_v1.4 currents by 2 μM TFP were 49.1 ± 3.9 ms (n = 13) and 62.6 ± 6.0 ms (n = 14), respectively and were not significantly different. The onset of Na_v1.7 and Na_v1.4 current inhibition by 500 nM TFP was significantly slower than that observed with 2 μM TFP giving time constants of 148 ± 24 ms (n = 5) and 139 ± 26 ms (n = 5), respectively. Figure 9B displays the protocol used to examine the recovery from TFP inhibition for Na_v1.7 and Na_v1.4 currents. TFP was present during this protocol; no washout was used. The recovery of Na_v1.7 currents from inhibition by 500 nM and 2 μM TFP (Figure 9C, top) had

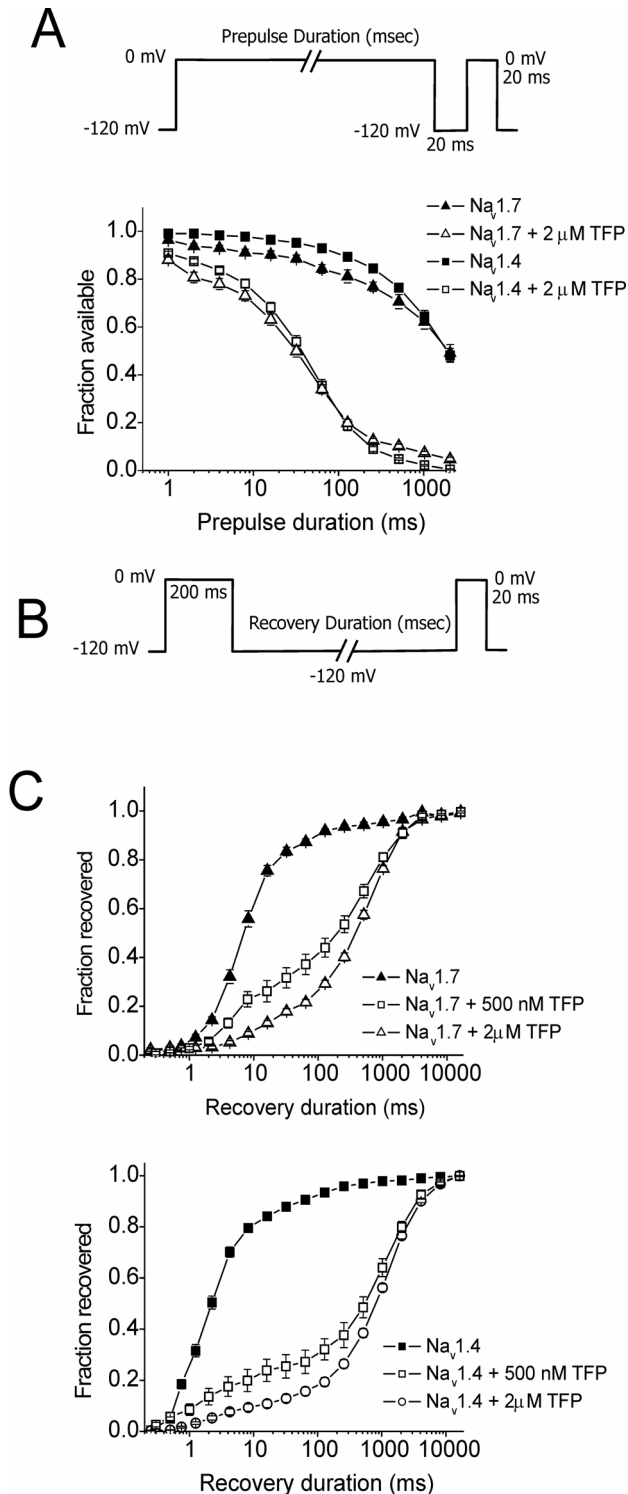


Figure 9. Onset of TFP inhibition and recovery from TFP inhibition for Na_v1.7 and Na_v1.4 channels. A (top), protocol for examining onset of TFP-induced Na_v1.7 and Na_v1.4 channel inhibition. A (bottom), onset of 2 μM TFP inhibition for Na_v1.7 and Na_v1.4 channels. Decrease in Na_v1.7 and Na_v1.4 current under control conditions is likely due to slow-inactivation. B, protocol for examining recovery from TFP-induced Na_v1.7 and Na_v1.4 channel inhibition. C (top), recovery from 500 nM and 2 μM TFP inhibition for Na_v1.7 channels. C (bottom), recovery from 500 nM and 2 μM TFP inhibition for Na_v1.4 channels.

time constants of 572 ± 36 ms ($n = 6$) and 686 ± 43 ms ($n = 9$), respectively. The recovery of $\text{Na}_v1.4$ currents from inhibition by 500 nM and 2 μM TFP (Figure 9C, bottom) was slower with time constants of 1.0 ± 0.1 s ($n = 5$) and 1.2 ± 0.06 s ($n = 10$), respectively. TFP concentration did not have a significant effect on the time constants of recovery for either $\text{Na}_v1.7$ or $\text{Na}_v1.4$. This is consistent with the interaction seen between LAs and sodium channels in which drug unbinding rate was unrelated to drug concentration, indicating a simple bimolecular reaction of drug and channel (Bean et al., 1983).

8. TFP showed attenuated effects on LA binding site mutations N434K and F1579K, but not L1280K

To confirm that TFP was acting as a LA on $\text{Na}_v1.7$ or $\text{Na}_v1.4$, the effects of TFP were tested on $\text{Na}_v1.4$ channels that have mutations in their LA binding site. LAs can directly bind to voltage-gated sodium channels and block the propagation of action potentials. Previous studies have shown that point mutations of residues located in the S6 transmembrane segments of domain 1 (DI), domain 3 (DIII), and domain 4 (DIV) of voltage-gated sodium channels can reduce high affinity binding of LAs to the inactivated state of the channel (Ragsdale, et al., 1994; Wright, et al., 1998; Li, et al., 1999; Nau, et al., 1999; Nau, et al., 2003). Furthermore, it has been shown that the tricyclic antidepressant amitriptyline, which blocks voltage-gated sodium channels with a high degree of use-dependent block under repetitive pulses, also interacts with the LA binding site on sodium channels (Barber, et al., 1991; Nau, et al., 2000).

Three specific S6 residues located at DI, DIII, and DIV have been characterized as crucial for both LAs and amitriptyline binding in rat skeletal muscle ($\text{Na}_v1.4$) sodium channels (Wang, et al., 2004). Lysine and arginine substitutions at residues N434 (DI-S6), L1280 (DIII-S6), and F1579 (DIV-S6) reduced the affinity for both amitriptyline and LA binding to the inactivated state of the channel (Wang, et al., 2004; Nau and Wang, 2004). In order to determine if TFP was acting through a possible LA mechanism, TFP was applied to rat $\text{Na}_v1.4$ channels having one of three amino acid substitutions (N434K, L1280K, F1579K) and the effectiveness of TFP inhibition was examined.

Since these LA binding-site mutations were performed with rat $\text{Na}_v1.4$, and the data shown in Figures 4-6 used human $\text{Na}_v1.4$, the control conditions involved application of TFP to wild-type rat $\text{Na}_v1.4$. Rat and human $\text{Na}_v1.4$ channels are highly conserved, and completely conserved in the CaM and LA binding site regions. Figure 10A displays the effects of application of 2 μM TFP to the external bath solution on sodium currents from the wild-type rat $\text{Na}_v1.4$ and the LA binding site mutant channels. The addition of 2 μM TFP to wild-type rat $\text{Na}_v1.4$ caused a decrease in peak sodium current of $83.7 \pm 2.6 \%$ ($n = 6$; Figure 10B). Two of the LA binding site mutant channels, N434K and F1579K, showed a significant attenuation in the decrease of peak sodium current caused by 2 μM TFP to $12.5 \pm 1.8 \%$ ($n = 5$) and $7.01 \pm 3.2 \%$ ($n = 5$), respectively. In contrast, the L1280K mutant channel showed a decrease of $80.3 \pm 3.1 \%$ ($n = 5$) in peak

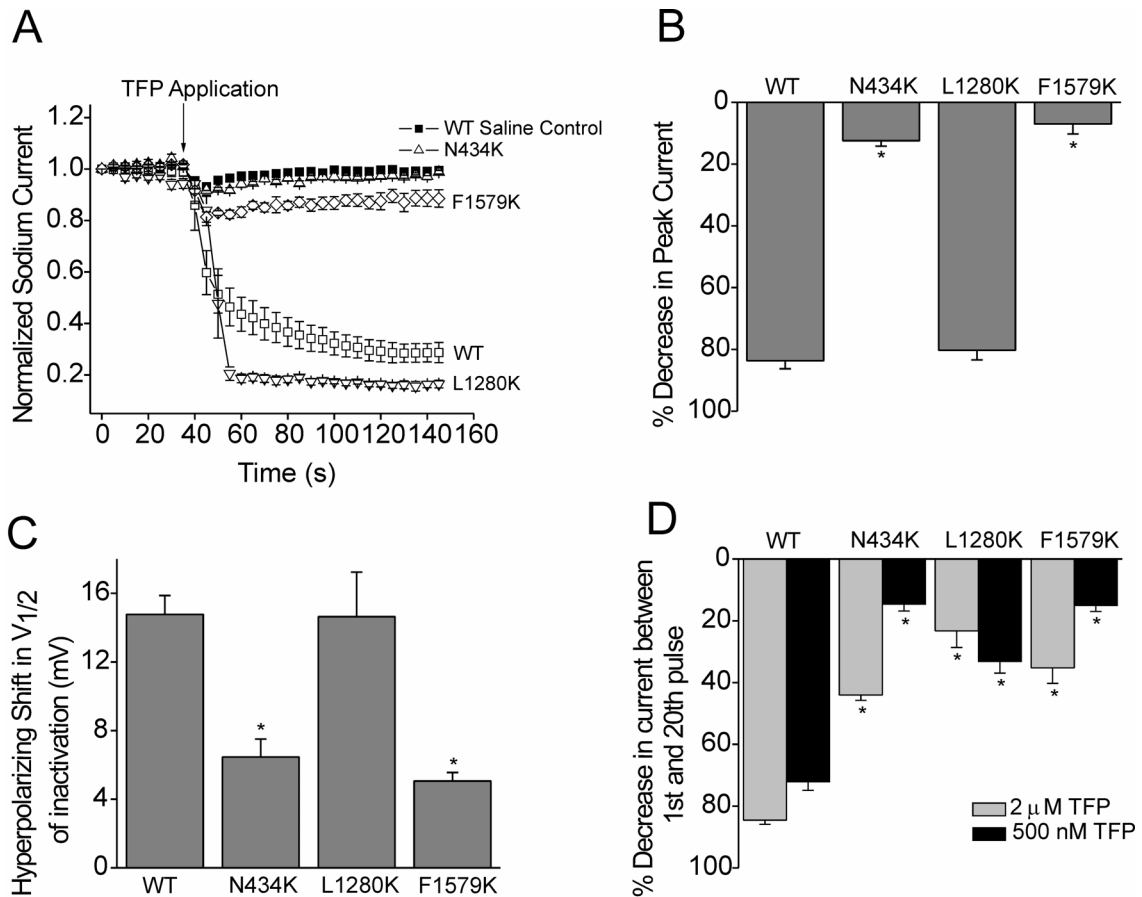


Figure 10. Effects of TFP on current produced from rat $Na_v1.4$ channels and rat channels containing the mutations, N434K, L1280K, or F1579K in the LA binding site. The protocols for A and B are described in the Figure 4 legend. A, 2 μ M TFP caused decreases in current produced by the all channels having a reduced effect on the N434K and F1579K channels. B, comparison of effects of 2 μ M TFP on the rat $Na_v1.4$ channels and rat LA mutant channels shows that the LA mutant channels, N434K and F1579K, displayed a significant reduction in % decrease of peak current. The protocol for C is described in the Figure 5 legend. C, shift in steady-state inactivation of rat $Na_v1.4$ channels and rat LA mutant $Na_v1.4$ channels, N434K, L1280K, F1579K in the presence of TFP. D, use-dependent block of the rat $Na_v1.4$ channels and rat LA mutant $Na_v1.4$ channels, N434K, L1280K, F1579K in the presence of 500 nM or 2 μ M TFP. High frequency stimulation followed the same protocol as shown in Figure 4. Statistical significance was determined using a one-way ANOVA analysis followed with a Tukey's comparison test (* = $p < 0.05$). Statistical comparisons were made against WT values.

sodium current which was not significantly different from the decrease observed with the wild-type channel (Figure 10B). As seen with human Na_v1.7 and Na_v1.4, TFP caused a significant hyperpolarizing shift in the $V_{1/2}$ of steady-state inactivation of rat Na_v1.4. Application of 2 μ M TFP to rat Na_v1.4 caused a hyperpolarizing shift of -14.8 ± 1.1 mV ($n = 6$; Figure 10C). The N434K and F1579K mutant channels showed significantly smaller hyperpolarizing shifts in $V_{1/2}$ of steady-state inactivation in the presence of 2 μ M TFP, having only shifts of -6.5 ± 1.1 mV ($n = 5$) and -5.0 ± 0.5 mV ($n = 5$), respectively (Figure 10C). The L1280K mutant channel in the presence of 2 μ M TFP exhibited a hyperpolarizing shift of -14.6 ± 2.6 mV ($n = 5$; Figure 10C), which was not significantly different than that seen with the wild-type channel.

Use-dependent effects of TFP were also studied with the rat Na_v1.4 as well as with the LA binding-site mutant channels by using the same 5 Hz pulse protocol that was used with the human Na_v1.7 and Na_v1.4. Current evoked by the last pulse of the protocol was $84.6 \pm 1.3\%$ ($n = 11$) less than current evoked by the first pulse of the protocol for the wild-type rat Na_v1.4 in the presence of 2 μ M TFP (Figure 10D). All three mutant channels showed significantly attenuated use-dependent decreases in current produced by high frequency stimulation in the presence of 2 μ M TFP compared to the wild-type rat Na_v1.4 channel (Figure 10D). The decreases observed in the presence of 2 μ M TFP were $44.1 \pm 1.7\%$ ($n = 5$), $23.3 \pm 5.4\%$ ($n = 5$), and $35.2 \pm 5.0\%$ ($n = 6$) for LA binding-site mutant channels N434K, L1280K, and F1579K, respectively (Figure 10D). However, the attenuated use-dependent decrease observed for the L1280K channel might not

accurately reflect a decreased sensitivity of the channel to use-dependent inhibition brought on by TFP because 2 μ M TFP decreased the steady-state L1280K current to the point at which additional use-dependent inhibition was difficult to determine. Therefore we also examined current produced from the LA binding-site mutant channels and the wild-type channel after high frequency stimulation (5 Hz) in the presence of 500 nM TFP in an attempt to limit the initial effects on the L1280K channel. Results show that 500 nM TFP produced a use-dependent decrease of $72.1 \pm 2.7\%$ ($n = 8$) in current evoked by the last pulse of the protocol compared to current evoked by the first pulse of the protocol for the wild-type rat $\text{Na}_v1.4$ channel. The decreases observed for channels containing mutations N434K, L1280K, or F1579K in the LA binding site were $14.7 \pm 2.2\%$ ($n = 6$), $33.2 \pm 3.8\%$ ($n = 6$), and $15.1 \pm 1.9\%$ ($n = 8$), respectively. All of these observed use-dependent decreases were significantly attenuated compared to the use-dependent decreases seen with the wild-type rat $\text{Na}_v1.4$ channel.

Interestingly, the steady-state inactivation curves for each of the local anesthetic binding site mutant channels, in the absence of TFP, show that the N434K and F1579K mutations shifted steady-state inactivation of the channel in the depolarizing direction while the L1280K mutation shifted it in the hyperpolarizing direction compared to the wild-type channel (Figure 11). Therefore with a holding potential of -100 mV, more of the L1280K channels are in the inactivated state than the N434K or F1579K channels and this raises the

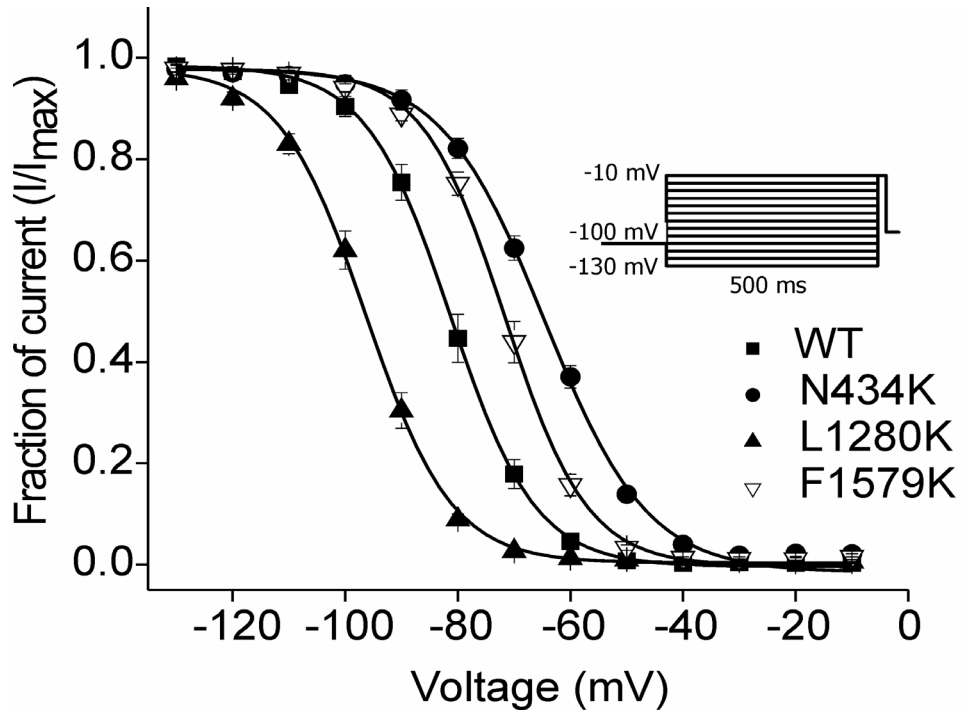


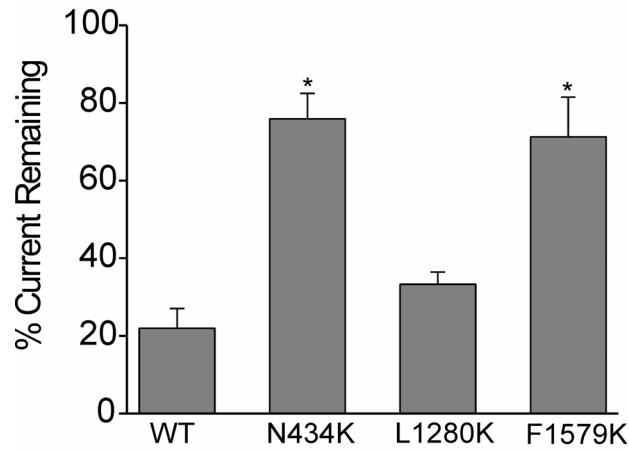
Figure. 11. Steady-state inactivation curves of rat wild-type channels (n = 11) and rat channels having the mutations N434K (n = 10), L1280K (n = 9), or F1579K (n = 10) in the LA binding site.

possibility that the differential effect of TFP on the mutant channels could be influenced by the differential shifts in steady-state inactivation and may not reflect differences in state-dependent binding. To address this, protocols designed to examine TFP interaction with either the inactivated or closed state of the channels were used. To examine TFP binding to the inactivated state of the channels, cells were held at -120 mV and pre-pulsed to -60 mV (wild-type, L1280K and F1579K channels) or -40 mV (N434K channels) for 10 seconds, pulsed to -120 mV for 100 ms to allow for recovery from fast inactivation, and then pulsed to 0 mV to elicit current. The steady-state inactivation curve for N434K and F1579K show a considerable amount of current available at -60 mV (~ 35—45%) compared to WT channels (Figure 11) and therefore to ensure that the mutant channels were inactivated to the same extent as WT channels, the cells expressing N434K and F1579K channels were pre-pulsed to -40 mV and -50 mV, respectively, instead of -60 mV. At -40 mV 96% of the N434K channels are inactivated, which is similar to the 97% of F1579K channels inactivated at -50 mV and 95% of WT channels inactivated at -60 mV. An initial current was measured in the absence of drug and a second current was measured in the presence of 500 nM TFP. After application of 500 nM TFP, only $21.9 \pm 5.1\%$ ($n = 8$) of the rat wild-type $\text{Na}_v1.4$ current remained (Figure 12A). The percentage of currents remaining for LA mutant channels N434K, L1280K, and F1579K after 500 nM TFP application were $75.9 \pm 6.6\%$ ($n = 6$), $33.3 \pm 3.2\%$ ($n = 6$), and $71.3 \pm 10.3\%$ ($n = 6$), respectively (Figure 12A). The percentage of remaining current was used to estimate the IC_{50} for TFP by using the equation: (% remaining

current)/((1-% remaining current) x [TFP]). The estimated IC_{50} of TFP for the inactivated state of the rat wild-type $Na_v1.4$ channel is approximately 140 nM. The estimated IC_{50} 's for TFP on the inactivated state of the N434K, L1280K, and F1579K channels are approximately 1.6 μ M, 250 nM, and 1.2 μ M, respectively. Although all mutant channels had more peak current remaining compared to the peak current remaining in the wild-type rat $Na_v1.4$, only the LA binding-site mutant channels N434K and F1579K showed a significance difference from the wild-type channel.

To examine TFP binding to the closed state of the channels, cells were pulsed to -140 mV for 10 seconds before pulsing to 0 mV to elicit a current. We were not able to see any significant changes in the percentage of remaining current from control conditions after application of 500 nM TFP. Therefore, we increased the concentration of TFP to 2 μ M to see if we could observe differences in inhibition of channels in the closed state. After application of 2 μ M TFP the wild-type rat $Na_v1.4$ had $93.0 \pm 4.5\%$ ($n = 8$) channel current remaining (Figure 12B) and, based on this data, the estimated IC_{50} of TFP for the closed state of the rat wild-type $Na_v1.4$ is approximately 27 μ M. LA mutant channels N434K and F1579K after 2 μ M TFP application had $103.9 \pm 2.5\%$ ($n = 6$) and $97.4 \pm 3.8\%$ ($n = 8$) of their current remaining, respectively, and these effects were not significantly different than those seen with the wild-type rat $Na_v1.4$ (Figure 12B). The L1280K mutant channel, however, showed a significant decrease in percent of remaining current in the presence of 2 μ M TFP, with only $41.6 \pm 3.3\%$ ($n = 5$) remaining (Figure 12B). The estimated IC_{50} 's for TFP on the

A Inactivated (500 nM TFP)



B Closed (2 μ M TFP)

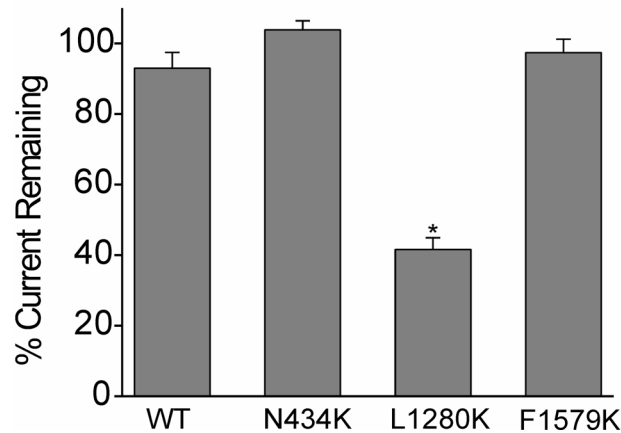


Figure 12. State-dependent inhibitory effects of 500 nM TFP on the rat $\text{Na}_v1.4$ wild-type channel and rat channels having the mutations N434K, L1280K, or F1579K in the LA binding site. A, percentage of control current remaining after application of 500 nM TFP to rat wild-type and LA mutant channels in their inactivated state. For the N434K channel, the pre-pulse voltage was -40 mV to ensure inactivation of the channels. B, Percentage of control current remaining after application of 2 μ M TFP to rat wild-type and LA mutant channels in their closed state. Statistical significance was determined using one-way ANOVA analysis followed with a Tukey's comparison test (* = $p < 0.05$). Statistical comparisons were made against WT values.

closed state of L1280K and F1579K channels are approximately 1.0 μM and 75 μM , respectively. The IC_{50} for TFP on the closed state of the N434K mutant channel could not be estimated due to the amount of current remaining after TFP treatment being over 100%. However, it is probable that the IC_{50} value is greater than 75 μM . Thus while the N434K and F1579K mutations reduced the apparent affinity of inactivated $\text{Na}_v1.4$ for TFP, the L1280K mutation increased the apparent affinity of $\text{Na}_v1.4$ in the closed state for TFP. To further investigate the possibility that these lysine substitutions directly affect TFP interaction rather than indirectly attenuating TFP inhibition by altering the inactivation of the untreated channel, the effects of TFP on the development of channel inhibition as well as on recovery from inhibition were examined. Surprisingly, the N434K channels showed an enhanced ($\sim 2.5 \times$) development of inhibition by 2 μM TFP compared to WT channels while the F1579K channels showed a slower ($\sim 12 \times$) development of inhibition by 2 μM TFP (Table 1). Based on the rates of channel inhibition by TFP observed for WT and N434K channels, inactivating pre-pulses used for examining recovery from channel inhibition by TFP were set at 200 ms. However, based on the rate of channel inhibition, a 200 ms pre-pulse would not be long enough to allow for adequate drug-binding to F1579K channels, and therefore a 500 ms inactivating pre-pulse was used for examining recovery of F1579K from inhibition by TFP. Table 1 shows the N434K and F1579K channels recover from 2 μM TFP inhibition approximately 4.5 and 3 times faster than do WT channels, respectively. These results indicate while the N434K enhances the onset of TFP interaction with inactivated $\text{Na}_v1.4$, the F1579K mutation

Table 1. Time constants for onset of TFP inhibition and recovery from TFP inhibition for WT, N434K, and F1579K channels.

Channel	2 μ M TFP	
	Recovery tau (ms)	Development tau (ms)
WT	1530 \pm 170	51 \pm 5
N434K	347 \pm 12*	20 \pm 2†
F1579K	502 \pm 13*	655 \pm 53†

Values are means \pm S.E.M. Data was examined using a one-way ANOVA. * value is significantly ($p < 0.05$) different from WT recovery tau. † Value is significantly ($p < 0.05$) different from WT development tau.

attenuates the onset of TFP interaction with the channel, and both mutations accelerate TFP unbinding from the inactivated Na_v1.4. These results strengthen the evidence that the differential effect of TFP on the mutant channels are due to differences in direct binding of the drug to the channel.

B. A channel mutation associated with primary hereditary erythromelalgia (N395K) alters electrophysiological properties of Na_v1.7 in addition to decreasing channel sensitivity to the local anesthetic lidocaine

1. The N395K mutation alters electrophysiological properties of Na_v1.7

The above results show a lysine substitution at the N434 residue (N434K) in the rat Na_v1.4 sodium channel reduces TFP inhibition of the channel. This same mutation causes decreased local anesthetic block of Na_v1.4 (Nau et al., 1999). One hereditary erythromelalgia mutation that has been associated with a severe phenotype is the N395K Nav1.7 mutation (Drenth et al., 2005), located in the S6 segment of domain I. This residue corresponds to the N434 residue in rat and human Na_v1.4 channels. Therefore, it was predicted that the N395K mutation in Na_v1.7 alters interaction of local anesthetics with the channel. Wild-type (WT) hNa_v1.7 or the mutant derivative channel N395K were transiently expressed with hβ-1 and hβ-2 subunits in HEK293 cells. An initial comparison of current traces from both channels did not suggest any major differences in channel kinetics (Figure 13, A and B). The voltage-dependence of activation was measured for each channel using a series of depolarizing test pulses from -100

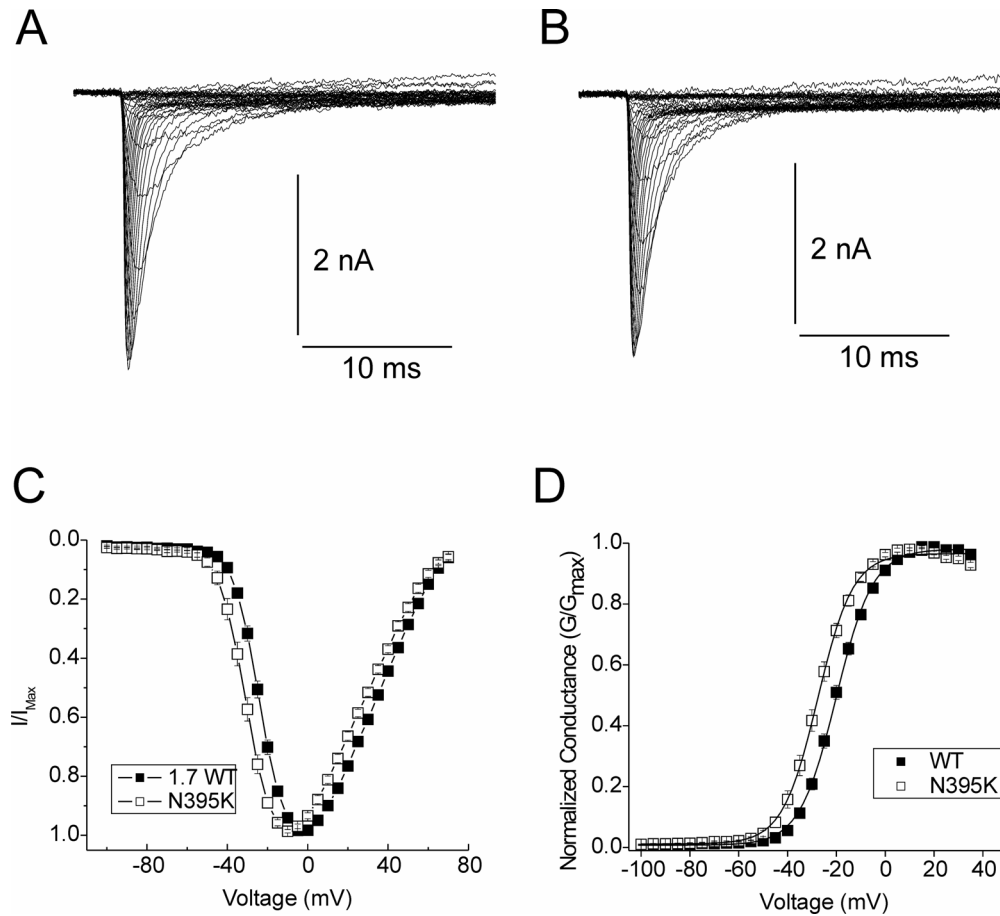


Figure 13. Comparison of the activation properties between the WT and N395K $\text{Na}_v1.7$ channels. A and B, representative current-voltage (IV) traces for HEK293 cells transfected with WT (A) or N395K (B) channels. Both channels were coexpressed with the human β_1 and β_2 subunits. C and D, the IV relationship (C) and steady-state conductance curve (D) for N395K was hyperpolarized compared to WT. Conductance was calculated using the equation $g = \frac{I}{(V - E_{\text{Na}})}$ where g = conductance, I = measured current, V = command voltage, and E_{Na} = estimated reversal potential for Na^+ ions.

to +70 mV. N395K channels exhibited a hyperpolarized current-voltage (IV) and conductance-voltage (GV) curve compared to wild-type channels (Figure 13, C and D). The midpoint of activation (estimated using a Boltzmann function) was significantly ($p < 0.05$) more negative (-28.0 ± 1.1 mV; slope: 6.7 ± 0.1 mV⁻¹; $n = 18$) for N395K channels than for WT channels (-20.3 ± 0.8 mV; slope: 7.27 ± 0.1 mV⁻¹; $n = 19$; Student's unpaired t-test). The voltage-dependence of steady-state fast inactivation was also evaluated for each channel using the protocol shown in Figure 14A and, in contrast to activation, did not differ between the WT and mutant channels (Figure 14, B and C). The midpoint of steady-state fast inactivation for the WT channels (-71.3 ± 0.8 mV; slope: 6.79 ± 0.2 mV⁻¹; $n = 19$) was not significantly different ($p = 0.76$) from that of the N395K channels (-70.9 ± 1.1 mV; slope: 6.14 ± 0.1 mV⁻¹; $n = 18$; Student's t-test).

Next, effects of the N395K mutation in Na_v1.7 on steady-state slow inactivation were examined. Mutations impairing steady-state slow inactivation in voltage-gated sodium channels have been implicated in hyperkalemic periodic paralysis, hereditary erythromelalgia, and epilepsy (Cummins & Sigworth, 1996; Bendahhou et al., 1999; Bendahhou et al., 2002; Rhodes et al., 2005; Cummins et al., 2004). It has further been shown that mutations in residues corresponding to N395 in the skeletal muscle Na_v1.4 channel (N434) and the brain Na_v1.2 channel (N418) alter slow inactivation (Wang & Wang, 1997; Nau et al., 1999; Chen et al., 2006). Figure 14D shows that steady-state slow inactivation was tested by holding the cells at -120 mV and stepping to an inactivating pre-pulse (ranging from -130 to 10 mV) for 30 s. This was followed by a 100 ms pulse to

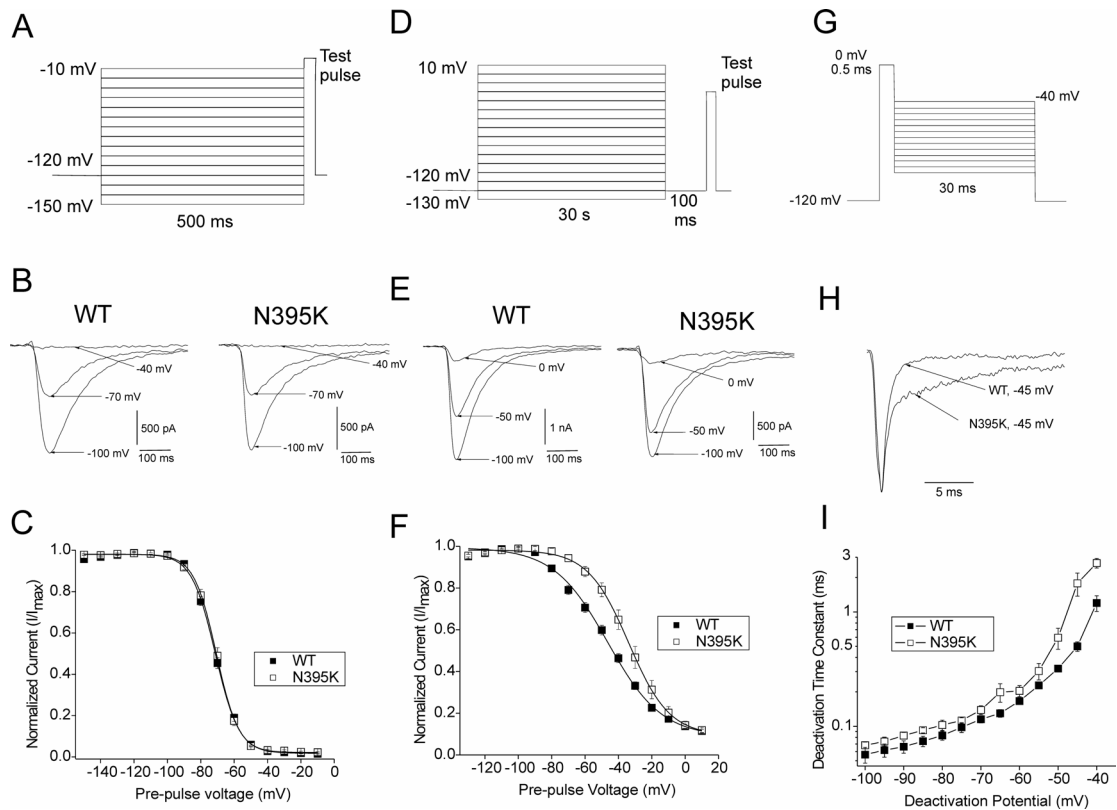


Figure 14. Comparison of electrophysiological properties between the WT and N395K $Na_v1.7$ channels. A, Protocol used to examine steady-state fast inactivation. B, Representative traces of WT and N395K currents produced after pulsing to the indicated voltage for 500 ms. C, The steady-state fast inactivation curves for WT and N395K channels were not significantly different. D, Protocol used to examine steady-state slow inactivation. E, Representative traces of WT and N395K currents produced after pulsing to the indicated voltage for 30 s. F, The N395K channel showed an impaired steady-state slow inactivation curve compared to WT. G, Protocol used to examine deactivation. H, Representative traces of WT and N395K currents produced during a 0.5 ms pulse to 0 mV followed by a 30 ms pulse to -45 mV. Deactivation time constants were determined using a single exponential fit to the rate of current decay during the 30 ms pulse to the indicated voltages. I, N395K channels displayed a slightly slower onset of deactivation than that of WT.

-120 mV to allow recovery from fast inactivation and a test pulse to -10 mV for 25 ms to assess the fraction of current remaining available for activation. The change in channel availability measured with this protocol reflects the fraction of channels that undergo slow inactivation. Figure 14E shows representative traces of WT and N395K current produced following a 30 s pulse to the indicated voltage. N395K channels showed an impaired steady-state slow inactivation compared to WT channels (Figure 14F). The midpoint of steady-state slow inactivation for N395K channels (-33.6 ± 2.6 mV; slope: 11.8 ± 0.2 mV⁻¹; n = 6) was significantly ($p < 0.05$) depolarized compared to WT channels (-46.7 ± 1.7 mV; slope: 16.1 ± 1.0 mV⁻¹; n = 6; Student's unpaired t-test).

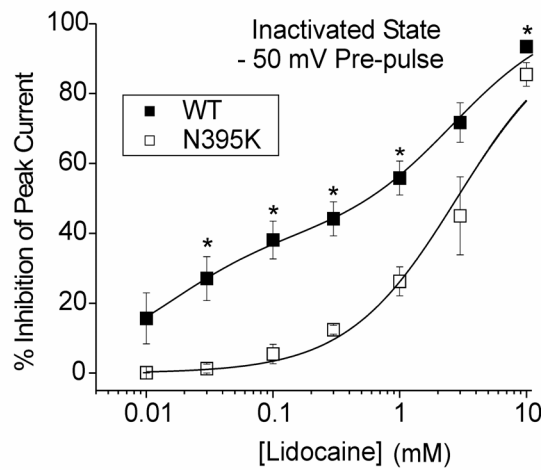
The kinetics of deactivation for WT and N395K channels was also examined (protocol shown in Figure 14G) by eliciting tail currents at a range of potentials after brief activation of the channels (0 mV for 0.5 ms). Deactivation reflects the transition of the channel from the open to closed state, and defects in skeletal muscle sodium channel deactivation have been implicated in paramyotonia congenita (Featherstone et al., 1998). Figure 14H shows an example of WT and N395K tail currents elicited by pulsing to -45 mV for 30 ms following a 0.5 ms pulse to 0 mV. The traces demonstrate the N395K channels undergo deactivation slower than WT channels. The time constant of deactivation (measured with single exponential fits) was slower for the N395K channel than that of the WT channel at potentials ranging from -100 mV to -40 mV (Figure 14C). The change in the kinetics of deactivation is consistent with the hyperpolarizing shift in the voltage-dependence of activation.

2. *The N395K mutation decreases Na_v1.7 sensitivity to lidocaine*

As mentioned earlier, lysine substitution at the residue corresponding to N395 in rat skeletal muscle Na_v1.4 channel (N434) reduced the affinity for both amitriptyline and local anesthetics for inactivated channels (Nau et al., 1999; Wang et al., 2004; Nau & Wang, 2004). Therefore, the impact of the N395K mutation on local anesthetic binding to Na_v1.7 was tested. Inhibition of channel current by a range of lidocaine concentrations (10 μM—10 mM) was examined for WT and N395K channels in the inactivated and resting state. Lidocaine binding to the inactivated state of the channels was tested by holding the cells at -120 mV and stepping to an inactivating pre-pulse (-50 mV) for 10 s, which is sufficient to inactivate all of the channels. This was followed by 100 ms pulses to -120 mV to allow recovery from fast inactivation, and the fraction of current remaining was measured in the absence and presence of lidocaine with a 20 ms test pulse to -10 mV.

Potency, but not efficacy, of lidocaine inhibition of inactivated N395K channels was attenuated compared to WT (Figure 15A). No data was obtained using lidocaine concentrations greater than 10 mM due to toxicity to the cells. Using a one-site binding fit, the IC₅₀ of lidocaine for inactivated WT channels was estimated at 500 μM while the IC₅₀ for inactivated N395K channels was estimated at 2.8 mM. However, the one-site binding model did not produce a good fit for the dose-inhibition relationship of lidocaine and inactivated WT channels. The data show that between 100 and 300 μM, lidocaine inhibition of WT inactivated channels reaches a plateau before increasing at doses of 1 mM

A



B

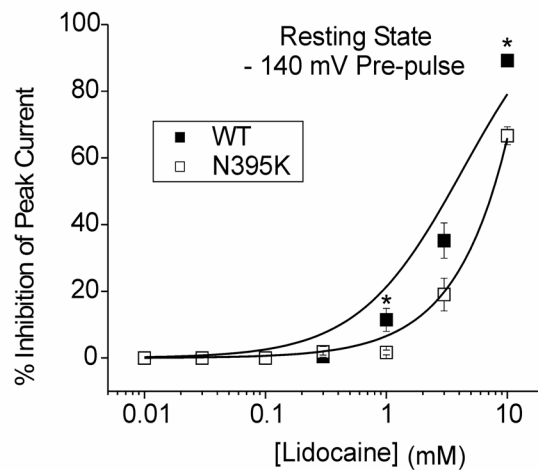


Figure 15. Effects of lidocaine on inactivated and resting WT and N395K channels. A, Dose-response of lidocaine inhibition was attenuated on inactivated N395K channels at all concentrations of lidocaine tested compared to inactivated WT. Two-site binding fit was used for WT ($R^2 = 0.99$) and a one-site binding fit was used for N395K ($R^2 = 0.98$) B, Dose-response of lidocaine inhibition was attenuated on resting N395K channels for 3 and 10 mM lidocaine compared to resting WT. A one-site binding fit was used for both WT ($R^2 = 0.91$) and N395K ($R^2 = 0.92$) channels. Data are presented as mean % inhibition of peak current \pm S.E.M. (* = $p < 0.05$).

and higher (Figure 15A). It was hypothesized that this plateau in the relationship was due to more than one-site being available for lidocaine binding. A two-site binding model gave a better fit to the WT data ($R^2 = 0.99$) than did a one-site binding model ($R^2 = 0.68$). The two-site binding model fit indicated that there are possibly two states of the WT sodium channels at -50 mV, one state that exhibits high affinity lidocaine binding while the other exhibits low affinity binding. Based on the two-site fit, the IC_{50} of lidocaine for the high affinity and low affinity binding to WT channels was 210 μ M and 4.3 mM, respectively. The high affinity and low affinity populations may represent channels in different inactivated conformations (see discussion). These data show that the N395K mutation significantly reduced lidocaine inhibition of $Na_v1.7$ channels at -50 mV, especially the high affinity binding.

Lidocaine binding to the resting state of the channels was tested by holding the cells at -120 mV and stepping to a pre-pulse of -140 mV for 10s. The fraction of current remaining was assessed by a test pulse to -10 mV for 25 ms. Lidocaine had little or no effect on resting WT and N395K channels at low concentrations (10 μ M—1 mM) while showing more inhibition at higher concentrations (3 mM, 10 mM) (Figure 15B). Using a one-site binding fit, the IC_{50} of lidocaine for resting WT channels was estimated at 4.3 mM while the IC_{50} for resting N395K channels was estimated at 7.9 mM. In contrast to the inactivated channel data, a two-site binding model did not give a better fit to the WT resting channel data. These data indicate the N395K mutation reduced the inhibition of resting channels by lidocaine, although to a lesser extent than that at -50 mV.

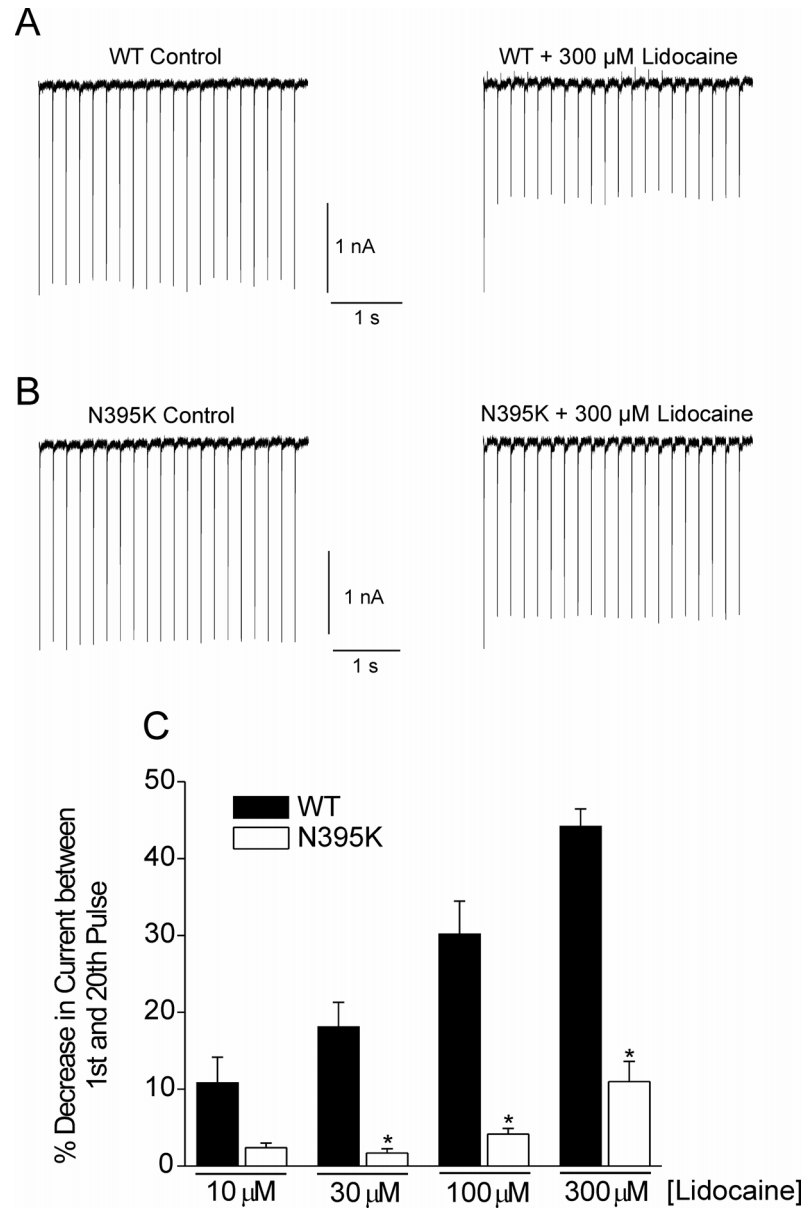


Figure. 16. Use-dependent inhibition of WT and N395K current by lidocaine. A, example of peak WT currents during high frequency stimulation under control conditions (left) and in the presence of 300 μ M lidocaine (right). B, example of peak N395K currents during high frequency stimulation under control conditions (left) and in the presence of 300 μ M lidocaine (right). C, Ratio of peak WT and N395K currents from the first pulse to the last pulse of the high frequency stimulation protocol in the presence of different concentrations of lidocaine. Data are presented as mean % decrease in current between the 1st and 20th pulse \pm S.E.M. (* = $p < 0.05$).

As local anesthetics are known to exhibit use-dependent inhibition of sodium currents, it was important determine if the N395K channels showed less use-dependent inhibition by lidocaine when compared to WT channels. Use-dependent effects were studied by pulsing the transfected cells to -10 mV at a frequency of 5 Hz in the absence and presence of drug. Figure 16 (A and B) displays examples of results under control conditions (left) and in the presence of 300 μ M lidocaine (right) for both the WT and N395K channels. WT current amplitude decreased 10.4 ± 3.3 % (n = 6), $18.1.4 \pm 3.2$ % (n = 6), 27.8 ± 3.3 % (n = 11), and 42.7 ± 2.0 % (n = 7) from the first pulse to the last pulse of the protocol in the presence of 10, 30, 100, 300 μ M lidocaine, respectively (Figure 16C). Decreases in N395K current amplitude were significantly ($p < 0.05$) smaller than decreases in WT current (one-way ANOVA followed by Tukey's comparison test) at 30, 100, 300 μ M lidocaine (Figure 16C). Decreases observed for the N395K channel were 2.4 ± 0.6 % (n = 6), 1.7 ± 0.6 % (n = 5), 4.3 ± 0.6 %, (n = 6) and 11.0 ± 2.6 %, (n = 5) for 10, 30, 100, 300 μ M lidocaine, respectively.

3. *An erythromelalgia mutation not found in the local anesthetic binding site (F216S) did not alter Na_v1.7 sensitivity to lidocaine*

Although the N395K mutation in Na_v1.7 showed resistance to inhibition by lidocaine, it is possible that other hereditary erythromelalgia mutations outside of the local anesthetic binding site might also alter lidocaine sensitivity. We therefore investigated the effects of lidocaine on Na_v1.7 containing another

mutation (F216S) that has been identified in erythromelalgia patients (Drenth et al., 2005). A recent study shows that the F216S channel has a hyperpolarized voltage-dependence of activation similar to the N395K mutation, but an enhanced steady-state slow inactivation (Choi et al., 2006). We examined the effects of 300 μ M and 1 mM lidocaine on inactivated F216S channels. These concentrations of lidocaine were chosen because both showed considerable inhibition of the WT channel in the inactivated (-50 mV pre-pulse) state. Figure 17A shows that the level of inhibition of inactivated F216S channels by 300 μ M (38.4 ± 2.1 %, $n = 6$) and 1 mM (58.2 ± 2.5 %; $n = 5$) were not significantly different from that of inactivated WT channels (300 μ M: 39.9 ± 7.3 %, $n = 11$; 1 mM: 55.9 ± 4.9 %, $n = 9$; Student's unpaired t-test). However, inhibition of inactivated F216S channels by 300 μ M and 1 mM lidocaine was significantly ($p < 0.05$) higher than inhibition of N395K channels by 300 μ M (12.4 ± 1.3 %, $n = 6$) and 1mM lidocaine (26.2 ± 4.2 %, $n = 8$; Student's unpaired t-test; Figure 17A). We also investigated use-dependent inhibition of F216S currents by 300 μ M by pulsing cells transfected with F216S to -10 mV at a frequency of 5 Hz in the presence of lidocaine. Figure 17B shows that F216S current amplitude decreased 42.7 ± 2.5 % ($n = 6$) from the first pulse to the last pulse of the protocol in the presence of 300 μ M lidocaine and was not significantly different from the decrease seen with WT channels (42.7 ± 2.0 %, $n = 11$; one-way ANOVA followed by a Tukey's comparison test). This decrease in F216S current amplitude was significantly ($p < 0.05$) higher than the decrease in N395K current amplitude (11.0 ± 2.6 %, $n = 5$; one-way ANOVA followed by a Tukey's

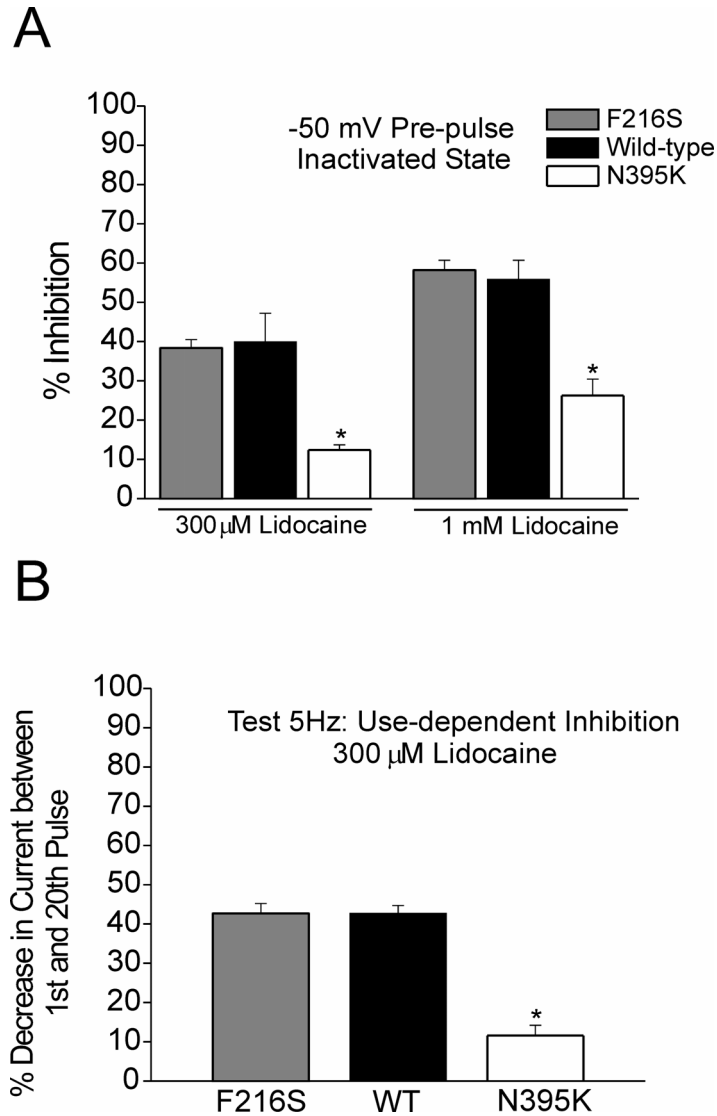


Figure 17. Inhibitory effects of lidocaine on the F216S channel compared to Na_v1.7 WT and N395K. A, Lidocaine (300 μ M and 1 mM) inhibition of inactivated F216S channels compared to inactivated WT channels and to inactivated N395K channels. B, Ratio of peak F216S currents from the first pulse to the last pulse of the high frequency stimulation protocol in the presence 300 μ M and 1 mM lidocaine compared to that of WT and N395K channels. Data are presented as mean % inhibition of peak current \pm S.E.M or mean % decrease in current between the 1st and 20th pulse \pm S.E.M (* = $p < 0.05$).

comparison test) induced by 300 μ M lidocaine (Figure 17B). These data show that a hereditary erythromelalgia mutation outside of the Na_v1.7 local anesthetic binding site does not affect lidocaine sensitivity of Na_v1.7.

C. Lidocaine stabilizes Na_v1.7 in a configuration that decreases transition to the slow-inactivated state of the channel

1. Lidocaine alters the recovery of Na_v1.7 channels from inactivation

As shown earlier, a two-site binding model gave a much better fit to the dose-response curve for lidocaine inhibition of Na_v1.7 channel current. This fit indicated there are possibly two interaction sites of Na_v1.7 at -50 mV, one that exhibits high affinity lidocaine binding while the other exhibits low affinity binding. The hypothesis was the high affinity and low affinity populations represent channels in different inactivated conformations. One explanation for this is the long pre-pulse (10 s) to -50 mV to test lidocaine inhibition of Na_v1.7 results in some channels entering into a fast-inactivated state and others entering into a slow-inactivated state. Slow-inactivated channels create a problem because they required prolonged hyperpolarizing pulses to recover. This long recovery pulse is likely to allow for unbinding of lidocaine thus its interaction with the slow-inactivated state may be masked. A second explanation for the two-site binding interaction of lidocaine with Na_v1.7 is at -50 mV the channels are a mixture of closed-inactivated and open-inactivated channels. In 1980 it was demonstrated sodium channels can inactivate without opening (Bean, 1981). One recent study

using squid giant axons showed closed-state inactivation is more likely to occur at hyperpolarized membrane potentials and less likely to occur as potentials become more depolarized (Armstrong, 2006). Therefore, to investigate the state dependence of lidocaine inhibition, the recovery profile for $\text{Na}_v1.7$ channels after being pulsed to various potentials for 10s in the absence and presence of 1 mM lidocaine was tested. This would establish a rate of recovery for fast and slow-inactivated channels at different potentials.

Figure 18A displays the protocol used to examine the recovery from fast and slow inactivation for $\text{Na}_v1.7$ channel. For these experiments cells containing $\text{Na}_v1.7$ were held at one of six different potentials (-100, -80, -60, -50, -40, or 0 mV) for 10 seconds in the absence and presence of 1 mM lidocaine and were allowed to recover to -120 mV for various durations before testing remaining current with a 20 ms pulse to 0 mV. The normalized amount of current was then plotted versus the duration of the recovery time in order to determine time constants for recovery from inactivation. All recovery of $\text{Na}_v1.7$ channels not treated with lidocaine showed a two or three-phase recovery profile (Figure 18, B thru G). The time constant values estimated from a non-linear curve fit for these two phases of recovery are summarized in Table 2. Due to the prolonged pre-pulse duration the two-phase recovery profile for control conditions likely represents a recovery from a fast and a slow-inactivated state with τ_1 representing the time constant for recovery of $\text{Na}_v1.7$ from fast inactivation and τ_2 representing the time constant for recovery of $\text{Na}_v1.7$ from slow inactivation. A third τ value (Figure 18, E thru G) likely represents recovery

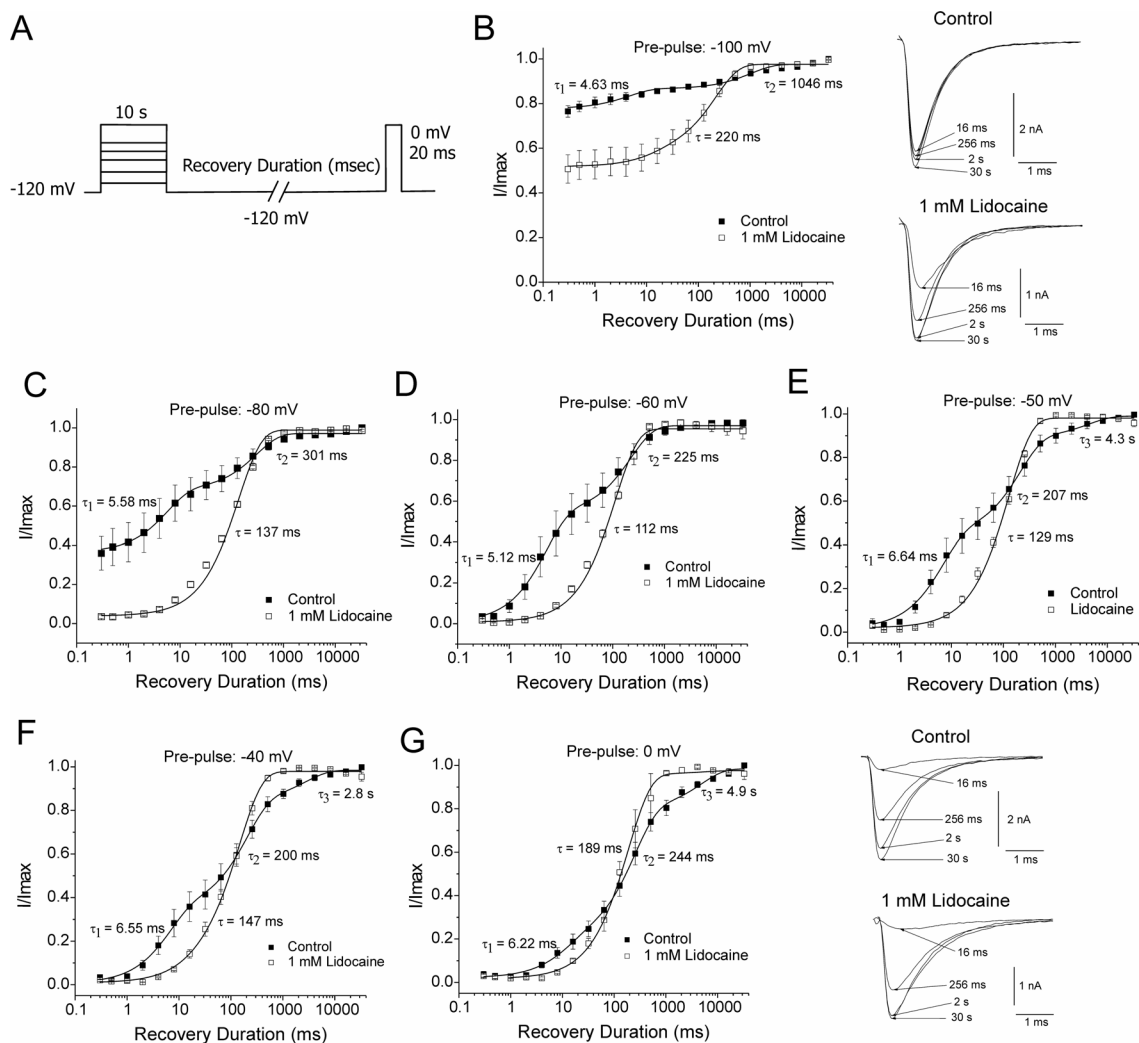


Figure 18. Recovery from prolonged inactivation and lidocaine inhibition for $\text{Na}_v1.7$ channels. A, protocol used for examining recovery from prolonged inactivation and lidocaine inhibition for $\text{Na}_v1.7$ channels. B (left), recovery profile of $\text{Na}_v1.7$ channels from a 10 s pulse to -100 mV in the absence and presence of 1 mM lidocaine. B (right), representative traces of recovery current at various durations of recovery after a 10 s pulse to -100 mV in the absence and presence of 1 mM lidocaine. C—G, recovery profiles of $\text{Na}_v1.7$ channels from different pre-pulse potentials. The pre-pulse value is given at the top of each graph. G (left), recovery profile of $\text{Na}_v1.7$ channels from a 10 s pulse to 0 mV in the absence and presence of 1 mM lidocaine. G (right), representative traces of recovery current at various durations of recovery after a 10 s pulse to 0 mV in the absence and presence of 1 mM lidocaine. Tau values are given for each trace. In the case of control conditions, the recovery profile fit better to a second or third-order exponential growth equation. All fits had $R^2 > 0.90$. As mentioned in the text, this likely represents recovery from 2 or 3 different forms of channel inactivation: fast and 2 types of slow.

Table 2. Estimated time constants recovery from prolonged inactivation and lidocaine inhibition for Na_v1.7 channels.

Pre-pulse voltage (mV)	No Lidocaine						1 mM lidocaine
	Tau 1 (ms)	A ₁	Tau 2 (ms)	A ₂	Tau 3 (s)	A ₃	Tau (ms)
-100 mV	4.63 +/- 1.6	0.14	1046 +/- 300	0.11	N/A	N/A	220 +/- 16
-80 mV	5.58 +/- 0.7	0.33	301 +/- 40	0.29	N/A	N/A	137 +/- 7.2
-60 mV	5.12 +/- 0.5	0.56	225 +/- 24	0.43	N/A	N/A	112 +/- 5.3
-50 mV	6.64 +/- 0.9	0.44	207 +/- 37	0.44	4.3 +/- 3.0	0.10	129 +/- 5.0
-40 mV	6.55 +/- 0.8	0.36	200 +/- 27	0.49	2.8 +/- 1.1	0.14	147 +/- 5.0
0 mV	6.22 +/- 4.3	0.21	245 +/- 26	0.61	4.9 +/- 1.4	0.18	189 +/- 12

Values are means estimated from the best fit line produced from a second-order exponential growth function for the no lidocaine group and first-order exponential decay for the 1 mM lidocaine group. The first-order exponential growth equation used is as follows: $y = y_o + A_1 e^{x/\tau_1}$. The second-order and third-order exponential growth equation used were as follows: $y = y_o + A_1 e^{x/\tau_1} + A_2 e^{x/\tau_2}$ and $y = y_o + A_1 e^{x/\tau_1} + A_2 e^{x/\tau_2} + A_3 e^{x/\tau_3}$ where for both equations y_o = the initial value at time 0, A_1 = weight factor (of total recovered) for fraction recovered with time constant τ_1 , A_2 = weight factor (of total recovered) for fraction recovered at τ_2 , A_3 = weight factor (of total recovered) for fraction recovered at τ_3 , x = the growth constant, and τ_1 = time constant for recovery of fast-inactivated channels, τ_2 and τ_3 = time constants for the recovery of potentially two distinct slow-inactivated states of the channels. N/A = not applicable. The τ value for the lidocaine group represents the time constant for the recovery of channels from a drug bound state.

from a possible second slow-inactivated state produced from the 10 s pre-pulse. Recovery of Na_v1.7 channels treated with 1 mM lidocaine displayed a one-phase profile and was fit using a first-order exponential growth equation for all pre-pulse voltages. The time constant values estimated from a non-linear curve fit for mean values of recovery from lidocaine at each voltage can also be found in a summarized format in Table 2. Figure 18, B and C, show that pulsing to -100 mV or -80 mV for 10 s does not completely inactivate Na_v1.7 under control conditions but is sufficient to transition some of the channels into a state that recovers slowly. Prolonged pulse durations (10 s) at -60, -50, -40 and 0 mV completely inactivate Na_v1.7 and the fraction of channels exhibiting slow recovery increases with more depolarized conditioning pulses (Figure 18, D thru G). When looking at the effects of 1 mM lidocaine, it is clear that recovery from inactivation is altered. This indicates interaction of lidocaine with Na_v1.7 induces a channel-drug configuration that, at least initially, takes longer to recover than un-treated channels. However, at more depolarized potentials (-50, -40, 0 mV) lidocaine paradoxically seemed to enhance the rate of recovery of Na_v1.7 channels at prolonged durations compared to control (Figure 18, E thru G). In addition, this enhancement of recovery rate by lidocaine corresponds to the durations at which the control channels were recovering from the slow-inactivated state. Lidocaine enhances recovery from inactivation after recovery durations of approximately 140 ms, 105 ms, and 75 ms for -50 mV, -40 mV, and 0 mV, respectively (Figure 18, E thru G). At shorter recovery durations at which control channels are recovering from a fast-inactivated state, 1 mM lidocaine still prolongs recovery.

These results indicate lidocaine reduces the transition of Na_v1.7 channels to the state with slow recovery from inactivation while stabilizing a configuration that normally recovers quickly from inactivation.

2. Lidocaine attenuates the ability of Na_v1.7 channels to transition to a state that recovers slowly from inactivation

Since lidocaine showed a difference in affecting the recovery of Na_v1.7 from a fast-inactivated state versus a slow-inactivated state, the next goal was to investigate the effects of lidocaine on the onset of slow inactivation in Na_v1.7 channels at the same membrane potentials used to examine recovery from inactivation. To assure that relief from fast-inactivation was complete, the time constants for recovery (Table 2, tau 1) of Na_v1.7 at -120 mV from fast inactivation at the different holding potentials used was multiplied by five and used as the recovery duration. Therefore, when examining the onset of slow inactivation for holding potentials -100, -80, and -60 mV the recovery time was set at 30 ms while for holding potentials -50, -40, and 0 mV the recovery time was set at 40 ms. The protocol used to examine the onset of slow inactivation is shown in Figure 19A. Pulsing to -100 mV did not induce any slow inactivation (Figure 19B). Pulsing to -80, -60, -50, -40, and 0 mV induced slow inactivation that developed with two distinct time courses in Na_v1.7 (Figure 19, C thru F). As the pulses became more depolarized the time constant for onset of the first slow-inactivated state decreased indicating that stronger depolarizations are more effective at inducing slow-inactivation in Na_v1.7. As the pulses were prolonged, a

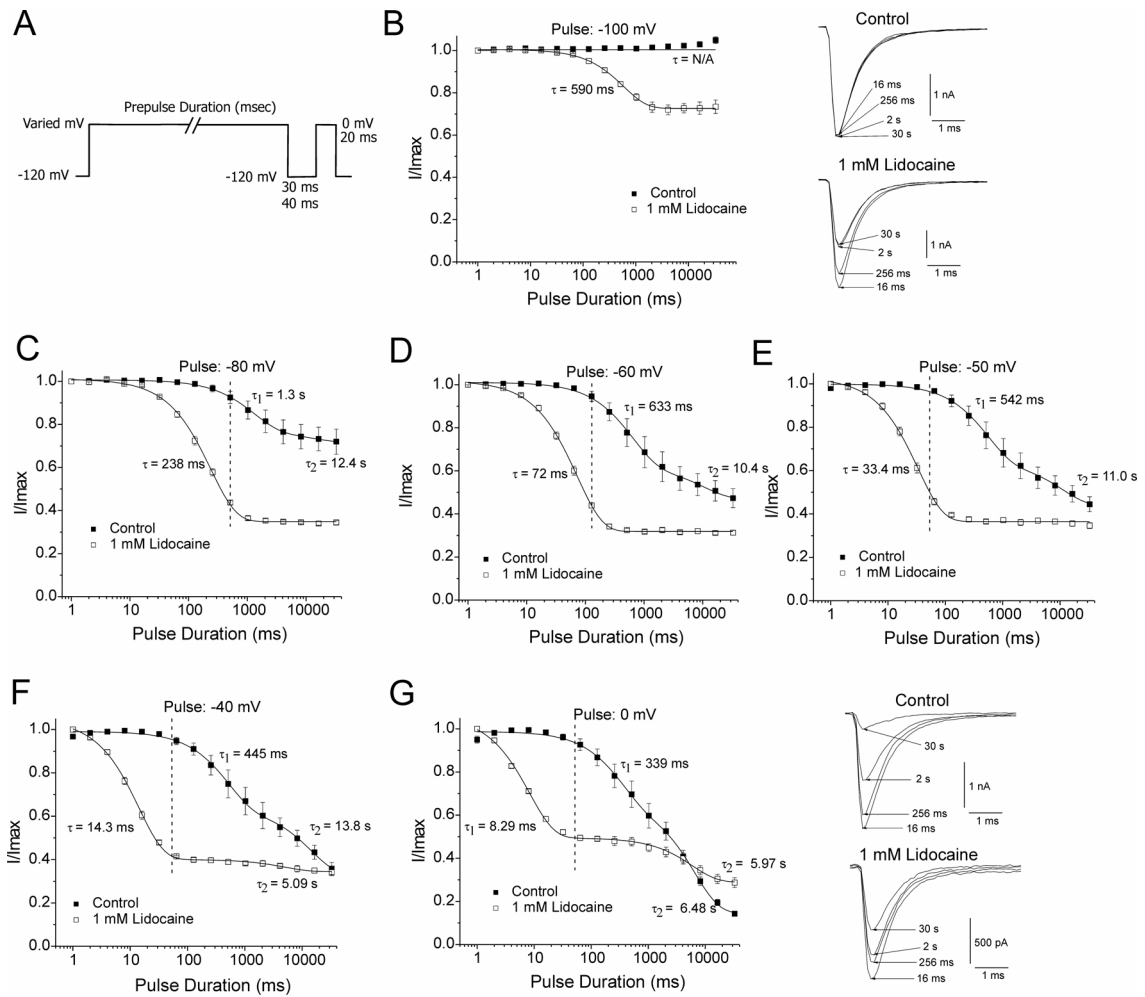


Figure 19. Onset of slow inactivation and lidocaine inhibition for $\text{Na}_v1.7$ channels. A, protocol used for examining onset of slow inactivation and lidocaine inhibition for $\text{Na}_v1.7$ channels. B (left), the onset of slow inactivation/lidocaine inhibition profile of $\text{Na}_v1.7$ channels pulsed to -100 mV for increasing durations in the absence and presence of 1 mM lidocaine. B (right), representative traces of current produced after various pulse durations to -100 mV in the absence and presence of 1 mM lidocaine. C—G, onset of slow inactivation/lidocaine inhibition profiles of $\text{Na}_v1.7$ channels from different pulse potentials. The pulse value is given at the top of each graph. G (left), the onset of slow inactivation/lidocaine inhibition profile of $\text{Na}_v1.7$ channels pulsed to 0 mV for increasing durations in the absence and presence of 1 mM lidocaine. G (right), representative traces of current produced after various pulse durations to 0 mV in the absence and presence of 1 mM lidocaine. Tau values are given for each trace. In the case of control conditions, the onset profile fit better to a second-order exponential growth equation possibly due to the onset of 2 different forms of channel slow inactivation. All fits had R^2 values > 0.90.

Table 3. Estimated time constants for onset of slow inactivation for Na_v1.7 channels.

Pre-pulse voltage (mV)	No Lidocaine			
	Tau 1 (ms)	A ₁	Tau 2 (ms)	A ₂
-100 mV	N/A	N/A	N/A	N/A
-80 mV	1300 +/- 120	0.24	12400 +/- 9100	0.05
-60 mV	633 +/- 49	0.45	10400 +/- 3300	0.15
-50 mV	540 +/- 50	0.45	11100 +/- 3100	0.21
-40 mV	508 +/- 48	0.46	14200 +/- 3300	0.31
0 mV	339 +/- 49	0.40	6510 +/- 785	0.52

Values are means estimated from the best fit line produced from a first-order or a second-order exponential growth. For -100 mV, no onset of slow inactivation was observed and therefore time constants could not be obtained. The first-order exponential growth equation used is as follows: $y = y_o + A_1 e^{x/\tau_1}$. The second-order exponential growth equation used is as follows: $y = y_o + A_1 e^{x/\tau_1} + A_2 e^{x/\tau_2}$ where for both equations y_o = the initial value at time 0, A_1 = weight factor (of total inactivated) for fraction inactivated with time constant τ_1 , A_2 = weight factor (of total inactivated) for fraction inactivated at τ_2 , x = the decay constant, and τ_1 and τ_2 = time constant for the onset of initial and prolonged slow inactivation in Na_v1.7 channels, respectively.

Table 4. Estimated time constants for onset of lidocaine inhibition of Na_v1.7 channels.

Pre-pulse voltage (mV)	1 mM Lidocaine			
	Tau 1 (ms)	A ₁	Tau 2 (ms)	A ₂
-100 mV	591.6 +/- 19.5	N/A	N/A	N/A
-80 mV	238.5 +/- 6.7	N/A	N/A	N/A
-60 mV	72.3 +/- 1.5	N/A	N/A	N/A
-50 mV	33.4 +/- 1.1	N/A	N/A	N/A
-40 mV	14.27 +/- 0.38	0.65	5094 +/- 1600	0.06
0 mV	8.29 +/- 0.39	0.71	5967 +/- 760	0.21

Values are means estimated from the best fit line produced from a first-order or a second-order exponential growth. The first-order and second-order exponential growth equations used were the same as used in Tables 2 and 3. Only at pulse voltages of -40 and 0 mV was the second-order exponential growth equation required. Again, A₁ = weight factor (of total inhibited) for fraction inhibited with time constant τ_1 , A₂ = weight factor (of total slow-inactivated) for fraction of channels inactivated at τ_2 , x = the decay constant, and τ_1 and τ_2 = time constant for the onset of lidocaine inhibition and prolonged slow inactivation in the presence of lidocaine for Na_v1.7 channels, respectively.

second slow-inactivation time course on the order of seconds could be observed at each potential (excluding -100 mV). The estimated time constants for onset of slow inactivation in Na_v1.7 channels are summarized in Table 3. The application of 1 mM lidocaine enhanced the transition of the Na_v1.7 channel to a non-conducting state at all pre-pulse potentials (Figure 19, B thru F). This non-conducting state corresponds to a drug bound state of the channel. The estimated time constants for the onset of lidocaine inhibition of Na_v1.7 channels are summarized in Table 4. Interestingly, after an initial fast decrease in current caused by lidocaine, inhibition levels off and very little additional drop in current is observed (Figure 19, B thru F). This is seen at all pre-pulse potentials including -100 mV. With increasing durations of depolarization this leveling off of current inhibition by lidocaine takes place at approximately the same time as slow inactivation is starting to occur in control channels. The dashed line in Figure 19 (B thru F) represents the approximate time at which slow inactivation begins to occur in control channels. As shown, the dashed line intersects with the time course of lidocaine inhibition on Na_v1.7 channels approximately where no additional inhibition can be observed. This raises the possibility that transition of Na_v1.7 into a slow-inactivated state decreases or abolishes the ability of lidocaine to interact with the channel. However, at pre-pulses of -40 or 0 mV, a second slow-inactivated state can be seen in lidocaine treated channels suggesting some slow inactivation may still take place in the presence of lidocaine given the depolarization is strong enough. In addition, when pulsing to 0 mV for approximately 6s or longer, lidocaine attenuates the magnitude of current

decrease compared to the decrease observed in control channels. This result is consistent with lidocaine interfering with the ability of Na_v1.7 channels to transition to a state that recovers slowly from inactivation.

3. Lidocaine exhibits different dose-response effects on Na_v1.7 current which are dependent on voltage and pulse duration

If the high affinity and low affinity populations represent channels in fast and slow-inactivated states, then lidocaine should display different concentration-response effects on channels pulsed to various potentials for 200 ms versus 10 s. The reason for this is that a 200 ms pulse would produce minimal transition to slow-inactivation in Na_v1.7 channels as opposed to a 10 s pulse which is efficient at inducing slow-inactivation. Therefore, Na_v1.7 channels were pulsed to the same potentials used previously for either 200 ms or 10 s protocols and shown in Figure 20A. Protocols were run before and after the application of 1 mM lidocaine and were analyzed as paired experiments. Dose-response effects of lidocaine on Na_v1.7 channel current when pulsing for 200 ms are better fit with a one-site dose-response model for all pulse potentials (Figure 20B). When pulsing Na_v1.7 channels to the various potentials for 10 s, the dose-response effects of lidocaine on channel current fit better to a two-site binding model (Figure 20C). This implies the extension of pulse duration transitions the Na_v1.7 channels into a mixture of high affinity and low affinity configurations that interact with lidocaine. The IC₅₀ values estimated for each voltage and duration are

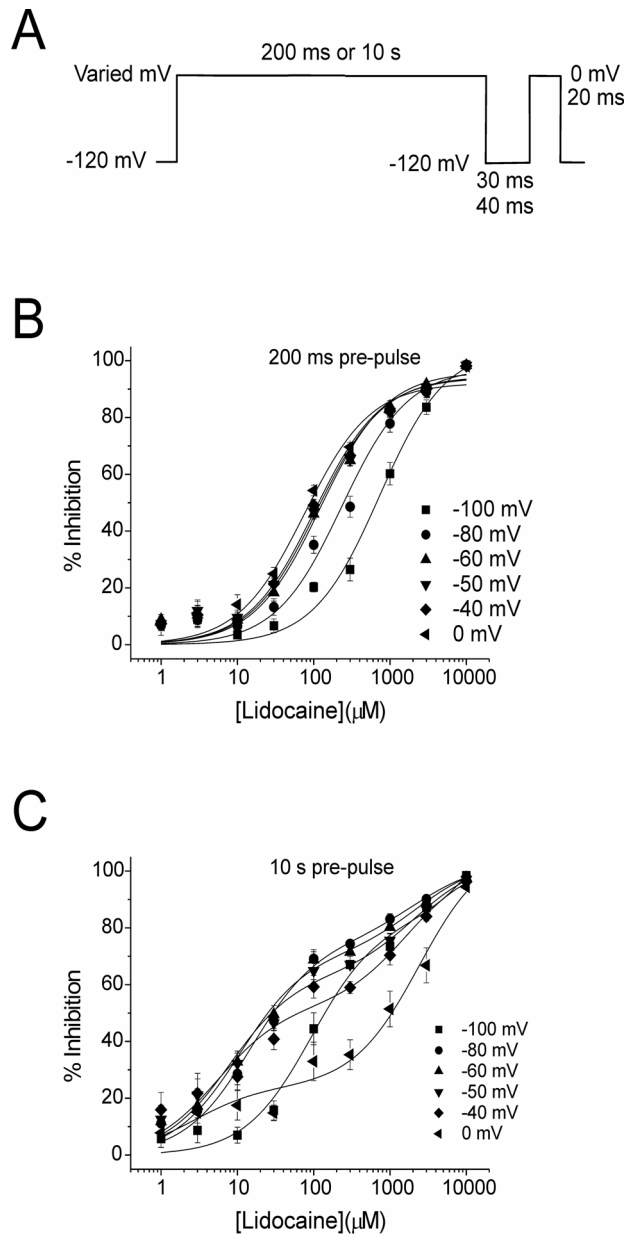


Figure 20. Dose-response curves of lidocaine inhibition of the Na_v1.7 at various holding potentials. A recovery pulse of 40 ms (for -100, -80, -60 mV pulses) and 30 ms (for -50, -40, 0 mV pulses) to -120 mV was given after each conditioning pulse. A, Dose-response curves of lidocaine inhibition of the Na_v1.7 when holding at the indicated potential for 200 ms. Data were fit using a one-site binding equation. B, Dose-response curves of lidocaine inhibition of the Na_v1.7 when holding at the indicated potential for 10 s. As seen previously in Figure 15, these data fit better using two-site binding equation. The one-site and two-site binding equations are explained in Table 5. All fits had $R^2 > 0.90$.

Table 5. Summary of IC₅₀ values established for lidocaine inhibition of Na_v1.7 current at different potentials and pulse durations.

Voltage (mV)	Pulse Duration		
	200 ms	10 s	
	IC ₅₀ (μM)	IC ₅₀ 1(μM)	IC ₅₀ 2 (mM)
-100 mV	727 +/- 154	91.7 +/- 29.3	34.2 +/- 350
-80 mV	234 +/- 44.0	15.1 +/- 3.4	2.26 +/- 2.6
-60 mV	121 +/- 20.5	10.7 +/- 2.2	2.32 +/- 2.0
-50 mV	110 +/- 19.7	7.92 +/- 2.2	2.12 +/- 1.7
-40 mV	102 +/- 16.9	5.46 +/- 2.5	1.68 +/- 1.4
0 mV	75.6 +/- 13.5	2.64 +/- 2.2	2.40 +/- 1.1

Values are mean IC₅₀ values ± S.E.M. estimated from the best fit line produced from a one-site or two-site binding equation. The one-site binding equation was

as follows: $y = \frac{Bx}{K + x}$. The two-site binding equation was as follows:

$y = \frac{B_1x}{K_1 + x} + \frac{B_2x}{K_2 + x}$. For these equations, y = percentage lidocaine inhibition, x =

lidocaine concentration, B = maximum amount of inhibition (thus B₁ and B₂ represent max inhibition for the high and low affinity configuration of Na_v1.7 for lidocaine, respectively), K = concentration at which 50% of Na_v1.7 channels are inhibited (i.e. IC₅₀ values, thus K₁ and K₂ represent IC₅₀ values for the high and low affinity configuration of Na_v1.7 for lidocaine, respectively). The average n value for all concentrations of lidocaine was 6 with no single concentration having an n < 4.

summarized in Table 5. When pulsing for 200 ms, the IC₅₀ values get progressively smaller in response to depolarizing the pulse potential. The first IC₅₀ values established from pulsing Na_v1.7 for 10 s also get progressively smaller in response to more depolarizing pulse potentials and are less than the IC₅₀ values observed when pulsing the channel for 200 ms. The second IC₅₀ values established for the 10 s pulse did not dramatically change with pulse potential. The -100 mV pulse is the exception with an IC₅₀ value of 34.2 ± 350 mM. The variability in this IC₅₀ value reflects the possibility that the low affinity configuration (IC₅₀ ~ 2 mM) is not established at a prolonged pulse to -100 mV. In addition, the onset of inactivation data shows Na_v1.7 does not transition to a slow-inactivated state during prolonged pulses to -100 mV (Figure 19B).

To further examine the effects of pulse duration on lidocaine inhibition of Na_v1.7 channels dose-response curves comparing the effects of 200 ms or 10 s pulses were plotted for each potential (Figure 21). When pulsing to -100 or -80 mV, it is clear that the 10 s pulse enhances lidocaine inhibition of Na_v1.7 compared to the 200 ms pulse (Figure 21, A and B). As the pulse potentials become more depolarized the dose-response curves for the 10 s pulse and the 200 ms pulse intersect with higher lidocaine concentrations showing more inhibition on Na_v1.7 channels pulsed for 200 ms than ones pulsed for 10 s (Figure 21, C thru F). The point of intersection for the separate dose-response curves was dependent on pulse potential. For example, the point at which the 200 ms pulse to -50 mV begins producing more lidocaine inhibition than the 10 s pulse to -50 mV was approximately at 260 μM (Figure 21D). If the pulse is

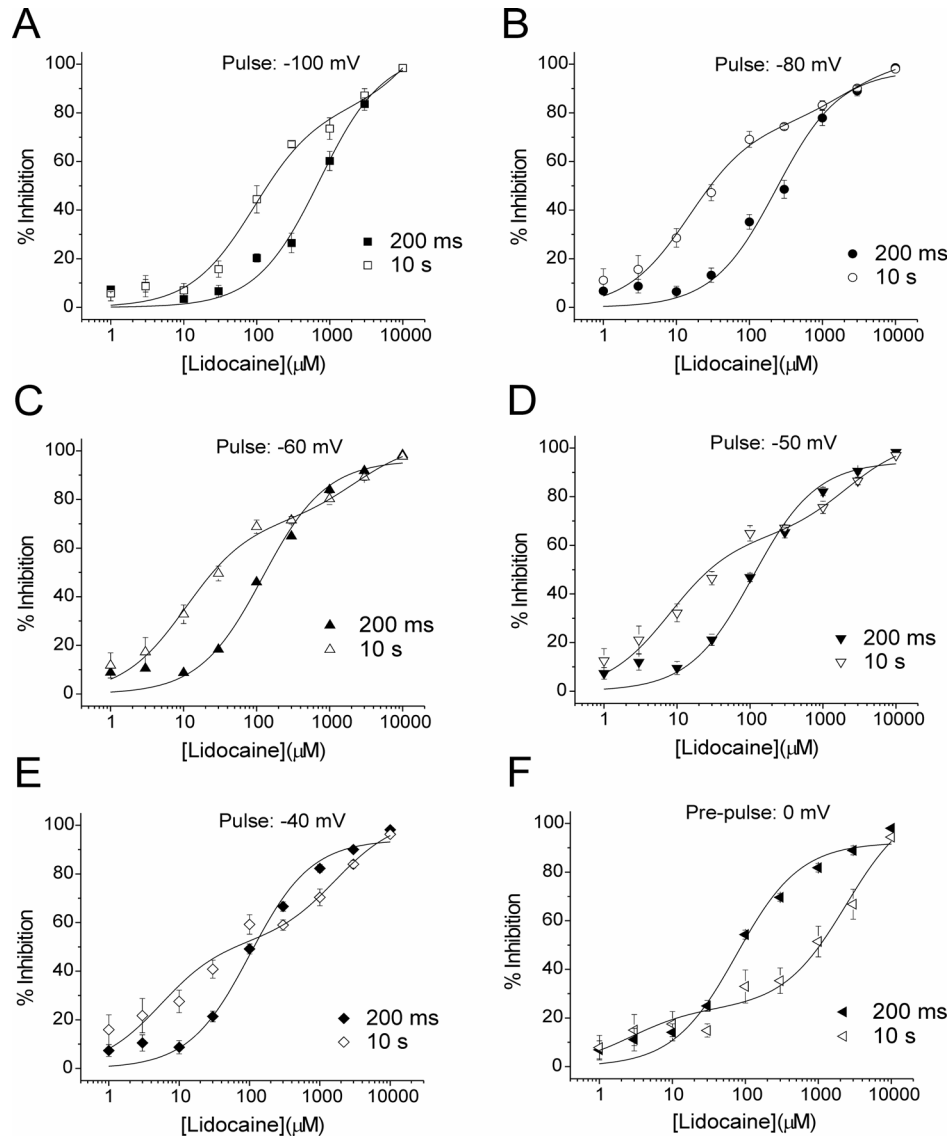


Figure 21. Dose-response curves of lidocaine inhibition on $Na_v1.7$ comparing the effects of pulse duration at various holding potentials on inhibition of channel current. The potential at which the channel was pulsed is indicated at the top of each set of dose-response curves. As mentioned previously dose-response data resulting from pulsing channels for 200 ms were fit using a one-site binding equation. Dose-response data resulting from pulsing channels for 10 s were fit using a two-site binding equation.

changed to 0 mV, this point of intersection shifts to approximately 25 μ M (Figure 21F). Interestingly, the point of intersection appears to happen during the plateau phase of the 10 s pulse dose-response curve for each potential. Again, this is consistent with the Na_v1.7 channel more effectively transitioning to the slow-inactivated state at depolarized potentials thus decreasing interaction of lidocaine with the channel.

4. PEPD mutations I1461T and T1464I do not alter lidocaine effects on the activation of the Na_v1.7 channel

A recent study has shown that families affected by paroxysmal extreme pain disorder (PEPD), characterized by rectal, ocular, and submandibular pain, have missense mutations in the SCN9A gene encoding for Na_v1.7 (Fertleman et al., 2006). PEPD mutations reportedly attenuate the voltage-dependence of fast inactivation as well as decrease the overall magnitude of fast inactivation for Na_v1.7 channels (Fertleman et al., 2006). These characteristics were used to evaluate how altering fast inactivation of Na_v1.7 may affect the lidocaine sensitivity of the channel. The hypothesis would be that attenuating the transition of Na_v1.7 to a fast-inactivated state will decrease the lidocaine sensitivity of the channel. To test this, two mutations implicated in PEPD, I1461T and T1464I, were inserted separately in the Na_v1.7 channel, and the effects of these mutations on channel function and lidocaine interaction were investigated. Figure 22 (B thru D) shows the current-voltage traces for WT, I1461T, and T1464I channels transiently transfected in HEK293 cells along with human β_1

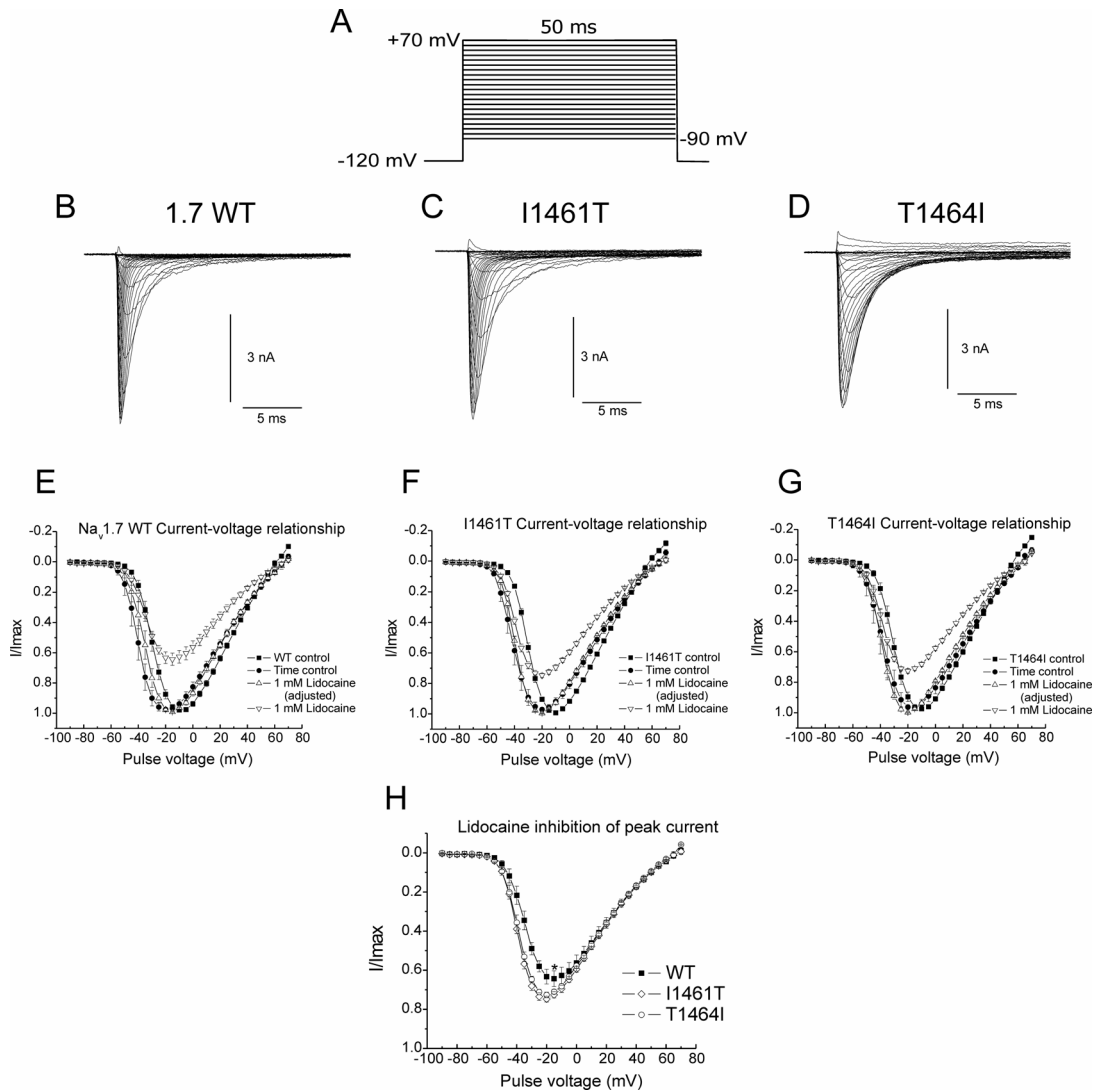


Figure 22. Effects of 1 mM lidocaine on the voltage-dependence of activation and peak current for $\text{Na}_v1.7$, I1461T, and T1464I channels. A, electrophysiological protocol used to obtain the current-voltage (IV) relationship for $\text{Na}_v1.7$, I1461T, and T1464I channels. B-D, representative IV traces for $\text{Na}_v1.7$ (B), I1461T (C), and T1464I channels (D). E-G, summarized IV curves of control conditions, time-dependent controls, and 1 mM lidocaine for $\text{Na}_v1.7$ (E), I1461T (F), and T1464I channels (G). H, effects of lidocaine on peak current for $\text{Na}_v1.7$, I1461T, and T1464I channels. Data are represented as normalized current \pm S.E.M. The 1 mM lidocaine (adjusted = normalized to peak control) group reflects the IV curve produced from normalizing the data to the peak current produced from control conditions. Statistical significance was determined using a one-way ANOVA analysis followed with a Tukey's comparison test (*= $p < 0.05$).

and β_2 subunits. The protocol used to obtain current-voltage relationships is shown in Figure 22A. Previous investigation showed the I1461T and T1464I mutations caused alterations in channel inactivation including a noticeable persistent current lasting several hundred milliseconds (Fertleman et al., 2006). In this study, the persistent currents were not as large ($\sim 4\%$ of peak current) as shown previously ($> 40\%$ of peak current) but were still present (Figure 22, B thru D). The effects of 1 mM lidocaine on the voltage-dependence of activation and peak current for $\text{Na}_v1.7$, I1461T, and T1464I channels were evaluated using paired experiments. Control values for $V_{1/2}$ of activation and peak current were measured and subsequently re-measured after application of 1 mM lidocaine. Controls were performed to measure any time-dependent changes that occurred in $V_{1/2}$ of activation and peak current. The values for $V_{1/2}$ of activation for WT, I146T, and T1464I were -26.3 ± 1.5 (n = 11), -27.2 ± 0.7 (n = 14), and -27.6 ± 1.5 mV (n = 11), respectively. These values were not significantly different from one another ($p > 0.05$, One-way ANOVA analysis) indicating the I1461T and T1464I mutations do not affect the voltage-dependence of activation for $\text{Na}_v1.7$ channels. After application of 1 mM lidocaine, the $V_{1/2}$ of activation for WT (Figure 22E), I1461T (Figure 22F), and T1464I (Figure 22G) was hyperpolarized by -8.9 ± 0.3 (n = 6), -10.8 ± 0.7 (n = 7), and -8.4 ± 0.8 (n = 6). However, for WT channels the time-dependent (~ 9 min.) shift in the $V_{1/2}$ of activation (-11.5 ± 1.0 mV; n = 5) was significantly larger ($p = 0.03$) than the shift caused by lidocaine. Yet the time dependent shifts in the $V_{1/2}$ of activation for I1461T (-11.2 ± 1.3 mV; n = 7) and T1464I (-10.1 ± 1.3 mV; n = 5) were not significantly different ($p >$

0.05) from the shifts caused by lidocaine (Figure 22, F and G). This indicates lidocaine has minimal effect the voltage-dependence of activation for Na_v1.7 and the I1461T and T1464I mutations do not alter this effect.

The I1461T and T1464I mutations did however have an effect on the decrease in peak current caused by the interaction of lidocaine with Na_v1.7. WT channels showed a 49.7 ± 3.0 % (n = 6) decrease in peak current after application of 1 mM lidocaine (Figure 22E). This value reflects the percent decrease in current adjusted for a time-dependent increase in current that occurred in Na_v1.7 channels. I1461T and T1464I channels showed a 39.9 ± 1.3 % (n = 7; Figure 22F) and a 37.9 ± 1.1 % (n = 6; Figure 22G) decrease in current after application of 1 mM lidocaine. Both of these decreases in current were significantly smaller ($p < 0.05$) than the decrease in current observed in WT Na_v1.7 channels caused by 1 mM lidocaine (Figure 22H). These values were also adjusted for a time-dependent increase in current. Taken together, these data indicate while the I1461T and T1464I mutations do not affect the $V_{1/2}$ of activation for Na_v1.7 channels, they do decrease the ability of lidocaine to inhibit peak current produced by Na_v1.7. In addition, this attenuation of lidocaine effect does not involve changes in Na_v1.7 voltage-dependence of activation.

5. PEPD mutations I1461T and T1464I alter inactivation of the Na_v1.7 channel

Since PEPD mutations I1461T and T1464I effectively decrease the lidocaine inhibition of Na_v1.7 peak current without showing effects on the voltage

dependence of activation for the channel, it was possible this decrease in lidocaine inhibition of the channel was due to a decreased interaction with the inactivated state of the channel. To examine this, the effects of the I1461T and T1464I mutations on the inactivation properties of the Na_v1.7 channel were tested. The voltage-dependence of steady-state fast-inactivation was examined for all the channels using the protocol shown in Figure 23A. The I1461T and T1464I mutations both caused depolarizing shifts of the voltage-dependence of fast-inactivation of Na_v1.7 channels (Figure 23C). The $V_{1/2}$ of fast activation for WT (-77.5 ± 1.4 mV; $n = 11$), was statistically different ($p < 0.05$) from those of I1461T (-60.8 ± 0.6 mV; $n = 14$) and T1464I (-63.7 ± 1.6 mV; $n = 11$). The $V_{1/2}$ of fast inactivation values for the I1461T and T1464I mutant channels were not statistically different. In addition, the slope for the fast inactivation curve for WT (7.09 ± 0.1 mV⁻¹; $n = 11$), was statistically different from the slopes of the I1461T (5.68 ± 0.1 mV⁻¹; $n = 14$) and T1464I (5.53 ± 0.2 mV⁻¹; $n = 11$) fast inactivation curves ($p < 0.05$ one-way ANOVA followed by a Tukey's comparison test). The slopes of the I1461T and T1464I steady-state inactivation curves did not significantly differ.

The protocol shown in Figure 23B was used to test the effects of I1461T and T1464I mutations on the slow inactivation properties of the Na_v1.7 channel. The Na_v1.7 channel produced a slow inactivation profile containing two distinct components that were fit with a double Boltzmann function instead of a single (Figure 23D). The first component of Na_v1.7 slow inactivation had a $V_{1/2}$ value of

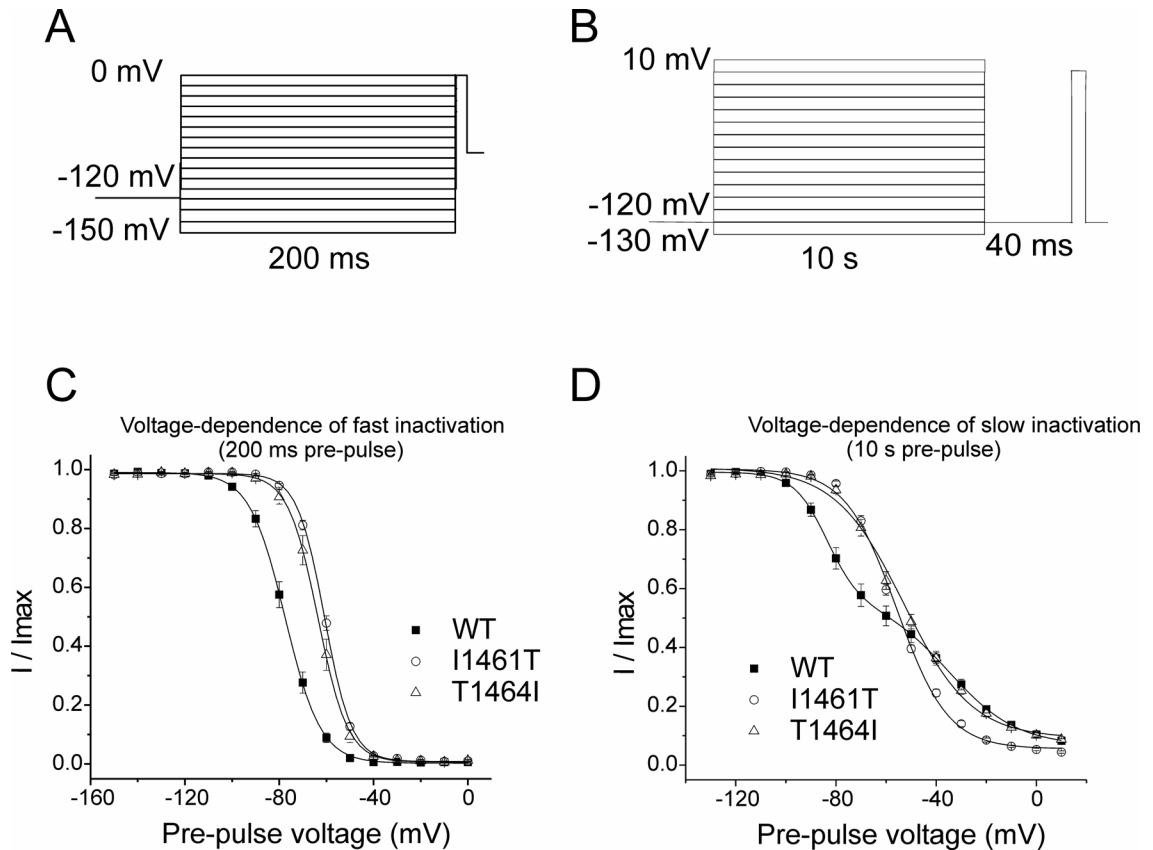


Figure 23. Effects of the I1461T and T1464I mutations on the inactivation properties of the Na_v1.7 channel. A, Protocol used to examine the voltage-dependence of fast inactivation for the Na_v1.7 channel. B, Protocol used to examine the voltage-dependence of slow inactivation for the Na_v1.7 channel. C, Voltage dependence of fast inactivation for the Na_v1.7 WT, I1461T, and T1464I channels. D, Voltage dependence of slow inactivation for the Na_v1.7 WT, I1461T, and T1464I channels. Slope factors of conductance-voltage and steady-state inactivation curves were calculated using the general single Boltzmann

function: $I / I_{\max} = \left(\frac{1}{1 + e^{(V - V_{0.5})/k}} \right)$ or double Boltzmann function:

$$I / I_{\max} = \left(\frac{1 - c}{1 + e^{(V - V_{0.51})/k_1}} \right) + \left(\frac{c}{1 + e^{(V - V_{0.52})/k_2}} \right)$$

-83.1 ± 1.6 mV (n = 11) and the second component had a $V_{1/2}$ value of -33.9 ± 1.5 mV (n = 11). The I1461T and T1464I mutations produced a profile that fits better with a single Boltzmann function giving $V_{1/2}$ values of -56.6 ± 0.7 mV (n = 14) and -53.5 ± 1.8 mV (n = 11), respectively (Figure 23D). The first and second $V_{1/2}$ values for the WT voltage-dependence of slow inactivation were statistically different ($p < 0.05$) from $V_{1/2}$ values for both the I1461T and T1464I channels. The $V_{1/2}$ values of slow activation for the I1461T and T1464I mutant channels were not statistically different. The slopes for the first ($6.08 \pm 0.2 \text{ mV}^{-1}$; n = 11) and second ($13.4 \pm 0.4 \text{ mV}^{-1}$; n = 11) components of slow inactivation curve for WT were statistically different ($p < 0.05$) from each other. The slopes of both the first and second component of slow inactivation for WT were statistically different ($p < 0.05$) from the slope of the I1461T ($10.1 \pm 0.4 \text{ mV}^{-1}$; n = 14) slow inactivation curve. However, only the slope of the first component for WT slow inactivation was statistically different ($p < 0.05$) from the slope the T1464I ($13.0 \pm 0.6 \text{ mV}^{-1}$; n = 11) slow inactivation curve. The slope of the second component for WT slow inactivation was not different from the slope the T1464I slow inactivation curve. These results demonstrate the voltage-sensitivity of slow inactivation for $\text{Na}_v1.7$ channels decreases as pulse voltages become more depolarized. With more depolarized voltages increasing the probability of channel opening, it is possible the voltage-dependence of slow inactivation for $\text{Na}_v1.7$ channels may differ between channels that have opened before inactivation and those that have not. The I1461T and T1464I mutations seem to eliminate this difference.

6. *PEPD mutations I1461T and T1464I alter the effects of lidocaine on slow inactivation of the Na_v1.7 channel but not fast inactivation*

The same protocols shown in Figure 23A and 23B were used to investigate the effects of 1 mM lidocaine on fast and slow inactivation properties of the Na_v1.7 WT, I1461T, and T1464I channels. The $V_{1/2}$ values were determined before and after application of lidocaine, and a control experiment was also performed to determine any time-dependent shifts in $V_{1/2}$ values. The average time-dependent effects are represented by the dotted lines in Figure 24, A thru F. All shifts in $V_{1/2}$ values caused by lidocaine were determined after accounting for the time-dependent shift observed in non-treated channels. Application of 1 mM lidocaine to WT channels caused hyperpolarizing shifts of -15.2 ± 1.9 mV ($n = 5$) in the $V_{1/2}$ of fast inactivation (Figure 24A). The slope factor of the fast inactivation curve for Na_v1.7 in the presence of lidocaine was 12.6 ± 0.6 mV⁻¹ ($n = 5$). Application of the same concentrations of lidocaine to I1461T and T1464I channels caused hyperpolarizing shifts in the $V_{1/2}$ of fast inactivation of -12.3 ± 0.5 mV ($n = 7$) and -13.2 ± 0.6 mV ($n = 6$), respectively (Figure 24, B and C). The shifts in the $V_{1/2}$ of fast inactivation caused by 1 mM lidocaine for the I1461T and T1464I channels were not statistically different ($p > 0.05$) from the shift observed in the WT channel. Following application of 1 mM lidocaine, the slope factors for of the fast inactivation curve for the I1461T and T1464I channels were 8.8 ± 0.2 mV⁻¹ and 7.6 ± 0.2 mV⁻¹, respectively. Both of these slope factors were significantly different ($p < 0.05$) from that observed in WT channels after application of 1 mM lidocaine. This indicates the I1461T and

T1464I mutations enhance the ability of lidocaine to increase the voltage sensitivity of Na_v1.7 inactivation gating while not affecting the overall shift in the voltage-dependence of fast-inactivation by lidocaine.

The effects of lidocaine on Na_v1.7 WT, I1461T, and T1464I channels were different using a slow inactivation protocol than those when using a fast inactivation protocol. As shown previously, WT channels display two components of slow inactivation (Figure 23D). The addition of 1 mM lidocaine hyperpolarized the $V_{1/2}$ value of the first component by -21.1 ± 0.6 mV to -108 ± 2.4 mV (Figure 24D). Lidocaine did not have a significant effect ($p > 0.05$; Student's unpaired t test) on the slope factor of the first component (6.6 ± 0.2 mV⁻¹; $n = 6$) compared to the slope factor of the first component in time-dependent control channels (6.08 ± 0.2 mV⁻¹; $n = 11$). The second component was nearly eliminated in the presence of lidocaine, comprising less than 7% of total normalized current (Figure 24D). When treating the I1461T and T1464I channels with 1 mM lidocaine, the slow inactivation profiles for the channels appear to change from having one component to two components (Figure 24, E and F). The first of the two components for I1461T and T1464I displayed $V_{1/2}$ values of -90.0 ± 1.1 mV ($n = 7$) and -93.7 ± 2.5 mV ($n = 6$), respectively (Figure 24, E and F). These values were significantly hyperpolarized compared to time-dependent control values of non-treated I1461T and T1464I channels ($p < 0.05$; Student's t test). The first of the two slow inactivation components for lidocaine treated I1461T and T1464I channels displayed hyperpolarizing shifts in $V_{1/2}$ values of -26.7 ± 1.3 mV ($n = 7$) and -33.0 ± 2.3 mV ($n = 6$), respectively

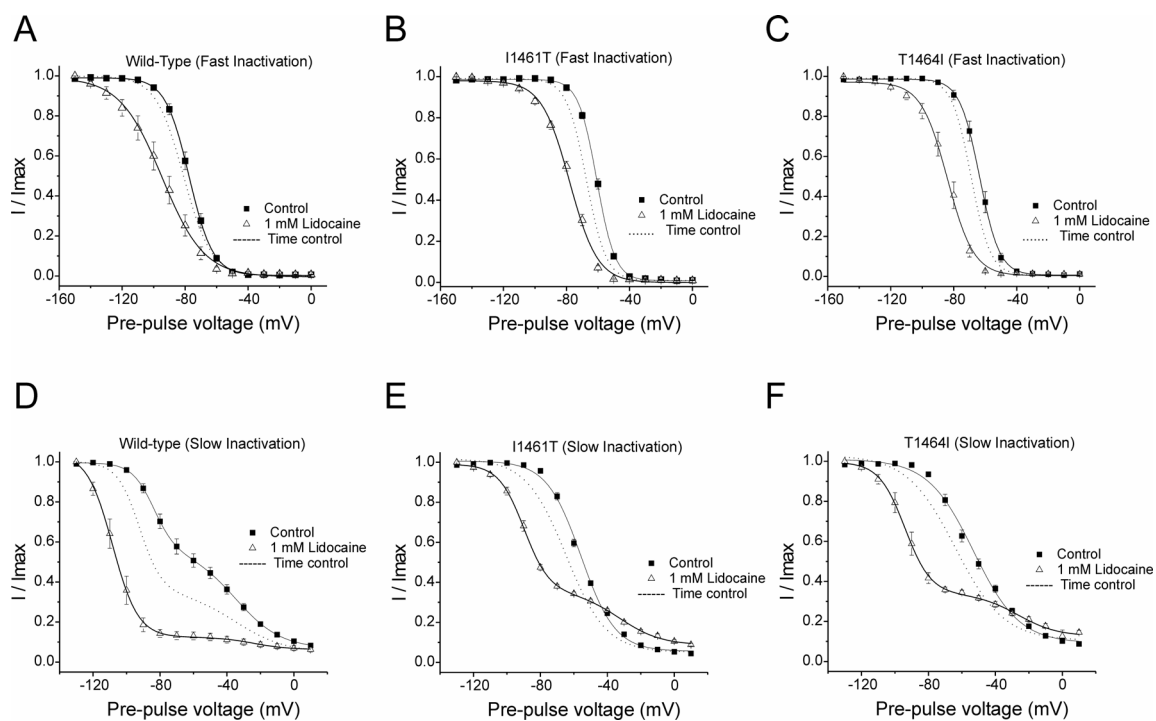


Figure 24. Effects of lidocaine on the fast and slow inactivation properties of the Na_v1.7 WT, I1461T, and T1464I channels. A thru C, effects of 1 mM lidocaine on the voltage-dependent properties of fast inactivation for Na_v1.7 WT (A), I1461T (B), and T1464I (C) channels. D thru F, effects of 1 mM lidocaine on the voltage-dependent properties of slow inactivation for Na_v1.7 WT (D), I1461T (E), and T1464I (F) channels. Traces represent inactivation profiles before and after lidocaine application. Time-dependent control values for each channel are represented by the dotted lines in each figure. Time-dependent recordings were obtained at the same time at which lidocaine would have been added to the bath solution.

(Figure 24, E and F). Both of these observed shifts were significantly larger than those observed in lidocaine treated WT channels ($p < 0.05$ for I1461T; $p < 0.05$ for T1464I; one-way ANOVA followed by a Tukey's comparison test). However, these shifts are difficult to interpret due to the I1461T and T1464I channels displaying only one slow inactivation component under control conditions.

The second of the two slow inactivation components for lidocaine treated I1461T and T1464I channels displayed lower voltage sensitivity to slow inactivation at depolarized potentials than non-treated channels (Figure 24, E and F). The second of the two components for I1461T and T1464I displayed $V_{1/2}$ values of -32.8 ± 1.2 mV ($n = 7$) and -30.1 ± 1.7 mV ($n = 5$), respectively (Figure 24, E and F). Since lidocaine eliminated the second component in the voltage-dependence of slow inactivation for WT channels, these $V_{1/2}$ values could not be compared to WT channels. However, these $V_{1/2}$ values were not significantly different from the $V_{1/2}$ value of the second component for non-treated WT channels. In addition these $V_{1/2}$ values were significantly depolarized compared to time-dependent control values of non-treated I1461T and T1464I channels ($p < 0.05$; Student's unpaired t test). The slope factors for the second of the two slow inactivation components for lidocaine treated I1461T (11.4 ± 0.5 mV⁻¹; $n = 7$) and T1464I channels (13.2 ± 1.0 mV⁻¹; $n = 5$) were not significantly different ($p > 0.05$; Student's unpaired t test) than the time-dependent slope factor values of non-treated I1461T (12.5 ± 0.5 mV⁻¹; $n = 7$) and T1464I channels (11.3 ± 1.0 mV⁻¹; $n = 5$) as well as the second component of non-treated WT channels (13.4 ± 0.4 mV⁻¹; $n = 11$). These findings suggest the presence of lidocaine produces

a voltage-dependence profile for I1461T and T1464I channels that is similar to non-treated WT channels.

7. PEPD mutations I1461T and T1464I decrease use-dependent inhibition of the Na_v1.7 channel by lidocaine

Since lidocaine is known to exhibit use-dependent inhibition of sodium currents, the use-dependent effects of lidocaine on the Na_v1.7 WT, I1461T, and T1464I channels were investigated by pulsing the transfected cells to -10 mV at a frequency of 5 Hz in the absence and presence of drug. Figure 25, A thru C displays representative traces of the effects of 1 mM lidocaine on the current amplitude when the channel is stimulated at high frequency. In the absence of lidocaine, Na_v1.7 WT, I1461T, and T1464I channels had decreases in current amplitudes evoked by the first pulse to the current amplitudes evoked by the last pulse of $20.5 \pm 2.5\%$ (n = 5), $22.3 \pm 2.0\%$ (n = 7), and $13.5 \pm 3.6\%$ (n = 5) respectively (Figure 25D). In the presence of 1 mM lidocaine decreases of $52.2 \pm 4.1\%$ (n = 6), $30.9 \pm 1.2\%$ (n = 7), and $31.6 \pm 1.5\%$ (n = 6) were observed for WT, I1461T, and T1464I, respectively (Figure 25D). All of these decreases in peak current amplitudes were significant compared to decreases observed in the time-dependent controls ($p < 0.05$; Student's t test). However, use-dependent decreases in current amplitude by lidocaine in I1461T and T1464I channels were significantly smaller than the decrease observed in the WT channel ($p < 0.05$; one-way ANOVA followed by a Tukey's comparison test).

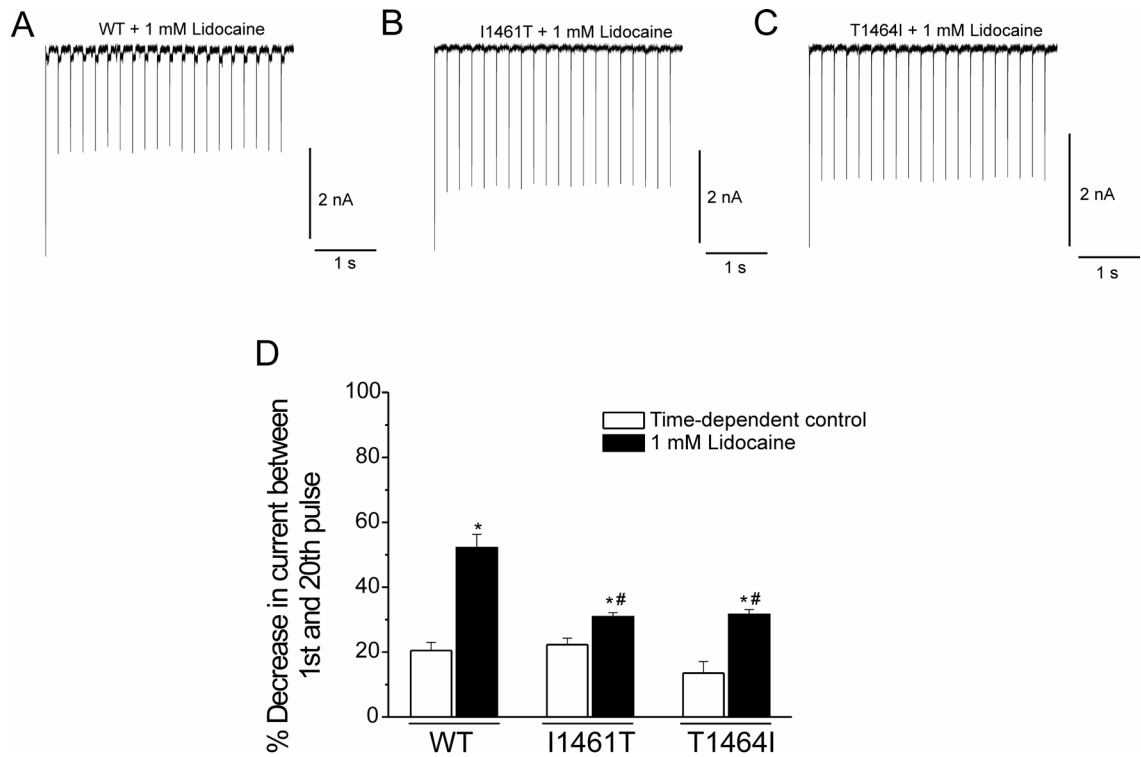


Figure 25. Use-dependent inhibition of $\text{Na}_v1.7$ WT, I1461T, and T1464I current by lidocaine. A thru C, representative traces of peak WT (A), I1461T (B), and T1464I (C) currents during high frequency stimulation in the presence of 1 mM lidocaine. D, ratio of peak WT, I1461T, and T1464I currents from the first pulse to the last pulse of the high frequency stimulation protocol for time-dependent controls and in the presence of 1 mM lidocaine. * represents a statistically significance difference from time-dependent controls. # represents a statistically significance difference WT lidocaine treated. Data are presented as mean % decrease in current between the 1st and 20th pulse \pm S.E.M (*/# = $p < 0.05$).

8. *The I1461T and T1464I mutations alter the recovery of Na_v1.7 channels from inactivation*

Since lidocaine decreased the transition of I1461T and T1464I to a slow-inactivated state at depolarized potentials, it was possible lidocaine enhances the ability of the I1461T and T1464I channel to recover after prolonged inactivation. Before this was determined, the recovery profile for I1461T and T1464I channels after being pulsed to -100 mV, -50 mV, or 0 mV for 10 s was established and compared to the recovery profile of WT channels. The protocol used for determining recovery profiles of I1461T and T1464I channels is shown in Figure 26A. Figure 26 (B thru D) shows the comparison of the recovery profile for I1461T and T1464I channels compared to wild-type channels. When pulsing I1461T (n = 4) and T1464I (n = 3) channels to -100 mV for 10 s, recovery from inactivation was similar to WT channels (Figure 26B). Table 6 displays tau values for recovery from fast inactivation for I1461T and T1464I channels compared to WT channels. These data indicate recovery from fast inactivation induced by -50 and 0 mV is faster for I1461T (n = 4) and T1464I (n = 3) channels than for WT channels. However, when pulsing at these voltages the effects of the I1461T and T1464I mutations on recovery from fast inactivation differ (Figure 26, C and D). For the T1464I channels, initial recovery from the -50 mV conditioning pulse is greater than observed in WT and I1461T channels while initial recovery from the 0 mV conditioning pulse was similar to that of WT, but still greater than that of I1461T channels (Figure 26, C and D).

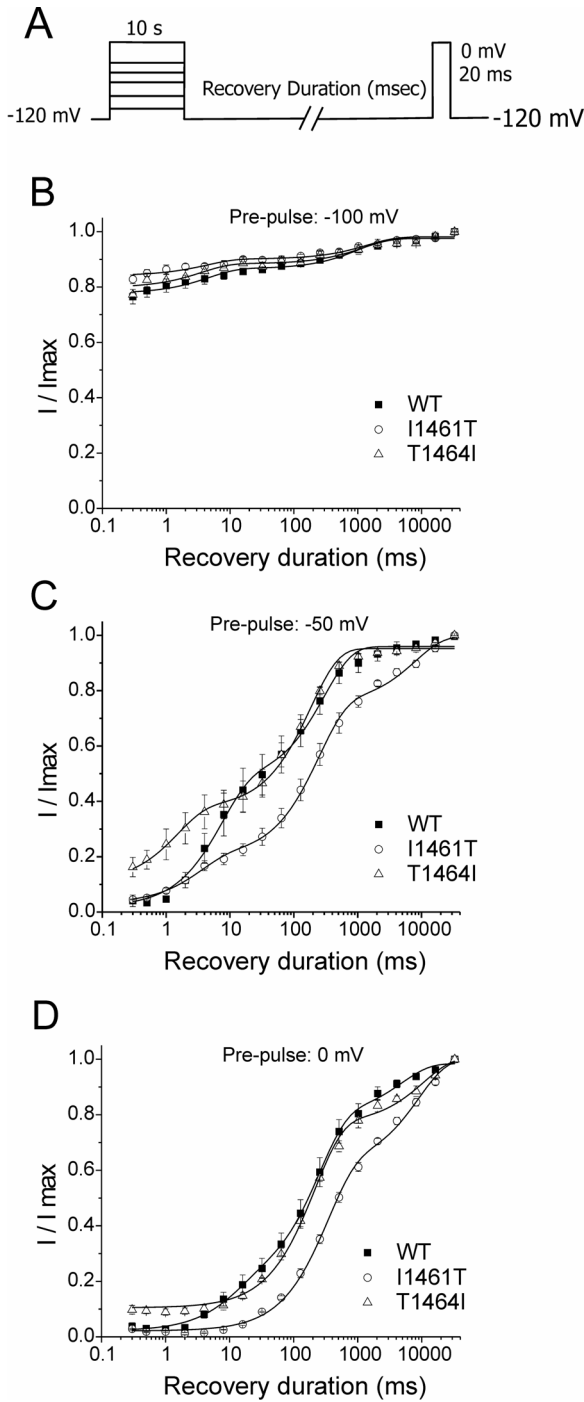


Figure 26. The effects of the I1461T and T1464I mutation on recovery from prolonged inactivation for $Na_v1.7$ channels. A, voltage protocol used to produce recovery from prolonged inactivation profiles for I1461T and T1464I $Na_v1.7$ channels. B—D, recovery profiles of $Na_v1.7$ WT, I1461T, and T1464I channels from different pre-pulse potentials. The pre-pulse value is given at the top of each graph. For these experiments, the channels were held at the indicated potential for 10 seconds before recovery pulses to -120 mV at various durations were elicited. This was followed by a 20 ms test pulse to 0 mV to test for available current. All profiles were fit with either a second or third-order exponential growth equation. All fits had $R^2 > 0.90$.

Table 6. Estimated time constants of recovery from fast inactivation for Na_v1.7 WT, I1461T, and T1464I channels.

Pre-pulse voltage (mV)	WT		I1461T		T1464I	
	Tau (ms)	A	Tau (ms)	A	Tau (ms)	A
-100 mV	4.6 +/- 1.6	0.14	4.3 +/- 1.7	0.11	3.6 +/- 1.6	0.09
-50 mV	7.3 +/- 1.2	0.45	3.3 +/- 0.7	0.19	1.5 +/- 0.3	0.40
0 mV	6.2 +/- 4.3	0.16	N/A	N/A	N/A	N/A

Values are means (\pm S.E.M.) estimated from the best fit line produced from the first component of a second or third-order exponential growth function. When pulsing to 0 mV, recovery for a fast-inactivated state was not observed for I1461T and T1464I channels. A = weight factor (of total recovered) for fraction recovered with time constant tau. Tau = time constant for the fast recovery of Na_v1.7 channels from inactivation.

For the I1461T channels pre-pulsed to -50 mV or 0 mV recovery from prolonged inactivation is slower than recovery observed in WT channels (Figure 26, C and D). This suggests the I1461T and T1464I mutations are altering the dynamics of fast inactivation by different means. One possibility is the I1461T mutation enhances the transition of Na_v1.7 to a slow-inactivated state in addition to the role it plays in impairing fast inactivation. The T1464 residue may only play a role in fast inactivation and does not affect the recovery of Na_v1.7 channels from the slow-inactivated state.

Table 7 displays tau values for recovery from the first slow inactivation component for I1461T and T1464I channels compared to WT channels. At -100 mV, there is some disparity in the estimated time constants of recovery for all three channels. However, Figure 26 shows there is very little transition to an inactivated state for I1461T and T1464I channels at -100 mV. This makes the comparison of tau values for all three channels at -100 mV difficult to interpret. A Interestingly, the recovery from the first slow inactivation component at potentials of -50 mV and 0 mV for I1461T was considerably delayed compared to WT channels (Figure 26, C and D). In contrast, recovery of T1464I channels from the first slow inactivation component at the same potentials was similar to WT (Figure 26, C and D). These data suggest the I1461T and T1464I mutations may affect the recovery of the Na_v1.7 channel from a closed slow-inactivated state in a similar manner while affecting the recovery from an open slow-inactivated state differently.

Table 7. Estimated time constants of recovery from the first slow inactivation component for Na_v1.7 WT, I1461T, and T1464I channels.

Pre-pulse voltage (mV)	WT		I1461T		T1464I	
	Tau (ms)	A	Tau (ms)	A	Tau (ms)	A
-100 mV	1046 +/- 300	0.11	1400 +/- 400	0.08	1200 +/- 470	0.09
-50 mV	301 +/- 43	0.49	243 +/- 20	0.57	185 +/- 15	0.58
0 mV	245 +/- 26	0.74	334 +/- 24	0.60	213 +/- 21	0.78

Values are means (\pm S.E.M.) estimated from the best fit line produced from the first component of a second or third-order exponential growth function. A = weight factor (of total recovered) for fraction recovered with time constant tau. Tau = time constant for the slow recovery of Na_v1.7 channels from inactivation.

9. *Lidocaine alters the recovery of I1461T and T1464I channels from inactivation differently than WT channels*

The effects of lidocaine on the recovery of I1461T and T1464I channels from inactivation were tested using the protocol shown in Figure 26A to determine if the I1461T and T1464I mutations alter the ability of Na_v1.7 to recover from lidocaine inhibition. After pulsing to -100 mV, lidocaine delayed recovery from inactivation for both I1461T (n = 3) and T1464I (n = 3) channels (Figure 27, A and D). After pulsing to -50 mV, lidocaine attenuated the fast recovery of T1464I (n = 3) channels but did not affect slow recovery compared to control conditions. However, after pulsing T1464I (n = 3) channels to 0 mV, recovery from slow inactivation becomes faster while recovery from fast inactivation is similar to control conditions (Figure 27, E and F). In contrast, lidocaine has little effect on the recovery of I1461T (n = 3) channels from fast inactivation after pulsing to -50 mV, but after pulsing to 0 mV, lidocaine enhances the recovery of I1461T (n = 3) channels from fast and slow inactivation (Figure 27, B and C).

To better understand how lidocaine may be interacting with WT channels, the information gathered on the effects of lidocaine on the recovery of I1461T and T1464I channels from inactivation was compared to the effects of lidocaine on the recovery of WT channels from inactivation. Lidocaine suppressed recovery from fast inactivation in WT channels to a greater extent than it did for

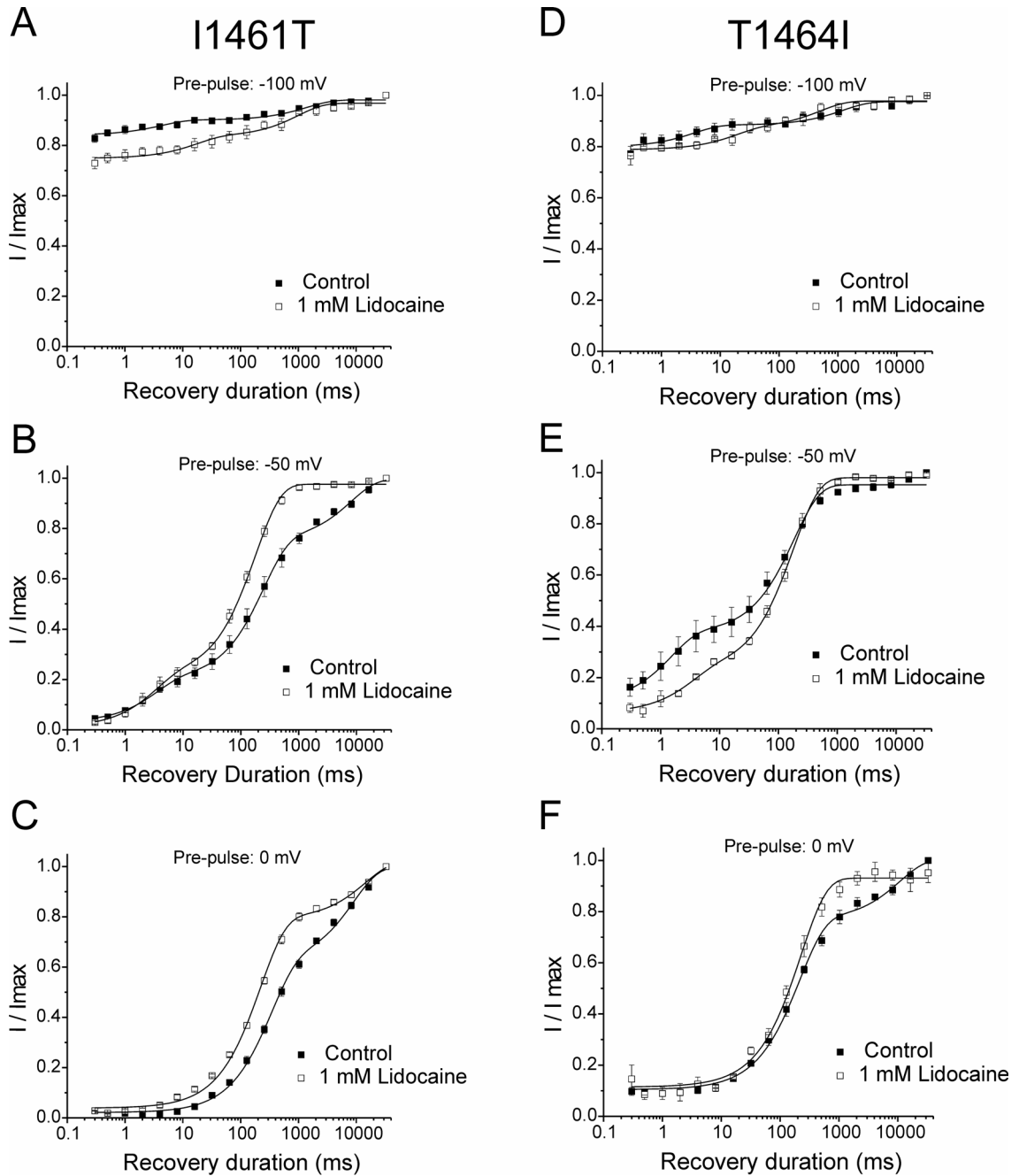


Figure 27. Lidocaine effects on recovery from prolonged inactivation at various potentials for $Na_v1.7$ channels having the I1461T or T1464I mutation. The protocol used for examining recovery from prolonged inactivation and lidocaine inhibition for I1461T and T1464I channels was the same as the one used in Figure 26A. The pre-pulse value (duration = 10 s) is given at the top of each graph. Under all conditions, the recovery profile was fit with a second-order exponential growth equation. All fits had $R^2 > 0.90$.

the I1461T and T1464I channels at -100 mV and -50 mV (Figure 28, A, B, D, and E). When recovering from 0 mV, the effect of lidocaine on recovery from inactivation is similar for T1464I and WT channels while recovery from inactivation for I1461T channels is attenuated at long recovery durations (Figure 28C). This implies at -100 mV and -50 mV, I1461T and T1464I mutations decrease the stabilization of lidocaine interaction with the fast-inactivated state of the Na_v1.7 channel and thus the recovery observed is a combination of channel recovery from a weaker lidocaine interaction and a less stable fast-inactivated state. At 0 mV, it is possible the I1461T mutation makes the channel more effective at transitioning to a slow-inactivated state in the presence of lidocaine. This is reflected in a lower magnitude of recovery compared to lidocaine treated WT channels.

10. The I1461T and T1464I mutations alter the onset of inactivation for Na_v1.7 channels

Using the protocol shown in Figure 29A, the onset of slow inactivation for I1461T and T1464I channels was compared to WT channels at -100 mV, -50 mV, and 0 mV. Table 8 displays the time constants for the onset of slow inactivation for the I1461T and T1464I channels compared to WT channels. As expected, pulsing I1461T and T1464I channels to -100 mV for increasing durations does not induce a significant transition to a slow-inactivated state (Figure 29B). Thus the small amount of recovery observed in Figure 26A is recovery of the I1461T and T1464I channels from a fast-inactivated state. The induction of slow inactivation is

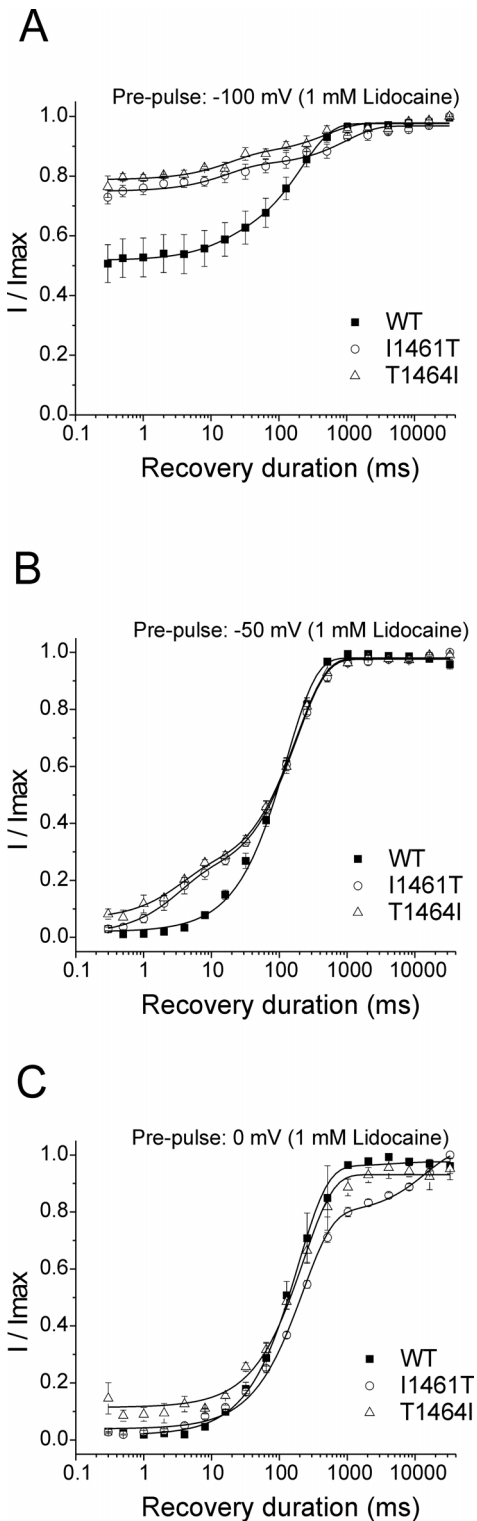


Figure 28. Comparison of lidocaine effects on the recovery from prolonged inactivation for WT, I1461T, and T1464I channels. A—C, recovery profiles of Na_v1.7 WT, I1461T, and T1464I channels from different pre-pulse potentials in the presence of 1 mM lidocaine. The pre-pulse value is given at the top of each graph. For these experiments, the channels were held at the indicated potential for 10 seconds before recovery pulses to -120 mV at various durations were elicited. This was followed by a 20 ms test pulse to 0 mV to test for available current. All profiles were fit with either a first or second-order exponential growth equation. All fits had $R^2 > 0.90$.

evident in I1461T and T1464I channels when pulsing to potentials of -50 mV and 0 mV (Figure 29, C and D). Although not significant, the initial fraction of slow-inactivated I1461T and T1464I channels appeared slightly attenuated compared to WT channels (Figure 29, C and D). However, the fraction of slow-inactivated channels is increased for I1461T and T1464I channels compared to WT channels as the durations become prolonged (-50 mV: > 10s, 0 mV: > 2s; Figure 29, C and D). Overall, the profile for the onset of slow inactivation for I1461T and T1464I channels are very similar. Interestingly, the recovery from inactivation profiles for I1461T and T1464I channels are much different in that recovery of I1461T channels after pulsing to potentials -50 and 0 mV was delayed compared to recovery of T1464I channels (Figure 26, C and D). This indicates the I1461T and T1464I mutations alter transition of Na_v1.7 to slow-inactivated state/s in a similar manner while affecting recovery from slow-inactivated state/s in a different manner.

11. The I1461T and T1464I mutations alter the onset of lidocaine inhibition for Na_v1.7 channels

Again using the protocol from Figure 29A, the effects of lidocaine on the onset of inactivation for I1461T and T1464I channels was tested. When pulsing to -100 mV, no lidocaine inhibition was observed for I1461T (n = 3) channels (Figure 30A). Only a small amount of lidocaine inhibition was observed for T1464I (n = 3) channels (Figure 30D). When pulsing to -50 mV, lidocaine inhibition of channel current was faster than the onset of slow inactivation for

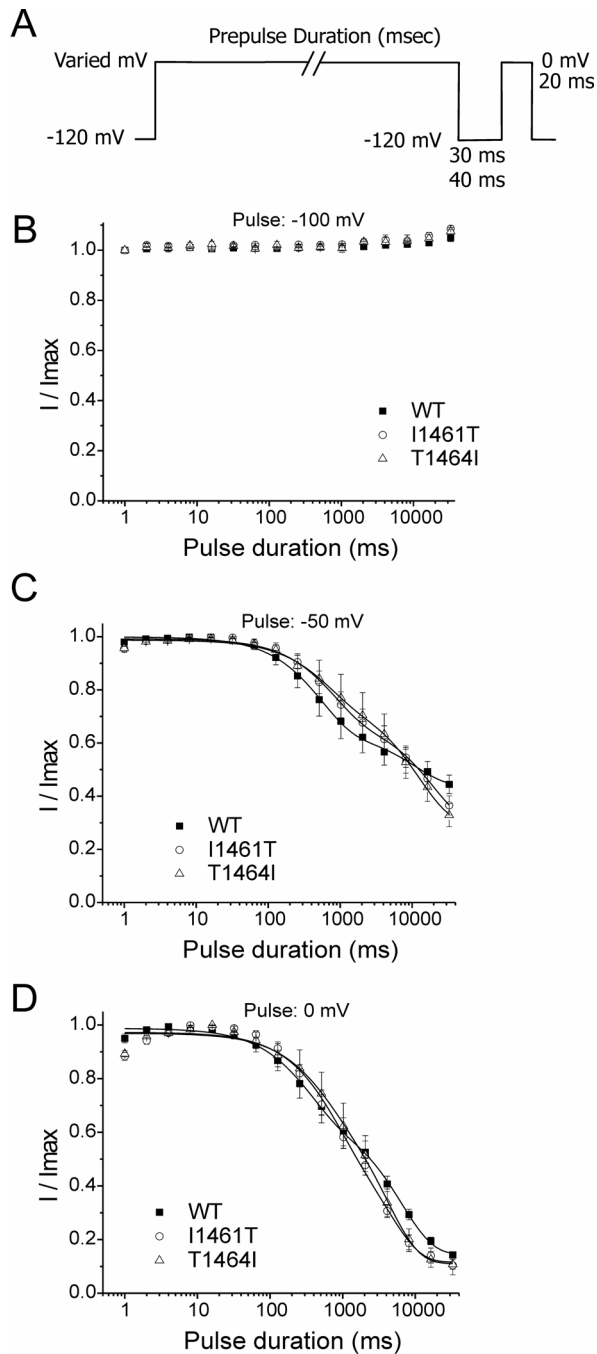


Figure 29. The effects of the I1461T and T1464I mutation on the onset of slow inactivation for $Na_v1.7$ channels. A, Voltage protocol used to obtain the onset of slow inactivation profiles for I1461T and T1464I $Na_v1.7$ channels. B—D, time course for the onset of slow inactivation for $Na_v1.7$ WT, I1461T, and T1464I channels from different pre-pulse potentials. The pre-pulse value is given at the top of each graph. For these experiments, the channels were held pulsed to the indicated potential for increasing durations before a recovery pulse to -120 mV for 30 or 40 ms was elicited. This was followed by a 20 ms test pulse to 0 mV to test for available current. All profiles were fit with a second-order exponential decay equation. All fits had $R^2 > 0.90$.

Table 8. Estimated time constants of the onset of slow inactivation for Na_v1.7 WT, I1461T, and T1464I channels.

Pre-pulse voltage (mV)	WT		I1461T		T1464I	
	Tau (ms)	A	Tau (ms)	A	Tau (ms)	A
-100 mV	N/A	N/A	N/A	N/A	N/A	N/A
-50 mV	540 +/- 50	0.45	800 +/- 130	0.37	640 +/- 130	0.32
0 mV	340 +/- 52	0.53	660 +/- 390	0.34	480 +/- 280	0.29

Values are means estimated from the best fit line produced from a second-order exponential growth function. The second-order exponential growth equation is as follows: $y = y_o + A_1e^{x/\tau_1} + A_2e^{x/\tau_2}$ where y_o = the initial value at time 0, A_1 = fraction of recovery at time τ_1 , A_2 = fraction of recovery at τ_2 , x = the growth constant, and τ_1 and τ_2 = time constant for the recovery of fast and slow-inactivated channels, respectively.

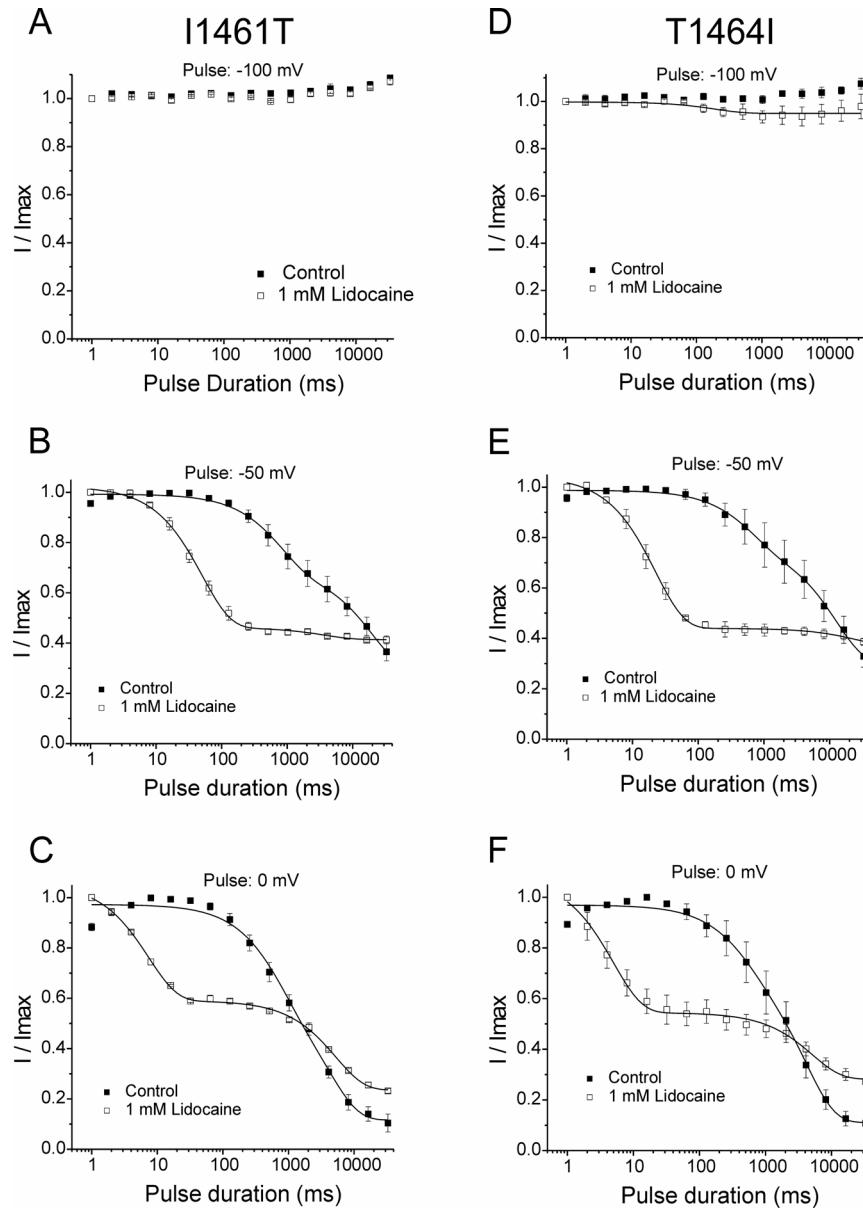


Figure 30. Lidocaine effects on the onset of slow inactivation at various potentials for $\text{Na}_v1.7$ channels having the I1461T or T1464I mutation. The protocol used for examining onset of slow inactivation and lidocaine inhibition for I1461T ($n = 3$) and T1464I ($n = 3$) channels was the same as the one used in Figure 19. The pulse value is given at the top of each graph. The recovery pulse for -100 mV was to -120 mV for 30 ms. The recovery pulse for -50 mV and 0 mV was to -120 mV for 40 ms. The onset of slow inactivation for I1461T (A) and T1464I (D), and the onset of lidocaine inhibition for I1461T (A) were not analyzed by curve fitting due to no decrease in current. All fits had $R^2 > 0.90$.

I1461T (n = 3) and T1464I (n = 3) channels (Figure 30, B and E). However, as the pulse duration reached close to 30 seconds, the magnitude of slow-inactivated channels exceeds the amount of channels inhibited by lidocaine (Figure 30, B and E). Consistent with results seen with WT channels, the rate of lidocaine inhibition for I1461T and T1464I channels reaches a plateau at approximately the same time that the onset of slow inactivation begins (Figure 30, B and E). When increasing the depolarizing pulse to 0 mV, the rate of lidocaine inhibition continued to be faster than the onset of slow inactivation for I1461T (n = 4) and T1464I (n = 3) channels (Figure 30, C and F). In addition, lidocaine inhibition for I1461T and T1464I channels reaches a plateau similar to that observed at -50 mV. However, at 0 mV a second component of current decay is observed in the presence of lidocaine for both I1461T and T1464I channels (Figure 30, C and F). This most likely represents the onset of a slow-inactivated state independent of lidocaine interaction with the channels. The magnitude of decrease in current of this second component was also less than that observed in control channels. This indicates lidocaine is impeding the transition of I1461T and T1464I channels to a second slow-inactivated state similar to that seen with WT channels. However, in control channels the transition to two separate slow-inactivated states at 0 mV is not observed (Figure 30, C and F).

The effects of lidocaine on the onset of inactivation for WT, I1461T, and T1464I channels were also compared (Figure 31). When pulsing to -100 mV, it is clear the I1461T and T1464I mutations decrease the ability of lidocaine to

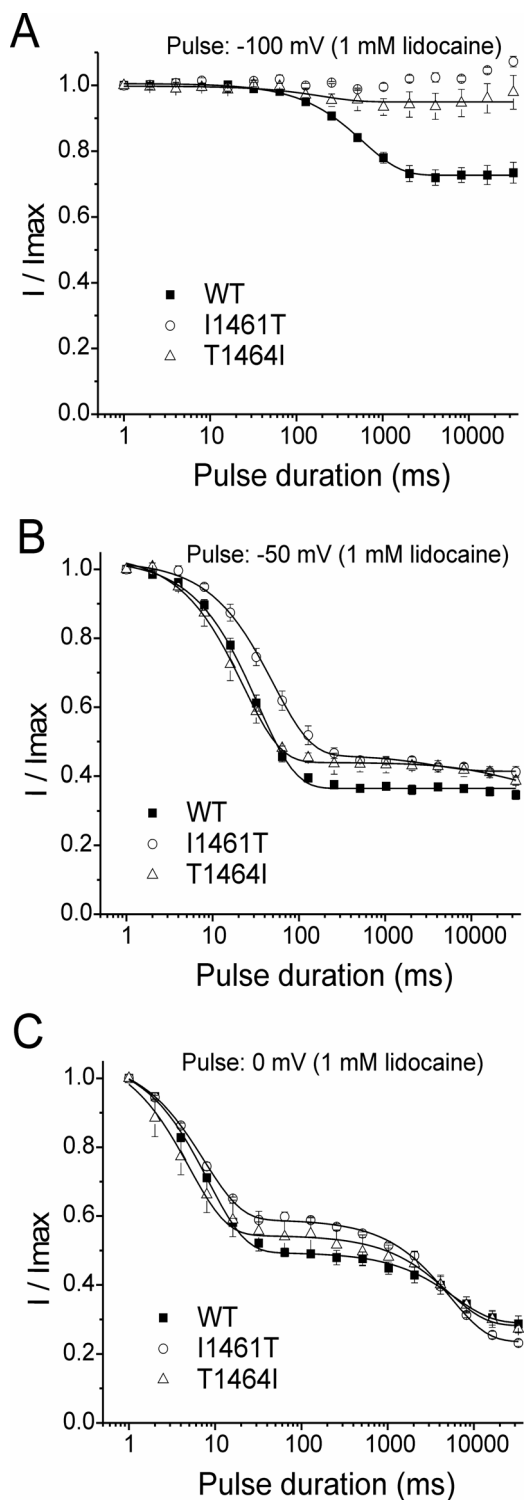


Figure 31. Comparison of lidocaine effects on the onset of slow inactivation for WT, I1461T, and T1464I channels. A—C, time course for the onset of slow inactivation for Na_v1.7 WT, I1461T (n = 3) and T1464I channels (n = 3) at different pre-pulse potentials in the presence of 1 mM lidocaine. The pre-pulse value is given at the top of each graph. For these experiments, the channels were held pulsed to the indicated potential for increasing durations before a recovery pulse to -120 mV for 30 or 40 ms was elicited. This was followed by a 20 ms test pulse to 0 mV to test for available current. All profiles were fit with either a first or second-order exponential decay equation. All fits had $R^2 > 0.90$.

produce channel inhibition (Figure 31A). The T1464I mutation did not change the initial enhancement of channel inhibition by lidocaine when pulsing to -50 mV (Figure 31B). However, as this pulse was extended the magnitude of inhibition was less for the T1464I channels than for WT channels (Figure 31B). In contrast, the I1461T mutation delayed the initial enhancement of channel inhibition by lidocaine as well as decreasing the magnitude of inhibition at prolonged durations at -50 mV (Figure 31B). The initial enhancement of channel inhibition by lidocaine did not seem to be affected by either mutation when pulsing to 0 mV (Figure 31C). The I1461T mutation did however decrease the magnitude of lidocaine inhibition at durations between 30 ms and 1000 ms (Figure 31C). As shown previously, lidocaine attenuates the fraction of WT channels inactivating at prolonged pulses (> 5 s) to 0 mV (Figure 19F). The T1464I mutation does not alter this transition compared to WT channels (Figure 31C). However, in the presence of lidocaine, the I1461T mutation enhances the magnitude of channels transitioning to a slow-inactivated state in the presence of lidocaine (Figure 31C). These results show that the I1461 and T1464 residues in Na_v1.7 channels are important in stabilizing the interaction of lidocaine with the channel. It also indicates the I1461 residue might be more important in this stabilization than the T1464 residue.

III. DISCUSSION

This dissertation focused primarily on 3 aspects of the electrophysiological and pharmacological properties of the neuronal VGSC subtype $\text{Na}_v1.7$. The first dealt with the possibility that the antipsychotic drug TFP could modulate $\text{Na}_v1.7$ currents through disruption of the CaM-channel interaction. Results showed TFP could directly interact with the $\text{Na}_v1.7$ through the LA binding site of the channel. The second aspect of this dissertation was an extension of the TFP findings which involved using a point mutation (N434K) in rat $\text{Na}_v1.4$ that affects LA and TFP interaction with VGSCs. The corresponding mutation in $\text{Na}_v1.7$ has been implicated in the painful neuropathy condition termed primary erythromelalgia. Therefore, it was predicted that the N395K mutation in $\text{Na}_v1.7$ alters electrophysiological properties of the channel as well as the interaction of lidocaine with the channel. The N395K $\text{Na}_v1.7$ channel displayed an altered electrophysiological profile as well as a decreased sensitivity to lidocaine. The third and final aspect of this dissertation investigated the interaction of the $\text{Na}_v1.7$ channel with the lidocaine. Findings indicate lidocaine decreases channel transition to slow inactivation and the fast inactivation gate (DIII-DIV linker) is necessary for stabilizing the interaction of lidocaine with the $\text{Na}_v1.7$ channel. Below is the detailed discussion of these results and how they impact $\text{Na}_v1.7$ pharmacology and electrophysiology.

A. Inhibition of Na_v1.7 and Na_v1.4 sodium channels by trifluoperazine (TFP)
involves the local anesthetic interaction site

In the first part of this dissertation, it was investigated whether the CaM inhibitor TFP can modulate Na_v1.7 and Na_v1.4 channels. Although these channels may exhibit very different affinities for binding CaM (Herzog et al., 2003b), TFP decreases current amplitude for both Na_v1.7 and Na_v1.4 and causes hyperpolarizing shifts in Na_v1.7 and Na_v1.4 steady-state inactivation while having no effect on the voltage-dependence of activation. TFP also had use-dependent inhibition effects on these channels which provides evidence that the predominant inhibitory effect of TFP is through interaction with the LA binding site of these channels. These data indicate only a minor component of the TFP effect is likely due to preventing CaM interaction with the channels. This dissertation further reveals the mechanism of TFP inhibition by identifying specific amino acid residues involved in the interaction of TFP on closed and inactivated Na_v1.4 channels.

The initial hypothesis for this work was blocking CaM interactions with the C-terminus of these channels by using TFP would influence the gating of the channels. However, the Na_v1.4 currents, which were dramatically inhibited by TFP, were largely unaffected by the specific CaM inhibitor, CaM inhibitory peptide, at high concentrations (1 μM; K_D = 6 pM). The CaM inhibitory peptide did show significant effects on Na_v1.7 steady-state inactivation, but the use-dependent effects were much smaller than those induced by TFP. This indicated while CaM could play a role in regulating steady-state inactivation of Na_v1.7, the

more profound effect of TFP on Na_v1.7 might be independent of CaM inhibition, suggesting TFP altered sodium currents through a different mechanism. Therefore, an alternative mechanism for the effects of TFP on Na_v1.7 and Na_v1.4 was investigated.

Previous studies have reported several phenothiazine neuroleptics structurally related to TFP can also block sodium currents in a use-dependent manner (Ogata et al., 1990; Bolotina et al., 1992; Liu et al., 1992; Ahmmed et al., 2002). However, the ability of TFP and these other neuroleptics to directly interact with sodium channels, and the molecular mechanism of this possible drug-channel interaction, has not previously been determined. LAs are known to produce hyperpolarizing shifts in steady-state inactivation and use-dependent inhibition of sodium currents by binding to a receptor site on the ion channel (Hille, 1977; Bean, et al., 1983). These studies and the observations of TFP causing hyperpolarizing shifts in steady-state inactivation, exhibiting a higher interaction with inactivated channels, and exhibiting a concentration independent recovery from inhibition led to the hypothesis that TFP might interact with Na_v1.7 and Na_v1.4 through the LA interaction site. To test this TFP inhibition was tested on channels having three separate mutations in the S6 segments that disrupt LA inhibition. The attenuation of the inhibitory effects of TFP on the N434K and F1579K mutant channel currents indicates these residues are important for the interaction of TFP with sodium channels and that TFP acts directly on the channel. Surprisingly, the inhibitory effects of TFP on L1280K mutant channel current were greater than (Figure 12B) or equal to (Figure 12A) the effects on

WT Na_v1.4. Although this is different from the effect the L1280K mutation has on LA and amitriptyline binding, it is consistent with the hypothesis the TFP binding site and the LA binding site overlap.

The results show TFP preferentially interacts with the inactivated state of voltage-gated sodium channels compared to the closed state. The N434K and F1579K mutant Na_v1.4 channels showed a significantly decreased mean response to 500 nM TFP in their inactivated state indicating the binding of TFP to the channel is reliant on these 2 residues when the channel is inactivated. Interestingly, the L1280K channel showed no significant difference in the apparent affinity of the inactivated state. However, inhibition of the L1280K channel in the closed state was potentiated compared to that of the wild-type, N434K, and F1579K channels. This result indicates the L1280K mutation enhances the interaction of TFP to the closed-state and not the inactivated state of the channel. Interestingly, it has been hypothesized the hydrophobic group of tertiary amine LAs interacts at the cytoplasmic mouth of the channel pore (Ragsdale et al., 1994). This interaction is believed to be through hydrophobic interactions (Butterworth and Strichartz, 1990) between the aromatic groups of the LA and Phe and Tyr residues at the mouth of the channel pore. However, it was further hypothesized mutating a Tyr residue (Y1586) in the Na_v1.4 channel pore to a positively charged Lys residue could induce a cation- π electron interaction (Heginbotham and MacKinnon, 1992) and increase the interaction of benzocaine with the channel (Wright et al., 1998). Therefore, it is possible that the L1280K mutation has somehow created an additional interaction site on the

resting Na_v1.4 channel for one of the aromatic moieties of TFP. This might explain the increased inhibitory effects of TFP on the resting state of the Na_v1.4. However, further experiments, such as mutating the L1280 residue to an alanine, would be necessary to confirm this possibility.

The data shows Na_v1.4 in its inactivated state displays high interaction with TFP and the N434 and F1579 residues are important for this high interaction of TFP to the inactivated state of the sodium channel. Furthermore, these results show that the L1280 residue has less involvement in the binding of TFP to the inactivated state of the channel than residues N434 and F1579. However, these results also show that out of the N434, L1280, and F1579 residues, only the L1280 residue is important for TFP binding to the closed-state of voltage-gated sodium channels. This is consistent with the L1280 residue being accessible by TFP in the closed-state while moving to an inaccessible position during activation and/or inactivation.

Due to conserved homology between the Na_v1.4 and Na_v1.7 LA binding site, it was hypothesized the inhibitory effects of TFP on human Na_v1.7 are due to direct interaction with this site. Direct interaction with neuronal sodium channels could help explain the finding that TFP injections in sciatic nerve produces motor and sensory blockade (Sheets et al., 2006). These findings were from experiments performed by Dr. Peter Gerner's laboratory in the Department of Anesthesiology at Brigham and Women's Hospital and Harvard Medical School. The nerve block by TFP was found to be robust and more potent than lidocaine suggesting that TFP or TFP analogs might be useful for

inducing prolonged nerve block. The ability of TFP to block $\text{Na}_v1.7$ at low doses could make it a potential therapeutic regimen for regional anesthesia and pain management that would be more potent than traditional local anesthetics.

Overall, these experiments show the inhibition of sodium current caused by TFP is largely independent of the inhibition of CaM. The majority of the inhibition by TFP can be attributed to direct interaction of the drug with the sodium channels in a state-dependent manner. Interestingly, TFP's label as a potent CaM inhibitor has resulted in its effects being commonly related to inhibition of the CaM/CaMKII pathway. Studies using TFP to inhibit CaM and its effectors could be overlooking the direct action of TFP on sodium channels. This inhibitory action might lead to inaccurate conclusions regarding CaM's involvement in physiological processes. More specifically, studies correlating CaM inhibition with nerve block using TFP could be demonstrating a direct interaction of TFP with voltage-gated sodium channels highly expressed in peripheral nerves.

B. A channel mutation associated with primary hereditary erythromelalgia (N395K) alters electrophysiological properties of $\text{Na}_v1.7$ in addition to decreasing channel sensitivity to the local anesthetic lidocaine

The decreased sensitivity of the N434K rat $\text{Na}_v1.4$ channel to TFP led to the design of the second part of this dissertation. As mentioned earlier, the N434K mutation in the rat $\text{Na}_v1.4$ channel decreased the inhibitory effects of LAs (Wang et al., 2004a; Nau and Wang, 2004). This same point mutation is found at

the homologous residue in the Na_v1.7 channel (N395K) and is implicated in the painful inherited neuropathy erythromelalgia (Drenth et al., 2005). Interestingly, one study showed treatment of primary erythromelalgia with lidocaine relieved pain in only 55% of afflicted patients (Davis and Sandroni, 2005). These findings gave basis for investigating the effects of the N395K mutation on lidocaine inhibition of the Na_v1.7 channel as well as the overall electrophysiological effects of this mutation on voltage-dependent properties of Na_v1.7.

Therefore, the second overall goal of this dissertation was to examine electrophysiological differences in Na_v1.7 caused by the N395K mutation. The hyperpolarizing shift in activation and slower onset of deactivation caused by N395K is similar to findings involving other hereditary erythromelalgia mutations (Cummins et al., 2004; Han et al., 2006; Harty et al., 2006). All of the other erythromelalgia mutations studied to date (F216S, S241T, I848T, L858H, L858F, F1449V, and A863P) shift the voltage-dependence of activation in the negative direction by 7 to 14 mV (Cummins et al., 2004; Dib-Hajj et al., 2005; Choi et al., 2006; Han et al., 2006; Harty et al., 2006; Lampert et al., 2006). All of the mutations, with the exception of F1449V, also slow deactivation, but they differ in the manner in which they affect deactivation. The N395K mutation, like the F216S mutation, simply shifts the voltage-dependence of the deactivation time constant curve in the negative direction in a manner that is consistent with the shift in activation. By contrast, many of the other mutations, such as the L858H mutation, alter deactivation in a more pronounced voltage-dependent fashion (see Figure 1D of Cummins et al., 2004). This suggests the different

erythromelalgia mutations alter $Na_v1.7$ gating in at least two distinct ways. The N395K mutation also caused impairment of steady-state slow inactivation which is seen with sodium channel mutations associated with disorders such as epilepsy, hyperkalemic periodic paralysis, and hereditary erythromelalgia (Cummins and Sigworth, 1996; Bendahhou et al., 1999; Bendahhou et al., 2002; Cummins et al., 2004; Rhodes et al., 2005). However, only the I848T and N395K erythromelalgia mutations impair slow inactivation. The F1449V mutation does not alter slow inactivation and the other erythromelalgia mutations enhance slow inactivation. This differential effect on slow inactivation might indicate that slow inactivation is not important for the pathophysiology of erythromelalgia. By contrast, the shift in activation is believed to decrease the threshold for action potential generation, leading to nociceptor hyperexcitability and chronic pain in erythromelalgia patients.

The third goal of this dissertation was to determine whether the N395K mutation changes the effects of lidocaine on $Na_v1.7$ current. The N395 residue is located in the S6 segment of domain I and was proposed to lie within the local anesthetic binding site of $Na_v1.7$. One study has shown lidocaine relieved pain in only 55% of erythromelalgia patients (Davis and Sandroni, 2005) raising the possibility that specific mutations such as N395K in $Na_v1.7$ might contribute to the unresponsiveness of some patients to lidocaine treatment. Therefore, the hypothesis was mutation of this residue would reduce the inhibitory effects of lidocaine on channel current. The results clearly demonstrate an attenuation of lidocaine inhibition on inactivated N395K channels at -50 mV. This reduction of

the lidocaine effect was seen at all concentrations tested including concentrations comparable to total lidocaine serum concentrations ($\sim 10\text{--}16\ \mu\text{M}$) that cause analgesia in neuropathic pain patients (Ferrante et al., 1996). Interestingly, the dose-response curve for lidocaine inhibition on $\text{Na}_v1.7$ WT inactivated channels showed there were potentially two distinct inhibition trends and was best fit using a two-site binding model. One possibility for this phenomenon is that holding the cell at $-50\ \text{mV}$ for prolonged periods of time causes a subset of channels to transition into a high affinity binding state and a subset into a low affinity binding state. These two distinct states could involve closed-state and open-state inactivation which may have different affinities for lidocaine. A recent study in the squid giant axon showed at $-50\ \text{mV}$ total inactivation is comprised of both closed-state and open-state inactivation (Armstrong, 2006). The possibility that the ratio of closed-state versus open-state inactivated channels during the prolonged $-50\ \text{mV}$ pre-pulse might explain the two-phase dose-inhibition curve for lidocaine on $\text{Na}_v1.7$ WT inactivated channels and was the focus of the final section of this thesis.

An alternative explanation for the two-phase dose-response of WT channels to lidocaine would be fast-inactivated and slow-inactivated states of $\text{Na}_v1.7$ interact differently with lidocaine. Indeed, one explanation for the reduction of lidocaine's effect on the N395K channel is the mutation impairs steady-state slow inactivation and thus there are fewer channels in the inactivated state. This could decrease the number of channels in a configuration that preferentially interact with lidocaine. However, F216S channels display

enhanced steady-state inactivation at -50 mV (Choi et al., 2006) and, in the present study, did not show enhanced inhibition with lidocaine in the inactivated state compared to wild-type. Furthermore, WT channels prepulsed to -70 mV for 30s and N395K channels prepulsed to -50 mV for 30s both have approximately 21% of their channels slow-inactivated (Figure 14B), yet WT channels still displayed a higher inhibition of channel current by lidocaine with a -70 mV prepulse than N395K channels with a -50 mV prepulse (data not shown). This indicates the N395K mutation in $Na_v1.7$ alters the direct interaction of lidocaine with the inactivated state of the channel, and suggests that changes in steady-state slow inactivation might not affect lidocaine inhibition of the channel. This was also investigated further in the final section of this thesis. In addition, the inhibitory effect of lidocaine at high concentrations on the resting N395K channel was reduced compared to the resting WT channel. This further confirms the N395K mutation affects the direct interaction of lidocaine with $Na_v1.7$ because the percentage of total channels in the resting state would be the same for N395K and WT using a -140 mV pre-pulse.

A recent study has reported loss of functional $Nav1.7$ channels in humans due to homozygous nonsense mutations leads to a complete inability to sense pain (Cox et al., 2006). Surprisingly, individuals with this profound inability to sense pain were deemed to be healthy in virtually every other way. Although $Na_v1.7$ is believed to be present in both sensory and sympathetic ganglion neurons, none of the individuals studied by Cox et al. exhibited symptoms of autonomic nervous system dysfunction. Furthermore, non-nociceptive sensory

functions appeared normal in the individuals with the homozygous nonsense mutations that eliminated functional Na_v1.7 currents. This study strongly indicates drugs that specifically target Na_v1.7 could have the potential to selectively ameliorate pain. Interestingly, it has been reported mice lacking Na_v1.7 and Na_v1.8 subtypes can develop neuropathic pain (Nassar et al., 2004) indicating Na_v1.7 may not be important in the production of neuropathic pain. To date, it has not been reported whether the humans lacking Na_v1.7 function can develop neuropathic pain. The fact that Na_v1.7 has not been implicated in neuropathic pain suggests the intriguing possibility these individuals may in fact have the ability to develop some type of neuropathic pain. Unfortunately, these individuals thus far have died very young (i.e. teenage years), and it is difficult to obtain this information at this time.

The variability in the response of erythromelalgia patients to local anesthetics that target sodium channels may be due, at least in part, to differing effects of the various hereditary erythromelalgia mutations in Na_v1.7 on lidocaine sensitivity. The data collected in this dissertation predicts the individuals with the N395K mutation are likely to be more resistant to lidocaine treatment than individuals with the F216S mutation. Genotype-phenotype correlations are needed to help determine if this is indeed the case. Although none of the other hereditary erythromelalgia mutations identified thus far are located in the local anesthetic binding site, the possibility that one or more of these mutations also alters lidocaine sensitivity merits examination in future experiments. Interestingly, all of the hereditary erythromelalgia mutations studied to date,

including the N395K mutation studied here, induce a hyperpolarizing shift in the voltage-dependence of activation of $\text{Na}_v1.7$ currents, suggesting this alteration is crucial to the development of the pain associated with hereditary erythromelalgia. It could be speculated other manipulations, such as phosphorylation, that might also induce hyperpolarizing shifts in activation could contribute to increased pain sensations. Thus observations on the N395K mutation gathered in this dissertation provide insight into the changes in $\text{Na}_v1.7$ channel activity contributing to abnormal pain sensations in erythromelalgia, and also suggest research focusing on the function and pharmacology of the $\text{Na}_v1.7$ channel is crucial to the understanding of pain pathophysiology and the advancement of pain management therapies.

C. Lidocaine stabilizes $\text{Na}_v1.7$ in a configuration that decreases transition to the slow-inactivated state of the channel

The two-site binding model gave a much better fit than the one-site binding model to the dose-response curve for lidocaine inhibition of $\text{Na}_v1.7$ channel current. This fit indicated there are two states of $\text{Na}_v1.7$ channels at -50 mV, one state exhibiting a high interaction with lidocaine and the other exhibiting a low interaction. To date there remains much debate as to the exact interaction of lidocaine with VGSCs. One explanation for the two-site binding model is the long pulse used to evaluate lidocaine inhibition of $\text{Na}_v1.7$ created fast and slow-inactivated configurations of the channel, and lidocaine interacts differently with these two states of the channel. Another possibility is a pulse to -50 mV creates

a mixture of closed-inactivated and open-inactivated configuration, and it is these two populations that have different interactions with lidocaine. A third potential explanation would be $\text{Na}_v1.7$ channels exist in a phosphorylated and unphosphorylated state in HEK293 cells and the interaction of lidocaine may be altered depending on the phosphorylation state of the channel.

The final hypothesis for this dissertation was the high affinity and low affinity populations represent channels in different inactivated conformations. Based on this hypothesis, the goals for the final part of this dissertation were to 1) determine how different inactivated conformations of $\text{Na}_v1.7$ affect lidocaine inhibition of the channel and 2) use PEPD mutations (I1461T and T1464I) that alter transitions between the different inactivated configurations of $\text{Na}_v1.7$ to determine how these alterations affect lidocaine's ability to inhibit channel current.

The first step in examining the effects of lidocaine on the $\text{Na}_v1.7$ channel was to establish recovery from fast and slow inactivation as well as from a lidocaine inhibited state. Recovery from fast and slow inactivation was dependent on the pulse potential used to inactivate the channels. The magnitude of channels recovering from inactivation became greater as the test pulse became more depolarized. Recovery from lidocaine inhibition displayed a single-exponential growth profile that was slower than the recovery from fast inactivation but faster than the recovery from slow inactivation. Interestingly, at depolarized conditioning pulse potentials (-50, -40 and 0 mV), the magnitude of recovery from lidocaine inhibited channels was greater than that observed for

slow-inactivated channels under control conditions. This suggests the interaction of lidocaine with $\text{Na}_v1.7$ is impairing the transition of the channel to a slow-inactivated state and, therefore following prolonged depolarizations, channels recover faster and are available for activation sooner in the presence of lidocaine. Lidocaine is likely stabilizing $\text{Na}_v1.7$ into a drug-channel confirmation that is energetically favorable and transition to a slow-inactivated state is less favorable.

Lidocaine also affects $\text{Na}_v1.7$ channels when using protocols that evaluate slow inactivation. Lidocaine increased the transition to a non-conducting state (likely a drug bound state) when compared to the onset of slow inactivation for $\text{Na}_v1.7$ channels (Figure 19, Tables 3 and 4). This was evident at all pulse potentials. After the initial fast decrease in current caused by lidocaine interaction with the channel, the inhibition levels off and very little additional drop in current is observed. This leveling off occurs at approximately the same time the onset of slow inactivation begins in control $\text{Na}_v1.7$ channels indicating transition to a slow-inactivated state possibly hinders further inhibition of channel current by lidocaine. This provides more evidence that lidocaine interacts with these fast-inactivated channels and transition to a slow-inactivated state is attenuated. This explains why in the presence of lidocaine 1) the $\text{Na}_v1.7$ current inhibition plateaus and 2) no additional decrease in $\text{Na}_v1.7$ current is observed due to slow inactivation. However, the second slow-inactivated state observed at very prolonged pulse durations still occurs in the presence of lidocaine demonstrating a slow-inactivated state of $\text{Na}_v1.7$ that can occur even with the

channel is the presence of lidocaine. However, these results did not answer if the initial slow-inactivated state is the low interaction configuration for lidocaine observed in the dose-response curve of Figure 15A. Thus, another approach was used to investigate this possibility.

The approach used to answer the hypothesis that the high lidocaine interaction and low lidocaine interaction states represent channels in different inactivated conformations was to observe the effects of different pulse potentials and durations (200 ms versus 10 s) on the dose-response relationship of lidocaine and Na_v1.7. The rationale was different pulse potentials would alter the fraction of channels in a closed fast-inactivated state versus open fast-inactivated state and different pulse durations would alter the proportion of fast versus slow-inactivated channels. However, the results suggest the two-site binding profile observed in Figure 15A for WT Na_v1.7 channels is not due to a mixture of closed fast-inactivated and open fast-inactivated channels. This is because at pulse potentials that would give a mixture of closed fast-inactivated and open fast-inactivated channels (i.e. -60, -50, and -40 mV) the dose-response relationship fits a one-site binding profile. This also indicates the increased potency of lidocaine caused by increased depolarization of the 200 ms pulse potential is due to a higher probability of the Na_v1.7 channel being in the fast-inactivated state irrespective of closed fast-inactivated versus open fast-inactivated.

The dose-response relationship of lidocaine and Na_v1.7 channels after being pulsed to various potentials for 10 s resulted in very different effects than those observed with the 200 ms pulse. The increase in pulse duration changed

the dose-response relationship from one-site binding profile to a two-site binding profile for all pulse potentials (Figure 20C). Surprisingly, as the pulse potentials become more depolarized the dose-response curves for the 10 s pulse and the 200 ms pulse intersect with higher lidocaine concentrations showing more inhibition on Na_v1.7 channels pulsed for 200 ms than ones pulsed for 10 s (e.g. Figure 21F). This suggests prolonging the pulse duration increases the probability of the Na_v1.7 channel transitioning to a slow-inactivated state that displays less interaction with lidocaine than does fast-inactivated channels.

An interesting finding is the estimated IC₅₀ value (4.3 mM) for lidocaine on resting Na_v1.7 channels (pulsed to -140 mV; Figure 15B) and the estimated IC₅₀ value (4.3 mM) for the second component of lidocaine inhibition on inactivated Na_v1.7 channels (pulsed to -50 mV; Figure 15A) are identical. The estimated IC₅₀ values for the second component of lidocaine inhibition on Na_v1.7 channels pulsed to various potentials for 10 s are also similar to the value observed for resting Na_v1.7. This indicates the pore configuration of Na_v1.7 channels in a slow-inactivated state may be similar to the pore configuration of resting channels.

As mention earlier, a recent study (Fertleman et al., 2006) reported three missense mutations in the SCN9A gene encoding for Na_v1.7 which are linked to PEPD, a familial rectal pain syndrome, do not cause a hyperpolarizing shift in activation, but rather impair fast inactivation. It is intriguing that Na_v1.7 mutations predominantly associated with rectal pain may consistently impair fast inactivation while mutations predominantly associated with burning pain

sensations in the hands and feet cause a hyperpolarizing shift in activation. Since PEPD mutations are thought to alter transitions between the different configurations of $\text{Na}_v1.7$, they can be used as tools to further understand the state-dependent inhibition of channel current by lidocaine. Two mutations implicated in PEPD, I1461T and T1464I, were inserted separately in the $\text{Na}_v1.7$ channel, and the effects of these mutations on channel function and lidocaine interaction were investigated. In contrast to what is observed in erythromelalgia mutations of $\text{Na}_v1.7$ channels, the I1461T and T1464I mutations showed no effect on the voltage-dependence of activation. However, the I1461T and T1464I mutations do decrease the ability of lidocaine to effectively inhibit channel current.

Since no affect of the I1461T and T1464I mutations could be observed on activation of $\text{Na}_v1.7$, it was likely this decrease in lidocaine inhibition of the channel was due to a decreased interaction with the inactivated state of the channel. These mutations lie within the DIII-DIV cytoplasmic linker and the attenuated voltage-dependence of fast inactivation and enhanced persistent component during inactivation for $\text{Na}_v1.7$ channels having either of the mutations confirms the importance of the DIII-DIV cytoplasmic linker in fast inactivation of VGSCs. The presence of a noticeable persistent component during the inactivation element of I1461T and T1464I current traces supports that these mutations attenuate the ability of the $\text{Na}_v1.7$ channel to completely inactivate. Interestingly, the I1461T and T1464I mutations did not affect the overall enhancement of fast-inactivation by lidocaine. Lidocaine created a similar shift in

the voltage-dependence of fast inactivation for WT, I1461T, and T1464I channels. Since these mutations do not lie within what is thought to be the LA interaction site of the channel, this means the interaction of lidocaine with the LA site must remain intact. But the question still remains as to why these mutant channels are displaying a decreased sensitivity to lidocaine? Thus, the effects of the I1461T and T1464I mutations on $\text{Na}_v1.7$ voltage-dependence of slow inactivation as well as lidocaine interaction with $\text{Na}_v1.7$ during slow inactivation protocols were examined.

The I1461T and T1464I mutations did affect the voltage-dependence of slow inactivation but in a very interesting manner. Both mutations caused attenuation in the extent of slow inactivation for $\text{Na}_v1.7$ channels at potentials ranging from -90 mV to -60 mV. However, once the pulse potential was depolarized to -50 mV or lower, the voltage-dependence of slow inactivation for I1461T channels was enhanced while T1464I channels displayed no difference from WT channels. Overall, the I1461T and T1464I mutations eliminate the two-phase profile for the voltage-dependence of slow inactivation of $\text{Na}_v1.7$ channels. This indicates the I1461 and T1464 residues play a role determining which slow-inactivated configuration the $\text{Na}_v1.7$ channel will be in at a given voltage.

Lidocaine enhances the voltage-dependence of slow inactivation/drug inhibition for I1461T and T1464I channels less than WT channels. In addition, this enhancement is only observed at potentials more hyperpolarized than -40 mV for both mutations. Thus, the presence of the I1461T and T1464I mutations alter lidocaine interaction with the channel after prolonged pulse durations and

allow for lidocaine to decrease the magnitude of channels transitioning to a slow-inactivated state at depolarized potentials compared to control channels. One thing to note is this protocol does have a repolarization step to allow for the relief of fast-inactivated channels which would involve the removal of the fast inactivation gate. Thus the I1461T and T1464I mutations may alter lidocaine interaction during the repolarization of the Na_v1.7 channel. This would explain why use-dependent decreases in current amplitude by lidocaine in I1461T and T1464I channels were significantly smaller than the decrease observed in the WT channel.

The time course of recovery from fast inactivation for I1461T and T1464I channels was slightly faster than that observed for WT channels after pre-pulsing to -100 mV for 10 s indicating the I1461T and T1464I channels are not stabilizing in a fast-inactivated state as completely as WT channels. Surprisingly, the I1461T channels recovered more slowly than WT channels after prolonged inactivation at -50 and 0 mV (Figure 26, C and D). By contrast the T1464I channels recover no differently than WT channels at the longer recovery durations (Figure 26, C and D). It has been hypothesized that fast inactivation state of VGSCs can decrease the transition of the channel to a subsequent slow inactivation state after alteration of the fast inactivation gate (DIII-DIV cytoplasmic linker) by intracellular proteolysis or mutation (Valenzuela and Bennett, Jr., 1994; Featherstone et al., 1996). Therefore, I1461T channels likely transition to the slow-inactivated state more readily due to a decreased ability of the channel to fast inactivate.

The effects of lidocaine on the recovery of I1461T and T1464I channels from inactivation were tested to further understand how lidocaine may be interacting with the $\text{Na}_v1.7$ channel. The most interesting observation was that lidocaine increases recovery of I1461T channels from from fast and slow inactivation (Figure 27, B and C). As shown in WT channels, at depolarized conditioning pulse potentials, the magnitude of recovery from lidocaine inhibited channels was greater than that observed for channels under control conditions, providing additional evidence that the interaction of lidocaine with $\text{Na}_v1.7$ is prohibiting the transition of the channel to a slow-inactivated state. The same can be suggested for the interaction of lidocaine with I1461T and T1464I channels. In addition, the delayed recovery of I1461T channels from lidocaine inhibition compared to WT channels (Figure 28C) shows that while lidocaine is delaying the transition to slow inactivation in WT channels, the I1461T mutation can attenuate this effect due to less stabilization of lidocaine interaction.

The I1461T and T1464I mutations also showed effects on the onset of slow inactivation in $\text{Na}_v1.7$ channels. As mentioned earlier, it is thought that decreasing the ability of the channel to stabilize in a fast-inactivated state may allow for a more effective transition to a slow-inactivated state. Thus, channels would transition to the slow-inactivated state more readily due to a decreased ability of the channel to fast inactivate. However, it was observed that I1461T and T1464I transition to a slow-inactivated state less than WT channels until reaching longer pulse durations where they slow-inactivated more. This suggests the $\text{Na}_v1.7$ channel's transition to an initial or first slow-inactivated state

is slightly hindered when the I1461 and T1464 are mutated. However, transition to the second slow-inactivated state seems to be enhanced when the same two mutations are present.

The main focus of these experiments was to investigate the effects of lidocaine on the onset of slow inactivation in $\text{Na}_v1.7$ channels. Interestingly, for the I1461T and T1464I channels an initial fast decrease in current caused by lidocaine interaction with the channel was observed, and just as with WT channels, the inhibition levels off and very little additional drop in current is observed (Figure 30). Yet, when the conditioning pulse is 0 mV, lidocaine seems to attenuate the transition of the I1461T and T1464I channels at prolonged durations. This demonstrates lidocaine is diminishing the transition of the channels to the potential second slow-inactivated state observed at prolonged pulse durations. When looking at the effects of lidocaine on the onset of lidocaine inhibition for WT, I1461T, and T1464I channels together, it is clear the I1461T and T1464I mutations decrease the magnitude of lidocaine inhibition. This once again demonstrates the I1461 and T1464 residues in $\text{Na}_v1.7$ channels are critical in stabilizing the interaction of lidocaine with the channel. The observation that the T1464I mutation does not have an effect on the initial onset of lidocaine inhibition shows that the T1464 residue, while critical for fast inactivation, may not be as important in lidocaine stabilization as the I1461 residue.

Taken together, these data suggest that while the closure of the fast inactivation gate is not absolutely necessary for lidocaine interaction with $\text{Na}_v1.7$,

the fast inactivation gate of Na_v1.7 is critical in the stabilization of the high lidocaine interaction with the channel. Figure 32 displays a theoretical schematic of how lidocaine interaction with the Na_v1.7 channel may be taking place. These data also show interaction of lidocaine with VGSCs can be altered by mutations that lie outside of the theoretical LA binding site of the channel. Moreover, the fact the channel mutations used in these final experiments are implicated in PEPD suggests LA treatment for these patients may be less effective.

The two-site binding model used to fit the dose-response curve for lidocaine inhibition of Na_v1.7 was likely a result of lidocaine having different affinities for the fast-inactivated configuration versus the slow-inactivated configuration of the channel. The explanation that lidocaine interacts with closed fast-inactivated and open fast-inactivated channels differently is unlikely due to dose-response curves using 200 ms conditioning pulses fitting better with a one-site binding profile. This also decreases the possibility that the interaction of lidocaine is altered due to different phosphorylated states of the channel which theoretically would be independent of pulse duration. However, differences in lidocaine interaction with Na_v1.7 due to phosphorylation of the channel was not tested directly and still needs to be examined. Overall, the results from the last aim of this dissertation indicate the interaction of lidocaine with Na_v1.7 creates a drug-channel confirmation that is energetically favorable compared to fast inactivation, and if lidocaine is bound, transition to a slow-inactivated state is less probable. Furthermore, Na_v1.7 channels in the initial slow-inactivated state may very well be in a confirmation that has a similar

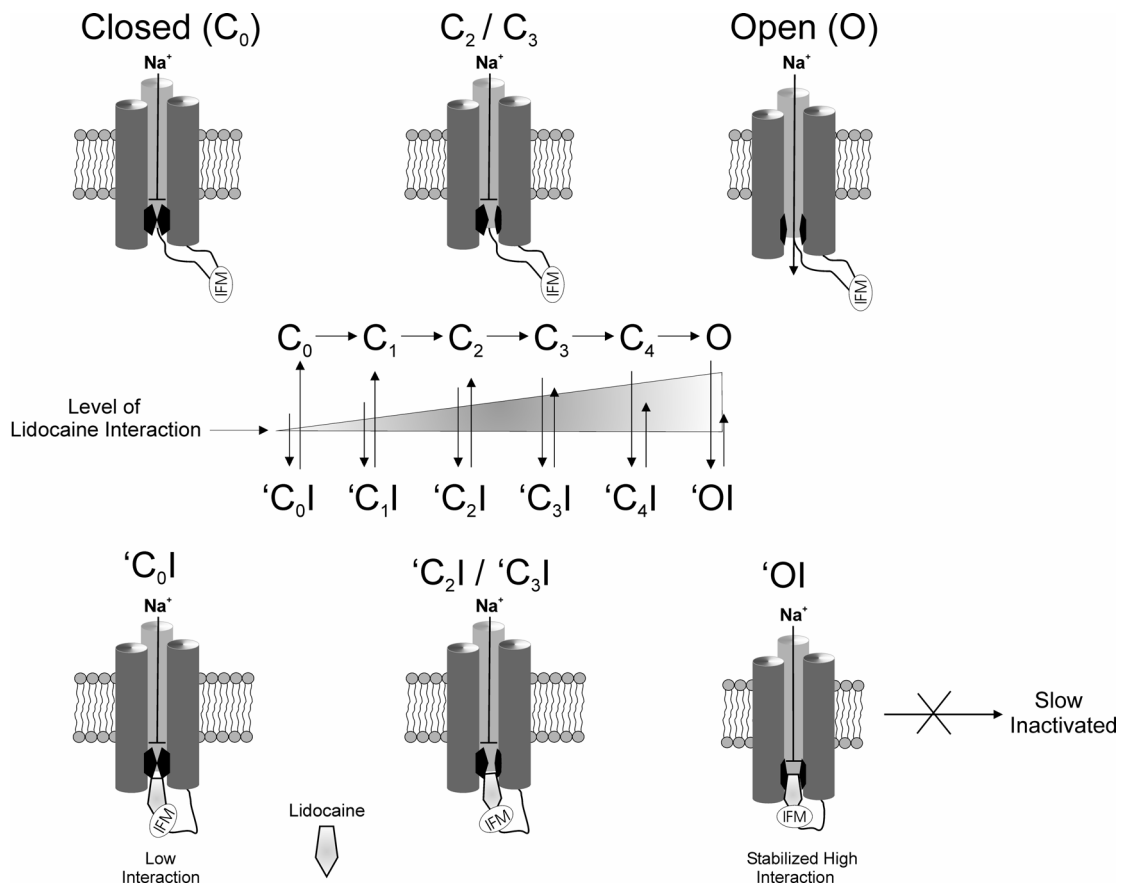


Figure 32. Theoretical schematic of lidocaine interaction with the Na_v1.7 channel. The top of the schematic represents simplified configurations of a Na_v1.7 channel at the instant before lidocaine interaction. The middle of schematic represents a modified form of the inactivation model (Armstrong and Gilly, 1979) with a theoretical level of lidocaine interaction with each state. As shown in the diagram as the channel transitions closer to the open state, the model suggests that lidocaine interaction increases. In addition, the model suggests recovery from the drug bound/inactivated ('C_i|' or 'O|') decreases as the channel transitions closer to the open state. In other words, the stabilization of lidocaine by the inactivation gate is greater when lidocaine can fully access its high affinity interaction site of the open channel. The bottom of the schematic represents simplified Na_v1.7 channel-lidocaine interactions induced from closed, partially activated (but still closed), and open channel configurations.

lidocaine interaction site to resting channels. Thus, slow inactivation takes place in a region of the Na_v1.7 channel that is not important for lidocaine interaction at high concentration.

D. Summation and future directions

Results from this dissertation demonstrate 1) TFP inhibits Na_v1.7 channels through the LA interaction site, 2) the N395K mutation alters electrophysiological properties of Na_v1.7 and decreases channel sensitivity to the local anesthetic lidocaine, 3) lidocaine stabilizes Na_v1.7 in a configuration that decreases transition to the slow-inactivated state of the channel, and 4) the fast inactivation gate of Na_v1.7 is critical in the stabilization of the high lidocaine interaction with the channel. Overall, this dissertation answers important questions regarding the pharmacology of Na_v1.7 and provides insight into the changes in Na_v1.7 channel properties caused by point mutations that may contribute to abnormal pain sensations. The results of this dissertation on the function and pharmacology of the Na_v1.7 channel are crucial to the understanding of pain pathophysiology and will provide insight for the advancement of pain management therapies.

An extension of this dissertation would involve mutating the phenylalanine of the IFM peptide in the inactivation loop to a cysteine that could be modified by methanethiosulfonate (MTS) derivatives. This modification would interfere with the inactivation peptide reaching its interaction site in the channel pore thus eliminating fast inactivation. The effect of lidocaine in the presence and absence of MTS would provide further evidence to the importance of the inactivation gate

in lidocaine stabilization. Much is still unknown as to how the Na_v1.7 may be modified during inflammation or nerve injury including expression and/or posttranslational modification (i.e. phosphorylation). As shown by mutation, changing the voltage-dependent properties of the Na_v1.7 is a factor that can lead to aberrant activity of nociceptive neurons. Understanding potential modulation of Na_v1.7 brought on by inflammation, injury, or other conditions such as cancer or cancer treatment would be helpful in understanding how these conditions affect the activity of sensory neurons and potentially lead to pain. In addition, studies could be done to alter the phosphorylated states of VGSCs and observe the role of these states in the pharmacology of the channel. Furthermore, the structure-function relationship of the various gating mechanisms that VGSCs undergo also remains unclear. Mutagenesis of VGSCs, while insightful, does not truly answer what is structurally important for the transition between the different gating mechanisms. Molecular modeling has been helpful in this area, but until a complete crystal structure is produced for VGSCs, the structure-function relationship of the various gating mechanisms cannot be confirmed. Advancements in these areas would be important in designing more selective and adequate pain therapeutics.

Overall, this dissertation answers important questions regarding the pharmacology and biophysics of the Na_v1.7 channel. This channel is fascinating in that removal of its function in the human body leads to the inability to sense pain thus creating a captivating and potential target for the treatment of pain. Furthermore, the role of Na_v1.7 (and VGSCs in general) in human physiology

remains intriguing and a continued effort to understand these roles is a critical step in discovering new ways to improve the quality and longevity of life.

V. REFERENCE LIST

Ahmad S, Dahllund L, Eriksson AB, Hellgren D, Karlsson U, Lund PE, Meijer IA, Meury L, Mills T, Moody A, Morinville A, Morten J, O'donnell D, Raynoschek C, Salter H, Rouleau GA, Krupp JJ (2007) A stop codon mutation in SCN9A causes lack of pain sensation. *Hum Mol Genet* 16:2114-2121.

Ahmed GU, Hisatome I, Kurata Y, Makita N, Tanaka Y, Tanaka H, Okamura T, Sonoyama K, Furuse Y, Kato M, Yamamoto Y, Ogura K, Shimoyama M, Miake J, Sasaki N, Ogino K, Igawa O, Yoshida A, Shigemasa C (2002) Analysis of moricizine block of sodium current in isolated guinea-pig atrial myocytes. Atrioventricular difference of moricizine block. *Vascul Pharmacol* 38:131-141.

Akopian AN, Souslova V, England S, Okuse K, Ogata N, Ure J, Smith A, Kerr BJ, McMahon SB, Boyce S, Hill R, Stanfa LC, Dickenson AH, Wood JN (1999) The tetrodotoxin-resistant sodium channel SNS has a specialized function in pain pathways. *Nat Neurosci* 2:541-548.

Amaya F, Decosterd I, Samad TA, Plumpton C, Tate S, Mannion RJ, Costigan M, Woolf CJ (2000) Diversity of expression of the sensory neuron-specific TTX-resistant voltage-gated sodium ion channels SNS and SNS2. *Mol Cell Neurosci* 15:331-342.

Armstrong CM (2006) Na channel inactivation from open and closed states. *Proc Natl Acad Sci U S A* 103:17991-17996.

Armstrong CM, Gilly WF (1979) Fast and slow steps in the activation of sodium channels. *J Gen Physiol* 74:691-711.

Baer M, Best PM, Reuter H (1976) Voltage-dependent action of tetrodotoxin in mammalian cardiac muscle. *Nature* 263:344-345.

Baker MD, Bostock H (1997) Low-threshold, persistent sodium current in rat large dorsal root ganglion neurons in culture. *J Neurophysiol* 77:1503-1513.

Baker MD, Wood JN (2001) Involvement of Na⁺ channels in pain pathways. *Trends Pharmacol Sci* 22:27-31.

Balser JR, Nuss HB, Romashko DN, Marban E, Tomaselli GF (1996a) Functional consequences of lidocaine binding to slow inactivated sodium channels. *J Gen Physiol* 107: 643-658.

Balser JR, Nuss HB, Orias DW, Johns DC, Marban E, Tomaselli GF, Lawrence JH (1996b) Local anesthetics as effectors of allosteric gating. Lidocaine effects on inactivation-deficient rat skeletal muscle Na channels. *J Clin Invest* 98:2874-2886.

- Bean BP, Cohen CJ, Tsien RW (1983) Lidocaine block of cardiac sodium channels. *J Gen Physiol* 81:613-642.
- Beckh S, Noda M, Lubbert H, Numa S (1989) Differential regulation of three sodium channel messenger RNAs in the rat central nervous system during development. *EMBO J* 8:3611-3616.
- Bendahhou S, Cummins TR, Kula RW, Fu YH, Ptacek LJ (2002) Impairment of slow inactivation as a common mechanism for periodic paralysis in DIIIS4-S5. *Neurology* 58:1266-1272.
- Bendahhou S, Cummins TR, Tawil R, Waxman SG, Ptacek LJ (1999) Activation and inactivation of the voltage-gated sodium channel: role of segment S5 revealed by a novel hyperkalaemic periodic paralysis mutation. *J Neurosci* 19:4762-4771.
- Bennett PB, Valenzuela C, Chen LQ, Kallen RG (1995) On the molecular nature of the lidocaine receptor of cardiac Na⁺ channels. Modification of block by alterations in the alpha-subunit III-IV interdomain. *Circ Res* 77:584-592.
- Black JA, Dib-Hajj S, McNabola K, Jeste S, Rizzo MA, Kocsis JD, Waxman SG (1996) Spinal sensory neurons express multiple sodium channel alpha-subunit mRNAs. *Brain Res Mol Brain Res* 43:117-131.
- Bolotina V, Courtney KR, Khodorov B (1992) Gate-dependent blockade of sodium channels by phenothiazine derivatives: structure-activity relationships. *Mol Pharmacol* 42:423-431.
- Boucher TJ, Okuse K, Bennett DL, Munson JB, Wood JN, McMahon SB (2000) Potent analgesic effects of GDNF in neuropathic pain states. *Science* 290:124-127.
- Brock JA, McLachlan EM, Belmonte C (1998) Tetrodotoxin-resistant impulses in single nociceptor nerve terminals in guinea-pig cornea. *J Physiol* 512 (Pt 1):211-217.
- Brostrom CO, Wolff DJ (1981) Properties and functions of calmodulin. *Biochem Pharmacol* 30:1395-1405.
- Butterworth JF, Strichartz GR (1990) Molecular mechanisms of local anesthesia: a review. *Anesthesiology* 72:711-734.
- Cahalan MD (1978) Local anesthetic block of sodium channels in normal and pronase-treated squid giant axons. *Biophys J* 23:285-311.
- Catterall WA (2000) From ionic currents to molecular mechanisms: the structure and function of voltage-gated sodium channels. *Neuron* 26:13-25.

Chen Z, Ong BH, Kambouris NG, Marban E, Tomaselli GF, Balsler JR (2000) Lidocaine induces a slow inactivated state in rat skeletal muscle sodium channels. *J Physiol* 524 Pt 1:37-49.

Chevrier P, Vijayaragavan K, Chahine M (2004) Differential modulation of Nav1.7 and Nav1.8 peripheral nerve sodium channels by the local anesthetic lidocaine. *Br J Pharmacol* 142:576-584.

Choi JS, Dib-Hajj SD, Waxman SG (2006) Inherited erythromelgia: limb pain from an S4 charge-neutral Na channelopathy. *Neurology* 67:1563-1567.

Courtney KR (1975) Mechanism of frequency-dependent inhibition of sodium currents in frog myelinated nerve by the lidocaine derivative GEA. *J Pharmacol Exp Ther* 195:225-236.

Cox JJ, Reimann F, Nicholas AK, Thornton G, Roberts E, Springell K, Karbani G, Jafri H, Mannan J, Raashid Y, Al-Gazali L, Hamamy H, Valente EM, Gorman S, Williams R, McHale DP, Wood JN, Gribble FM, Woods CG (2006) An SCN9A channelopathy causes congenital inability to experience pain. *Nature* 444:894-898.

Crill WE (1996) Persistent sodium current in mammalian central neurons. *Annu Rev Physiol* 58:349-362.

Cummins TR, Aglieco F, Renganathan M, Herzog RI, Dib-Hajj SD, Waxman SG (2001) Nav1.3 sodium channels: rapid repriming and slow closed-state inactivation display quantitative differences after expression in a mammalian cell line and in spinal sensory neurons. *J Neurosci* 21:5952-5961.

Cummins TR, Dib-Hajj SD, Waxman SG (2004) Electrophysiological properties of mutant Nav1.7 sodium channels in a painful inherited neuropathy. *J Neurosci* 24:8232-8236.

Cummins TR, Howe JR, Waxman SG (1998) Slow closed-state inactivation: a novel mechanism underlying ramp currents in cells expressing the hNE/PN1 sodium channel. *J Neurosci* 18:9607-9619.

Cummins TR, Sigworth FJ (1996) Impaired slow inactivation in mutant sodium channels. *Biophys J* 71:227-236.

Cummins TR, Waxman SG (1997) Downregulation of tetrodotoxin-resistant sodium currents and upregulation of a rapidly repriming tetrodotoxin-sensitive sodium current in small spinal sensory neurons after nerve injury. *J Neurosci* 17:3503-3514.

Davis MD, Sandroni P (2005) Lidocaine patch for pain of erythromelalgia: follow-up of 34 patients. *Arch Dermatol* 141:1320-1321.

Deschenes I, Neyroud N, DiSilvestre D, Marban E, Yue DT, Tomaselli GF (2002) Isoform-specific modulation of voltage-gated Na(+) channels by calmodulin. *Circ Res* 90:E49-E57.

Dib-Hajj SD, Rush AM, Cummins TR, Hisama FM, Novella S, Tyrrell L, Marshall L, Waxman SG (2005) Gain-of-function mutation in Nav1.7 in familial erythromelalgia induces bursting of sensory neurons. *Brain* 128:1847-1854.

Dib-Hajj SD, Tyrrell L, Black JA, Waxman SG (1998) NaN, a novel voltage-gated Na channel, is expressed preferentially in peripheral sensory neurons and down-regulated after axotomy. *Proc Natl Acad Sci U S A* 95:8963-8968.

Djoughri L, Newton R, Levinson SR, Berry CM, Carruthers B, Lawson SN (2003) Sensory and electrophysiological properties of guinea-pig sensory neurones expressing Nav 1.7 (PN1) Na⁺ channel alpha subunit protein. *J Physiol* 546:565-576.

Drenth JP, te Morsche RH, Guillet G, Taieb A, Kirby RL, Jansen JB (2005) SCN9A mutations define primary erythromelalgia as a neuropathic disorder of voltage gated sodium channels. *J Invest Dermatol* 124:1333-1338.

England S, Bevan S, Docherty RJ (1996) PGE2 modulates the tetrodotoxin-resistant sodium current in neonatal rat dorsal root ganglion neurones via the cyclic AMP-protein kinase A cascade. *J Physiol* 495 (Pt 2):429-440.

Featherstone DE, Richmond JE, Ruben PC (1996) Interaction between fast and slow inactivation in Skm1 sodium channels. *Biophys J* 71:3098-3109.

Ferrante FM, Paggioli J, Cherukuri S, Arthur GR (1996) The analgesic response to intravenous lidocaine in the treatment of neuropathic pain. *Anesth Analg* 82:91-97.

Fertleman CR, Baker MD, Parker KA, Moffatt S, Elmslie FV, Abrahamsen B, Ostman J, Klugbauer N, Wood JN, Gardiner RM, Rees M (2006) SCN9A mutations in paroxysmal extreme pain disorder: allelic variants underlie distinct channel defects and phenotypes. *Neuron* 52:767-774.

Fozzard HA, Hanck DA (1996) Structure and function of voltage-dependent sodium channels: comparison of brain II and cardiac isoforms. *Physiol Rev* 76:887-926.

Fukuda K, Nakajima T, Viswanathan PC, Balser JR (2005) Compound-specific Na⁺ channel pore conformational changes induced by local anaesthetics. *J Physiol* 564:21-31.

Golbidi S, Moriuchi H, Irie T, Ghafghazi T, Hajhashemi V (2002) Involvement of calmodulin inhibition in analgesia induced with low doses of intrathecal trifluoperazine. *Jpn J Pharmacol* 88:151-157.

- Gold MS, Reichling DB, Shuster MJ, Levine JD (1996) Hyperalgesic agents increase a tetrodotoxin-resistant Na⁺ current in nociceptors. *Proc Natl Acad Sci U S A* 93:1108-1112.
- Goldberg Y, et al. (2007) Loss-of-function mutations in the Na(v)1.7 gene underlie congenital indifference to pain in multiple human populations. *Clin Genet* 71:311-319.
- Goldin AL (2001) Resurgence of sodium channel research. *Annu Rev Physiol* 63:871-894.
- Goldin AL (2002) Evolution of voltage-gated Na(+) channels. *J Exp Biol* 205:575-584.
- Grieco TM, Malhotra JD, Chen C, Isom LL, Raman IM (2005) Open-channel block by the cytoplasmic tail of sodium channel beta4 as a mechanism for resurgent sodium current. *Neuron* 45:233-244.
- Hamill OP, Marty A, Neher E, Sakmann B, Sigworth FJ (1981) Improved patch-clamp techniques for high-resolution current recording from cells and cell-free membrane patches. *Pflugers Arch* 391:85-100.
- Han C, Rush AM, Dib-Hajj SD, Li S, Xu Z, Wang Y, Tyrrell L, Wang X, Yang Y, Waxman SG (2006) Sporadic onset of erythromelgia: A gain-of-function mutation in Na(v)1.7. *Ann Neurol* 59:553-558.
- Harty TP, Dib-Hajj SD, Tyrrell L, Blackman R, Hisama FM, Rose JB, Waxman SG (2006) Na(V)1.7 mutant A863P in erythromelgia: effects of altered activation and steady-state inactivation on excitability of nociceptive dorsal root ganglion neurons. *J Neurosci* 26:12566-12575.
- Heginbotham L, MacKinnon R (1992) The aromatic binding site for tetraethylammonium ion on potassium channels. *Neuron* 8:483-491.
- Herzog RI, Cummins TR, Ghassemi F, Dib-Hajj SD, Waxman SG (2003a) Distinct repriming and closed-state inactivation kinetics of Nav1.6 and Nav1.7 sodium channels in mouse spinal sensory neurons. *J Physiol* 551:741-750.
- Herzog RI, Liu C, Waxman SG, Cummins TR (2003b) Calmodulin binds to the C terminus of sodium channels Nav1.4 and Nav1.6 and differentially modulates their functional properties. *J Neurosci* 23:8261-8270.
- Hille B (1977) Local anesthetics: hydrophilic and hydrophobic pathways for the drug-receptor reaction. *J Gen Physiol* 69:497-515.
- Hille B (1966) Common mode of action of three agents that decrease the transient change in sodium permeability in nerves. *Nature* 210:1220-1222.

Hille B (1968) Pharmacological modifications of the sodium channels of frog nerve. *J Gen Physiol* 51:199-219.

Hodgkin AL, Huxley AF (1952a) Currents carried by sodium and potassium ions through the membrane of the giant axon of *Loligo*. *J Physiol* 116:449-472.

Hodgkin AL, Huxley AF (1952b) The components of membrane conductance in the giant axon of *Loligo*. *J Physiol* 116:473-496.

Hodgkin AL, Huxley AF (1952c) The dual effect of membrane potential on sodium conductance in the giant axon of *Loligo*. *J Physiol* 116:497-506.

Hodgkin AL, Huxley AF (1952) A quantitative description of membrane current and its application to conduction and excitation in nerve. *J Physiol* 117:500-544.

Hong S, Morrow TJ, Paulson PE, Isom LL, Wiley JW (2004) Early painful diabetic neuropathy is associated with differential changes in tetrodotoxin-sensitive and -resistant sodium channels in dorsal root ganglion neurons in the rat 3. *J Biol Chem* 279:29341-29350.

Ichikawa M, Urayama M, Matsumoto G (1991) Anticalmodulin drugs block the sodium gating current of squid giant axons. *J Membr Biol* 120:211-222.

Isom LL (2001) Sodium channel beta subunits: anything but auxiliary. *Neuroscientist* 7:42-54.

Khodorov BI, Vornovitskii EG, Ignat'eva VB, Mukumov MR, Kitaigorodskaja GM (1976) [Mechanism of excitation and contraction uncoupling in frog and guinea pig myocardial fibers during block of slow sodium-calcium channels by compound D-600]. *Biofizika* 21:1024-1030.

Klugbauer N, Lacinova L, Flockerzi V, Hofmann F (1995) Structure and functional expression of a new member of the tetrodotoxin-sensitive voltage-activated sodium channel family from human neuroendocrine cells. *EMBO J* 14:1084-1090.

Kostyuk PG, Veselovsky NS, Tsyndrenko AY (1981) Ionic currents in the somatic membrane of rat dorsal root ganglion neurons-I. Sodium currents. *Neuroscience* 6:2423-2430.

Lampert A, Dib-Hajj SD, Tyrrell L, Waxman SG (2006) Size matters: Erythromelalgia mutation S241T in Nav1.7 alters channel gating. *J Biol Chem* 281:36029-36035.

Levin RM, Weiss B (1979) Selective binding of antipsychotics and other psychoactive agents to the calcium-dependent activator of cyclic nucleotide phosphodiesterase. *J Pharmacol Exp Ther* 208:454-459.

- Li HL, Galue A, Meadows L, Ragsdale DS (1999) A molecular basis for the different local anesthetic affinities of resting versus open and inactivated states of the sodium channel. *Mol Pharmacol* 55:134-141.
- Liu W, Clarkson CW, Yamasaki S, Chang C, Stolfi A, Pickoff AS (1992) Characterization of the rate-dependent effects of ethmozine on conduction, in vivo, and on the sodium current, in vitro, in the newborn heart. *J Pharmacol Exp Ther* 263:608-616.
- Lossin C, Rhodes TH, Desai RR, Vanoye CG, Wang D, Carniciu S, Devinsky O, George AL, Jr. (2003) Epilepsy-associated dysfunction in the voltage-gated neuronal sodium channel SCN1A. *J Neurosci* 23:11289-11295.
- Lossin C, Wang DW, Rhodes TH, Vanoye CG, George AL, Jr. (2002) Molecular basis of an inherited epilepsy. *Neuron* 34:877-884.
- Marban E, Yamagishi T, Tomaselli GF (1998) Structure and function of voltage-gated sodium channels. *J Physiol* 508 (Pt 3):647-657.
- Matzner O, Devor M (1994) Hyperexcitability at sites of nerve injury depends on voltage-sensitive Na⁺ channels. *J Neurophysiol* 72:349-359.
- Michiels JJ, te Morsche RH, Jansen JB, Drenth JP (2005) Autosomal dominant erythralgia associated with a novel mutation in the voltage-gated sodium channel alpha subunit Nav1.7. *Arch Neurol* 62:1587-1590.
- Mickus T, Jung H, Spruston N (1999) Properties of slow, cumulative sodium channel inactivation in rat hippocampal CA1 pyramidal neurons. *Biophys J* 76:846-860.
- Nassar MA, Stirling LC, Forlani G, Baker MD, Matthews EA, Dickenson AH, Wood JN (2004) Nociceptor-specific gene deletion reveals a major role for Nav1.7 (PN1) in acute and inflammatory pain. *Proc Natl Acad Sci U S A* 101:12706-12711.
- Nau C, Wang GK (2004) Interactions of local anesthetics with voltage-gated Na⁺ channels. *J Membr Biol* 201:1-8.
- Nau C, Wang SY, Strichartz GR, Wang GK (1999) Point mutations at N434 in D1-S6 of mu1 Na(+) channels modulate binding affinity and stereoselectivity of local anesthetic enantiomers. *Mol Pharmacol* 56:404-413.
- Nau C, Wang SY, Wang GK (2003) Point mutations at L1280 in Nav1.4 channel D3-S6 modulate binding affinity and stereoselectivity of bupivacaine enantiomers. *Mol Pharmacol* 63:1398-1406.

Noda M, Shimizu S, Tanabe T, Takai T, Kayano T, Ikeda T, Takahashi H, Nakayama H, Kanaoka Y, Minamino N, . (1984) Primary structure of *Electrophorus electricus* sodium channel deduced from cDNA sequence. *Nature* 312:121-127.

Ogata N, Tatebayashi H (1992) Slow inactivation of tetrodotoxin-insensitive Na⁺ channels in neurons of rat dorsal root ganglia. *J Membr Biol* 129:71-80.

Ogata N, Yoshii M, Narahashi T (1990) Differential block of sodium and calcium channels by chlorpromazine in mouse neuroblastoma cells. *J Physiol* 420:165-183.

Okuse K, Malik-Hall M, Baker MD, Poon WY, Kong H, Chao MV, Wood JN (2002) Annexin II light chain regulates sensory neuron-specific sodium channel expression. *Nature* 417:653-656.

Ong BH, Tomaselli GF, Balse JR (2000) A structural rearrangement in the sodium channel pore linked to slow inactivation and use dependence. *J Gen Physiol* 116:653-662.

Ragsdale DS, McPhee JC, Scheuer T, Catterall WA (1994) Molecular determinants of state-dependent block of Na⁺ channels by local anesthetics. *Science* 265:1724-1728.

Renganathan M, Dib-Hajj S, Waxman SG (2002) Na^v1.5 underlies the 'third TTX-R sodium current' in rat small DRG neurons. *Brain Res Mol Brain Res* 106:70-82.

Rhodes TH, Vanoye CG, Ohmori I, Ogiwara I, Yamakawa K, George AL, Jr. (2005) Sodium channel dysfunction in intractable childhood epilepsy with generalized tonic-clonic seizures. *J Physiol* 569:433-445.

Richmond JE, Featherstone DE, Hartmann HA, Ruben PC (1998) Slow inactivation in human cardiac sodium channels. *Biophys J* 74:2945-2952.

Ritchie JM, Rogart RB (1977) The binding of saxitoxin and tetrodotoxin to excitable tissue. *Rev Physiol Biochem Pharmacol* 79:1-50.

Ritchie JM, Rogart RB, Strichartz GR (1976) A new method for labelling saxitoxin and its binding to non-myelinated fibres of the rabbit vagus, lobster walking leg, and garfish olfactory nerves. *J Physiol* 261:477-494.

Ritter AM, Mendell LM (1992) Somal membrane properties of physiologically identified sensory neurons in the rat: effects of nerve growth factor 3. *J Neurophysiol* 68:2033-2041.

Rogart RB, Cribbs LL, Muglia LK, Kephart DD, Kaiser MW (1989) Molecular cloning of a putative tetrodotoxin-resistant rat heart Na⁺ channel isoform. *Proc Natl Acad Sci U S A* 86:8170-8174.

Roy ML, Narahashi T (1992) Differential properties of tetrodotoxin-sensitive and tetrodotoxin-resistant sodium channels in rat dorsal root ganglion neurons. *J Neurosci* 12:2104-2111.

Rush AM, Dib-Hajj SD, Liu S, Cummins TR, Black JA, Waxman SG (2006) A single sodium channel mutation produces hyper- or hypoexcitability in different types of neurons. *Proc Natl Acad Sci U S A* 103:8245-8250.

Sakmann B, Neher E (1984) Patch clamp techniques for studying ionic channels in excitable membranes. *Annu Rev Physiol* 46:455-472.

Sangameswaran L, Fish LM, Koch BD, Rabert DK, Delgado SG, Ilnicka M, Jakeman LB, Novakovic S, Wong K, Sze P, Tzoumaka E, Stewart GR, Herman RC, Chan H, Eglon RM, Hunter JC (1997) A novel tetrodotoxin-sensitive, voltage-gated sodium channel expressed in rat and human dorsal root ganglia. *J Biol Chem* 272:14805-14809.

Schwarz W, Palade PT, Hille B (1977) Local anesthetics. Effect of pH on use-dependent block of sodium channels in frog muscle. *Biophys J* 20:343-368.

Sheets MF, Hanck DA (2007) Outward stabilization of the S4 segments in domains III and IV enhances lidocaine block of sodium channels. *J Physiol* 582:317-334.

Sheets PL, Jackson JO, Waxman SG, Dib-Hajj SD, Cummins TR (2007) A Nav1.7 channel mutation associated with hereditary erythromelalgia contributes to neuronal hyperexcitability and displays reduced lidocaine sensitivity. *J Physiol* 581:1019-1031.

Sheets PL, Heers C, Stoehr T, Cummins TR (2007) Differential block of sensory neuronal voltage-gated sodium channels by lacosamide, lidocaine and carbamazepine. *JPET* (submitted).

Starmer CF, Grant AO (1985) Phasic ion channel blockade. A kinetic model and parameter estimation procedure. *Mol Pharmacol* 28:348-356.

Starmer CF, Grant AO, Strauss HC (1984) Mechanisms of use-dependent block of sodium channels in excitable membranes by local anesthetics. *Biophys J* 46:15-27.

Strichartz GR (1973) The inhibition of sodium currents in myelinated nerve by quaternary derivatives of lidocaine. *J Gen Physiol* 62:37-57.

Tan HL, Kupersmidt S, Zhang R, Stepanovic S, Roden DM, Wilde AA, Anderson ME, Balsler JR (2002) A calcium sensor in the sodium channel modulates cardiac excitability. *Nature* 415:442-447.

Taylor RE (1959) Effect of procaine on electrical properties of squid axon membrane. *Am J Physiol* 196:1071-1078.

Toledo-Aral JJ, Moss BL, He ZJ, Koszowski AG, Whisenand T, Levinson SR, Wolf JJ, Silos-Santiago I, Halegoua S, Mandel G (1997) Identification of PN1, a predominant voltage-dependent sodium channel expressed principally in peripheral neurons. *Proc Natl Acad Sci U S A* 94:1527-1532.

Trimmer JS, Cooperman SS, Tomiko SA, Zhou JY, Crean SM, Boyle MB, Kallen RG, Sheng ZH, Barchi RL, Sigworth FJ, . (1989) Primary structure and functional expression of a mammalian skeletal muscle sodium channel. *Neuron* 3:33-49.

Trimmer JS, Rhodes KJ (2004) Localization of voltage-gated ion channels in mammalian brain. *Annu Rev Physiol* 66:477-519.

Valenzuela C, Bennett PB, Jr. (1994) Gating of cardiac Na⁺ channels in excised membrane patches after modification by alpha-chymotrypsin. *Biophys J* 67:161-171.

Van Genderen PJ, Michiels JJ, Drenth JP (1993) Hereditary erythremalgia and acquired erythromelalgia. *Am J Med Genet* 45:530-532.

Vedantham V, Cannon SC (1999) The position of the fast-inactivation gate during lidocaine block of voltage-gated Na⁺ channels. *J Gen Physiol* 113:7-16.

Vijayaragavan K, Boutjdir M, Chahine M (2004) Modulation of Nav1.7 and Nav1.8 peripheral nerve sodium channels by protein kinase A and protein kinase C. *J Neurophysiol* 91:1556-1569.

Vilin YY, Makita N, George AL, Jr., Ruben PC (1999) Structural determinants of slow inactivation in human cardiac and skeletal muscle sodium channels. *Biophys J* 77:1384-1393.

Wang GK, Brodwick MS, Eaton DC, Strichartz GR (1987) Inhibition of sodium currents by local anesthetics in chloramine-T-treated squid axons. The role of channel activation. *J Gen Physiol* 89:645-667.

Wang GK, Russell C, Wang SY (2004a) State-dependent block of voltage-gated Na⁺ channels by amitriptyline via the local anesthetic receptor and its implication for neuropathic pain. *Pain* 110:166-174.

- Wang SY, Mitchell J, Moczydlowski E, Wang GK (2004b) Block of inactivation-deficient Na⁺ channels by local anesthetics in stably transfected mammalian cells: evidence for drug binding along the activation pathway. *J Gen Physiol* 124:691-701.
- Wang SY, Nau C, Wang GK (2000) Residues in Na⁽⁺⁾ channel D3-S6 segment modulate both batrachotoxin and local anesthetic affinities. *Biophys J* 79:1379-1387.
- Waxman SG, Kocsis JD, Black JA (1994) Type III sodium channel mRNA is expressed in embryonic but not adult spinal sensory neurons, and is reexpressed following axotomy. *J Neurophysiol* 72:466-470.
- Weskamp G and Otten U (1987) An Enzyme-Linked Immunoassay for Nerve Growth Factor (NGF): a Tool for Studying Regulatory Mechanisms Involved in NGF Production in Brain and in Peripheral Tissues. *J Neurochem* 48:1779-1786.
- West JW, Patton DE, Scheuer T, Wang Y, Goldin AL, Catterall WA (1992) A cluster of hydrophobic amino acid residues required for fast Na⁽⁺⁾-channel inactivation. *Proc Natl Acad Sci U S A* 89:10910-10914.
- Wright SN, Wang SY, Wang GK (1998) Lysine point mutations in Na⁺ channel D4-S6 reduce inactivated channel block by local anesthetics. *Mol Pharmacol* 54:733-739.
- Yang Y, Wang Y, Li S, Xu Z, Li H, Ma L, Fan J, Bu D, Liu B, Fan Z, Wu G, Jin J, Ding B, Zhu X, Shen Y (2004) Mutations in SCN9A, encoding a sodium channel alpha subunit, in patients with primary erythralgia. *J Med Genet* 41:171-174.
- Yarov-Yarovoy V, Brown J, Sharp EM, Clare JJ, Scheuer T, Catterall WA (2001) Molecular determinants of voltage-dependent gating and binding of pore-blocking drugs in transmembrane segment IIS6 of the Na⁽⁺⁾ channel alpha subunit. *J Biol Chem* 276:20-27.
- Yarov-Yarovoy V, McPhee JC, Idsvoog D, Pate C, Scheuer T, Catterall WA (2002) Role of amino acid residues in transmembrane segments IS6 and IIS6 of the Na⁺ channel alpha subunit in voltage-dependent gating and drug block. *J Biol Chem* 277:35393-35401.
- Yeh JZ (1978) Sodium inactivation mechanism modulates QX-314 block of sodium channels in squid axons. *Biophys J* 24:569-574.
- Yeh JZ, Oxford GS (1985) Interactions of monovalent cations with sodium channels in squid axon. II. Modification of pharmacological inactivation gating. *J Gen Physiol* 85:603-620.

Yeomans DC, Levinson SR, Peters MC, Koszowski AG, Tzabazis AZ, Gilly WF, Wilson SP (2005) Decrease in Inflammatory Hyperalgesia by Herpes Vector-Mediated Knockdown of Na(v)1.7 Sodium Channels in Primary Afferents. *Hum Gene Ther* 16:271-277.

Yu FH, Westenbroek RE, Silos-Santiago I, McCormick KA, Lawson D, Ge P, Ferriera H, Lilly J, DiStefano PS, Catterall WA, Scheuer T, Curtis R (2003) Sodium channel beta4, a new disulfide-linked auxiliary subunit with similarity to beta2. *J Neurosci* 23:7577-7585.

Zhang YH, Vasko MR, Nicol GD (2002) Ceramide, a putative second messenger for nerve growth factor, modulates the TTX-resistant Na(+) current and delayed rectifier K(+) current in rat sensory neurons. *J Physiol* 544:385-402.

Zhou Z, Davar G, Strichartz G (2002) Endothelin-1 (ET-1) selectively enhances the activation gating of slowly inactivating tetrodotoxin-resistant sodium currents in rat sensory neurons: a mechanism for the pain-inducing actions of ET-1. *J Neurosci* 22:6325-6330.

CIRRICULUM VITAE

Patrick L. Sheets

EDUCATION

- August 2003—December 2007
Indiana University, Indianapolis, IN
Department of Pharmacology and Toxicology
Doctor of Philosophy
- August 2001—August 2003
Purdue University, West Lafayette, IN
School of Health Sciences
Master of Science in Industrial Hygiene/Toxicology
- August 1997—May 2001
Purdue University, West Lafayette, IN
School of Health Sciences
Bachelor of Science in General Health Science

PUBLICATIONS

1. Sheets PL, Heers C, Stoehr T, Cummins TR. Differential block of sensory neuronal voltage-gated sodium channels by lacosamide, lidocaine and carbamazepine. *JPET* (submitted).
2. Cummins TR, Sheets PL, Waxman, SG. The roles of sodium channels in nociception: implications for mechanisms of pain. *Pain* 131(3): 243-257, 2007.
3. Sheets PL, Jackson JO, Waxman SG, Dib-Hajj SD, Cummins TR. A Na_v1.7 channel mutation associated with hereditary erythromelalgia contributes to neuronal hyperexcitability and displays reduced lidocaine sensitivity. *J Physiol.* 581 (Pt. 3): 1019-1031, 2007.
4. Sheets PL, Gerner P, Wang CF, Wang SY, Wang GK, Cummins TR. Inhibition of Na_v1.7 and Na_v1.4 sodium channels by trifluoperazine involves the local anesthetic receptor. *J Neurophysiol.* 96: 1848-1859, 2006.
5. Sheets P, Carlson G. Kinetic factors involved in the metabolism of benzene in mouse lung and liver. *Journal of Toxicology and Environmental Health.* 67(5): 421-430, 2004.

6. Sheets PL, Yost GS, Carlson GP. Benzene metabolism in human lung cell lines BEAS-2B and A549 and cells overexpressing CYP2E1. *Journal of Biochemical and Molecular Toxicology*. 18(2):92-99, 2004.

SELECTED PRESENTATIONS

1. Sheets PL, Jarecki BW, Jackson JO, Cummins TR. Erythromelalgia and Paroxysmal Pain Disorder Alter the Pharmacology of Na_v1.7 Channels. Society for Neuroscience National Meeting, San Diego, CA, November 2007 (to be completed). Poster Presentation.
2. Sheets PL, Jackson JO, Waxman SG, Dib-Hajj SD, Cummins TR. Reduced Lidocaine Sensitivity of a Mutant Na_v1.7 Sodium Channel Associated with Painful Hereditary Erythromelalgia. Society for Neuroscience Local Meeting, Indianapolis, IN, October 2006. Platform Presentation.
3. Sheets PL, Jackson JO, Waxman SG, Dib-Hajj SD, Cummins TR. Reduced Lidocaine Sensitivity of a Mutant Na_v1.7 Sodium Channel Associated with Painful Hereditary Erythromelalgia. Society for Neuroscience National Meeting, Atlanta, GA, October 2006. Poster Presentation.
4. Sheets PL and Cummins TR. Changes in the voltage-dependent kinetics of the Na_v1.7 channel induced by the general phosphatase inhibitor sodium orthovanadate. Society for Neuroscience National Meeting, Washington, DC, 2005. Poster Presentation.
5. Sheets PL, Gerner P, Wang CF, Wang SY, Wang GK, Cummins TR. Modulation of Na_v 1.4 and Na_v1.7 currents by calmodulin antagonists. Society for Neuroscience Indianapolis Chapter Meeting, Indianapolis, IN, 2005. Poster Presentation.
6. Sheets PL, Gerner P, Wang CF, Wang SY, Wang GK, Cummins TR. Modulation of Na_v 1.4 and Na_v1.7 currents by calmodulin antagonists. Society for Neuroscience National Meeting, San Diego, CA, 2004. Poster Presentation.
7. Sheets PL and Carlson G. Benzene Metabolism in the Mouse Lung and Liver by CYP2E1. American Industrial Hygiene Conference and Exposition, Dallas, TX 2003. Poster Presentation.
8. Sheets PL and McGlothlin J. An Ergonomic and Cardiovascular Evaluation of Beverage Delivery Workers during Beverage Delivery. American Industrial Hygiene Association Conference and Exposition, San Diego, CA, 2002. Platform Presentation.

SCHOLARSHIPS AND AWARDS

1. Indiana University School of Medicine Graduate Student Organization Travel Award for Outstanding Abstract, June 2007.
2. Society for Neuroscience Travel Award for Outstanding Abstract, October 2006.
3. Paul and Carole Stark Research Fellowship Recipient, September 2005—August 2006.
4. First place in poster competition: Society for Neuroscience Indianapolis Chapter Meeting. Indianapolis, IN, April 2005.
5. School of Health Sciences Distinguished Student Award for academic excellence, Purdue University, West Lafayette, IN, Spring 2002.

RESEARCH EXPERIENCE

1. Indiana University School of Medicine, Indianapolis, IN, April 2004—December 2007.
 - a) Department of Pharmacology & Toxicology—Ph.D. Thesis Project
 - b) Pharmacology and modulation of the neuronal Na_v1.7 voltage-gated sodium channel.
 - c) Mentor: Theodore Cummins, Ph.D.
2. Indiana University School of Medicine, Indianapolis, IN, December 2003—April 2004.
 - a) Department of Pharmacology & Toxicology—Research Rotation
 - b) Investigated the response of DRG neurons to capsaicin stimulation using calcium imaging.
 - c) Mentor: Gerry Oxford, Ph.D.
3. Indiana University School of Medicine, Indianapolis, IN, August 2003—November 2003.
 - a) Department of Pharmacology & Toxicology—Research Rotation
 - b) Assisted in the purification of TgGCN5, a histone acetyltransferase in *Toxoplasma gondii*.
 - c) Mentor: William Sullivan Jr., Ph.D.
4. Purdue University, West Lafayette, IN, June 2002—August 2003
 - a) School of Health Sciences—M.S. Thesis Project
 - b) Metabolism of Benzene in Mouse Lung and Liver and Human Lung Cell Lines by CYP2E1 and CYP2F2.
 - c) Mentor: Gary Carlson, Ph.D.

5. Purdue University, West Lafayette, IN, August 2001—June 2002
 - a) School of Health Sciences—Initial M.S. Research Project
 - b) Analyzed heart rate and labor activity of beverage-delivery workers using video-based ergonomic assessment.
 - c) Mentor: James McGlothlin, Ph.D.

PROFESSIONAL ACTIVITIES

1. Department of Pharmacology and Toxicology Student Seminar Series, Indiana University School of Medicine, Indianapolis, IN, 2005—2007.
 - a) Organized schedule, hosts, and structure of seminar series
2. Chair of Pharmacology and Toxicology Graduate Student Organization and Graduate Student Representative for Department of Pharmacology & Toxicology, Indiana University School of Medicine, Indianapolis, IN 2004—2007.
 - a) Developed charity events and student social gatherings
 - b) Assisted in developing IUSM graduate student travel awards
 - c) Student representative for judging of travel awards
 - d) Organized student meetings for voicing concerns or problems
3. Student Representative of Committee on Open Enrollment for Graduate Studies, Indiana University School of Medicine, Indianapolis, IN, 2005—2007.
4. Society for Neuroscience Student Member, 2004—2007.
5. Society of Toxicology Student Member, 2003—2004.
6. American Association for the Advancement of Science Student Member, 2006—2007.